processes

Review

Nitinol Type Alloys General Characteristics and Applications in Endodontics

Leszek A. Dobrzański [1,2,*], Lech B. Dobrzański [1,3], Anna D. Dobrzańska-Danikiewicz [4] and Joanna Dobrzańska [1,3]

1 Medical and Dental Engineering Centre for Research, Design and Production ASKLEPIOS, 12/1 King Jana III Sobieskiego St., 44-100 Gliwice, Poland; dobrzanski@centrumasklepios.pl (L.B.D.); joanna.dobrzanska@centrumasklepios.pl (J.D.)
2 Department of Biomedical Engineering, Koszalin University of Technology, 2 Sniadeckich St., 75-453 Koszalin, Poland
3 Medical and Dental Centre SOBIESKI, 12/1 King Jana III Sobieskiego St., 44-100 Gliwice, Poland
4 Faculty of Mechanical Engineering, University of Zielona Gora, 4 Prof. Z. Szafrana St., 65-516 Zielona Gora, Poland; anna.dobrzanska.danikiewicz@gmail.com
* Correspondence: leszek.dobrzanski@centrumasklepios.pl

Abstract: A very extensive literature review presents the possibilities and needs of using, in endodontics, the alloys commonly known as nitinol. Nitinol, as the most modern group of engineering materials used to develop root canals, is equilibrium nickel and titanium alloys in terms of the elements' atomic concentration, or very similar. The main audience of this paper is engineers, tool designers and manufacturers, PhD students, and students of materials and manufacturing engineering but this article can also certainly be used by dentists. The paper aims to present a full material science characterization of the structure and properties of nitinol alloys and to discuss all structural phenomena that determine the performance properties of these alloys, including those applied to manufacture the endodontic tools. The paper presents the selection of these alloys' chemical composition and processing conditions and their importance in the endodontic treatment of teeth. The results of laboratory studies on the analysis of changes during the sterilization of endodontic instruments made of nitinol alloys are also included. The summary of all the literature analyses is an SWOT analysis of strengths, weaknesses, opportunities, and threats, and is a forecast of the development strategy of this material in a specific application such as endodontics.

Keywords: material science and engineering; dental engineering; dentistry sustainable development; endodontics; nitinol alloys; austenite B2; martensite B19′; phase R; heat treatment; thermomechanical treatment; sterilization; mechanical properties; fatigue life; SWOT analysis

check for updates

Citation: Dobrzański, L.A.; Dobrzański, L.B.; Dobrzańska-Danikiewicz, A.D.; Dobrzańska, J. Nitinol Type Alloys General Characteristics and Applications in Endodontics. *Processes* **2022**, *10*, 101. https://doi.org/10.3390/pr10010101

Academic Editors: Prashant K Sarswat and Antonino Recca

Received: 27 November 2021
Accepted: 28 December 2021
Published: 4 January 2022

1. Endodontic Treatment Social Significance and General Objectives of the Paper

Tooth loss has been a problem with the human population since the beginning. For example, in the skeleton of an approximately 25-year-old man, found in a melted glacier from the Ripari Villabruna rock shelter in the Italian Dolomites Veneto near Belluno, from the late Upper Paleolithic, around 14,000 years ago, an infected molar with a large cavity, partially cleaned with flint tools, was found [1,2] (Figure 1). It is considered to be the first-ever evidence of deliberate dental intervention. Research carried out in 2017 allows for adopting the concept [3] that Neanderthals used dental tools known to them even 130,000 years ago [4].

Extraction has been recognized as the only effective method of treating dental diseases for centuries. According to epidemiological data, the most common cause of tooth extractions is caries [5–10]. Tooth decay, which affects 3–5 billion people [2], is currently the most common infectious disease globally. Caries includes interactions between the bacterial biofilm and the surface of teeth, saliva, and genes, dietary carbohydrates, including sugars and starches, and the interaction of behavioral, social, and psychological factors [11–13]. The overwhelming majority of the causes of pulp inflammation and necrosis are extrinsic factors, which include bacterial, thermal, mechanical, chemical, and electrical factors [14,15]. There is also a possibility of infection through the blood vessels that penetrate the pulp through the apical opening. Then, the infection is caused by the intrinsic route due to nutritional deficiencies, metabolic disorders, anemia, or bacterial diseases. The elimination of bacteria from the vicinity of potential infection foci in the oral cavity is extremely important for the health of the whole organism due to the risk of local and systemic complications resulting from pulp diseases [16]. About 80% of all primary foci of systemic infection develop within the teeth, periodontal tissues, and tonsils [16], which means that early diagnosis and effective treatment, eliminating bacteria from the vicinity of potential infection foci in the oral cavity, are extremely important for the health of the whole organism. A focal disease is defined as a secondary focus's clinical systemic and local symptoms, i.e., a pathological change in another organ due to the primary focus [17]. The primary focus of infection is local chronic pathological changes, which are the source of adverse effects on distant organs, causing or maintaining pathological changes in distant organs [18]. It is now well known that, regardless of the direct effects of the disease, caries causes numerous systemic diseases [17,19–39], causing tooth loss and toothlessness, and other serious health complications [18,40–44]. It is the cause of a significant deterioration in the wellbeing, quality, and length of human life. Obviously, missing teeth, especially large ones, significantly impact the oral health-related quality of life (OHRQoL) [45]. A measure of disease prevalence is the disability-adjusted life-years (DALY) indicator, often referring to 100,000 inhabitants, which is used to determine the health condition of a given society [46]. It expresses the total number of years of life lost due to premature death or damage to health due to an injury or disease.

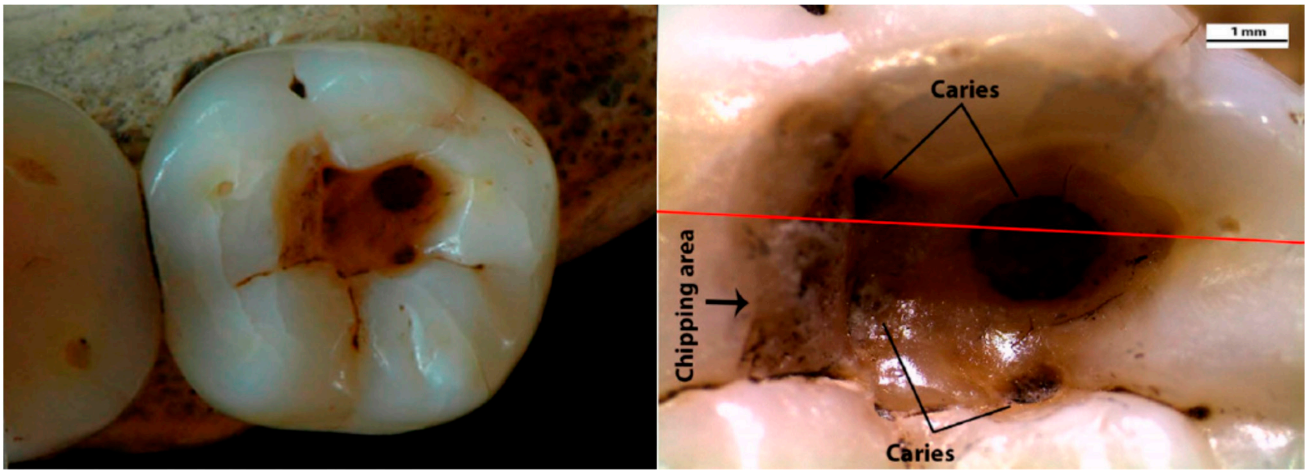

(**a**) (**b**)

Figure 1. Top view of the lower right third molar (RM3) of the Villabrun man; (**a**) occlusal view; (**b**) detailed view of the occlusal cavity with four carious lesions and the area of chipping on the mesial wall; a red line directed mesially–distally runs through the major carious lesion [1].

The DALY index may reach even 40–50 years [2]. It has a major impact on many aspects of social and economic life, although the problem is underestimated by many individuals and by many governments [47]. It is imperative to recognize that the public's overall health is closely related to oral hygiene, prevention, and effective treatment of oral diseases at the earliest possible stage of the disease once it has developed. The most popular and most frequently used treatment method is conservative treatment, which consists of preparing carious lesions and then the direct reconstruction of hard tooth tissues using filling material. Progress in this regard is obvious. If the disease is more advanced, endodontic treatment is needed, which is shown schematically in Figure 2, which includes the matrix of advancement and treatment of oral diseases according to the general authors' concept [2].

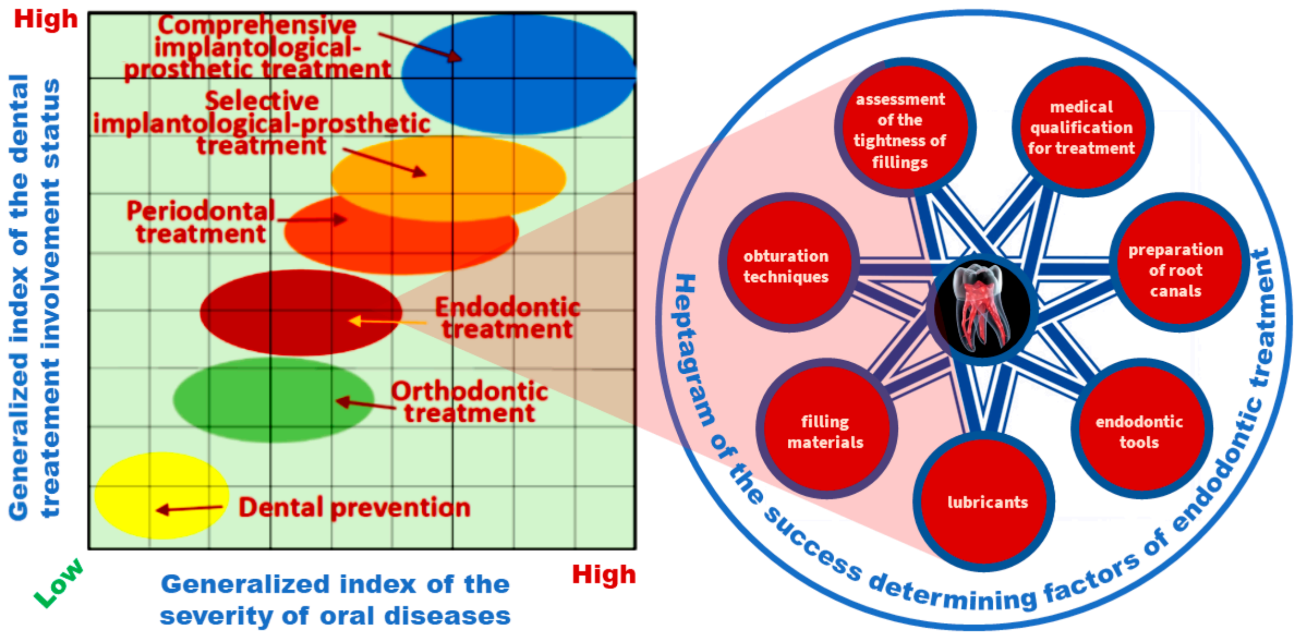

Figure 2. Oral cavity disease treatment advancement matrix with heptogram of the success-determining factors of endodontic treatment.

The inspiration for the development of methodological assumptions during the creation of this matrix (Figure 2) were the portfolio methods commonly known in management sciences, allowing for a graphic presentation of the comparative analysis, the results of which are based on two criteria/factors placed on the horizontal (x) and vertical (y) axis of the matrix.

Historically, conservative treatments instead of dental extractions appeared very late. The history of endodontics dates back to the 17th century. Initially, efforts were made to eliminate pulp ailments by anesthesia with clove oil, cauterization of the pulp with a hot tool, and even devitalization with arsenic trioxide. It was not until 1836 that E. Maynard used the tool for the first time to evacuate the pulp from the inside of the tooth [48]. Understanding the causes and factors causing pulp diseases that make up the epidemiology of pulp diseases has become a significant problem. Currently, in many clinical situations in which tooth extraction is, or may be, performed, it can be successfully replaced by endodontic treatment (Figure 2), which will allow the tooth to be preserved as a pillar, being a component of the stomatognathic system. A human tooth can successfully play the role of a natural dental implant, thus fulfilling both cosmetic functions and recreating appropriate functions in the stomatognathic system, despite losing its living part after proper preparation of the interior and replacing the living tissue with a biocompatible substitute material, also known as filling. Dentists, identifying themselves with the patients' aesthetic needs but at the same time having health considerations in mind, prefer endodontic treatment to extraction [49,50]. Currently, endodontic treatment is more and more common, which is related to the increase in the general level of culture and health awareness of societies [51] and the need to eliminate the effects of inadequate prophylaxis of oral diseases [52], with promotional government actions in many countries [51] resulting from the awareness of the costs of treating complications caused by diseases of the oral cavity, mainly due to the ageing of societies and an increase in the geriatric population [53], more frequently exposed to oral cavity diseases due to their age. As a result of the impact of these factors, the endodontics market is growing, and the forecast predicts that in 2026 it will reach USD 2.1 billion with a CAGR of 4.1% [47,52], and the related dental consumables market in 2023 will reach USD 55.584 million with a CAGR of 5.2% [47,51].

The matrix in Figure 2 is in the Dentistry Sustainable Development (DSD) > 2020 model, consisting of three component models: Global Dental Prevention (GDP), Advanced Interventionist Dentistry 4.0 (AID 4.0), and Dentistry Safety System (DSS) [2,54–57] (Figure 3).

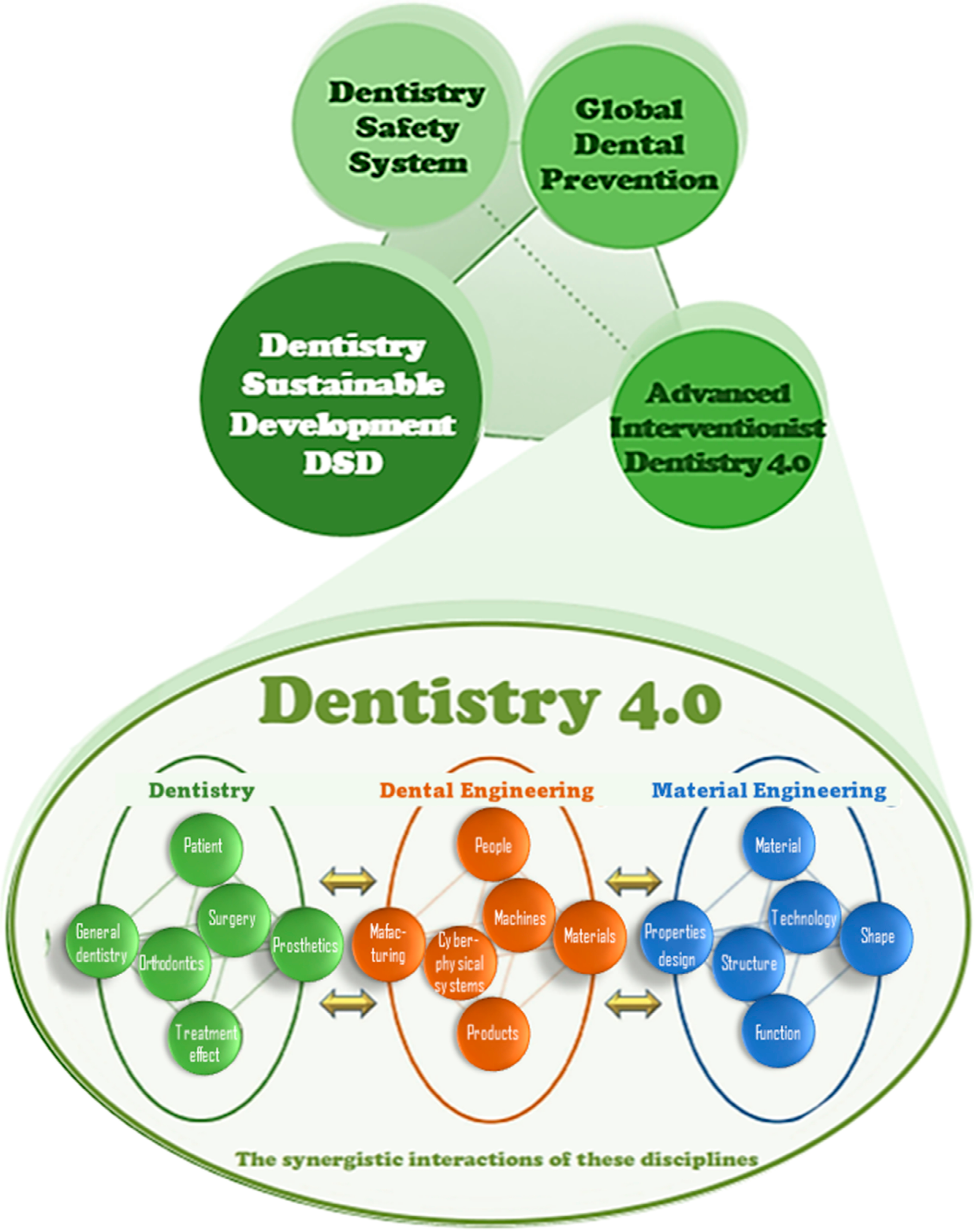

Figure 3. The original concept of the Dentistry Sustainable Development (DSD) > 2020 model and synergistic interactions of dentistry, dental, and material engineering.

This model is an original response to outstanding specialists presented in a series of works [58,59] who expect the practical elimination of interventionist dentistry. It is impossible to disagree with these views regarding waiting for egalitarianism in dental care, increasing the scope of prevention and eliminating discrimination in this area due to exclusion and poverty. However, prophylaxis cannot replace the necessary therapeutic activities defined as interventionist dentistry, including, among others, endodontic treatment.

The effect of endodontic treatment is coronal, lateral, and apical sealing of the previously infected and then prepared root canals, thus preventing the spread of bacteria with possible toxins, also from saliva [60], towards the root apex [61–63]. The correctly performed endodontic procedure should end with leaving the tooth as a natural abutment and leaving a healthy marginal and periapical periodontium.

Requirements for an ideal material for filling the root canal were developed by Grossman [64]. In his own work [47], a virtual analysis of all factors influencing effective endodontic treatment was performed and indicated effective methods of assessing the results of this treatment. In the authors' own works [65–67], it was indicated that the filling material with the best functional properties now has a gutta-percha matrix, and the material with a synthetic resilon matrix is giving way to it. However, it would be most advantageous to develop another, even better, material for this purpose.

The development of root canals consists of removing the contents inside the root canal, disinfecting it, and giving it a shape that will ensure the best hermetization of the root canal with filling material. In endodontics, various techniques can be used to prepare the dentine of the root canal for connection with the filling material (Figure 2). It is possible to use the classic mechanical preparation and disinfection methods by cutting the dentin with hand or rotary tools. It is also possible to use the laser technique, which causes the dentin to fuse, recrystallize, and close the lumen of the dentinal tubules or ultrasound. The preparation and disinfection of the canal are carried out thanks to sound vortices and cavitation [68–72].

The most frequently used methods of preparing the canal for subsequent obturation are mechanical techniques, which, in combination with appropriate rinsing liquids and lubricants, play the role of a universal technique for the preparation and disinfection of the root canal. The virtual analysis performed in [47] limits the considerations only to this group of methods or only to some of them. Classic steel hand and rotary tools are very popular endodontic instruments and can be used in virtually any clinical situation. Unfortunately, as the size increases, the tool's flexibility decreases, and thus the risk of tool breakage increases, especially in curved channels. Due to the inability to adjust the tool to the natural curvature and course of the root canal, their elimination occurs as a consequence of what causes the inevitability of various complications, including perforation of the canal, creation of an unnatural step along the axis of the root canal, or excessive preparation of one of the canal walls [73].

An alternative is a nickel–titanium alloy that was introduced for endodontics in 1988 [74–76]. It allowed increasing the effectiveness of the work of these tools in curved canals. In addition to the traditionally used tools made of corrosion-resistant steel, but with relatively low elasticity, an experienced dentist has gained, by using Ni–Ti alloys for this purpose, much wider possibilities of complementary selection of tools with much greater elasticity and better adaptability to the anatomical features of the root canals, showing increased torsional fracture resistance compared to corrosion-resistant steel tools [74]. It is particularly important when motor-driven rotational endodontic tools are used [77], limiting the incidental fracture of such tools in clinical conditions [78,79]. Endodontic tools made of nickel–titanium alloys require the necessary structural changes and dedicated technological processes to provide them with increased resistance to cracking and increased flexibility. These alloys are known as nitinol, an acronym for Nickel Titanium-Naval Ordnance Laboratory derived from its chemical composition and site of its discovery at the Naval Ordnance Laboratory in 1959 [80–83], although the accidental heating of a harmonica made of this alloy by an accidental participant in the presentation decided the actual discovery of its most important property, which is shape memory [84]. However, this effect was already known concerning gold–cadmium alloys [85] and Cu–Zn brass [86] and is present in many other alloys [87]. However, practical attempts to commercialize nitinol were undertaken only ten years later, and for economic reasons, it gained practical significance only in the 1980s. Nitinol alloys can be used in many areas of technology, including for many medical applications. It is very important to adapt this alloy to long-term work in the working environment inside the human body [88]. The superelastic phenomena may be of significant importance, as in the case of transcatheter delivery, enabling spontaneous expansion and adaptation of the geometric features of the device to the patient's anatomy [76,88,89]. Examples of applications of nitinol in medicine include examples of self-expanding devices such as heart valves [90], arterial stents [91], and inferior vena cava filters [92]. There are, however, examples of unsuccessful or premature applications of nitinol in medicine due to fatigue damage, e.g., in implanted inferior vena cava filters [93] or arterial stents [91]. It is extremely important to meet the high requirements for fatigue life [94,95]. Many natural processes in the human body, such as walking [96], but mainly respiration [97], the cardiac cycle [98], the vena caval dynamics [99], and others, cause the cyclic imposition of deformations. It must be realized that, for example, within 10 years, as a result of the cardiac cycle, there are almost 400 million load cycles of each prosthetic device cyclically deformed by the heart, e.g., heart valves, while at the same time any devices burdened with the respiratory cycle undergo almost 80 million cycle deformations, such as the inferior vena cava filter [88]. Therefore, the prediction of test results for this material with a standard number of, e.g., 10 million cycles, recommended by relevant standards, must seem doubtful. Including this situation makes it necessary to carry out numerous new research in this field for medical applications without unacceptable risk, contrary to the Hippocratic Oath and the indispensable ethical requirements addressed to doctors and medical engineers [100].

One of the possibilities of using nitinol are dental applications in orthodontics [101] and for endodontic instruments [74,102,103], which took place from 1988 [74–76], both for manual and rotational preparation of root canals [73,104], due to the high fatigue strength [74–76,105–128] and mechanical resistance to fracture [75]. The main advantage of these endodontic tools compared to those made of corrosion-resistant steels is their increased flexibility and torsional strength [74]. It applies not only to hand tools but mainly motor-driven rotary tools [77]. However, also, in this case, it is difficult to avoid incidental breakage of such tools during clinical practice [78,79].

In the last dozen or so years, many economic entities in the world have developed new technological procedures, thanks to which new endodontic tools with better functional properties than those used so far were introduced into clinical practice, especially in the case of motor-driven rotary tools [77]. It significantly improved the efficiency of root canal preparation due to the much lower than before canal transport [129–132] and the minimization of lateral forces, provided by the flexibility of these tools [133,134]. There have been valuable studies in the literature review that systematize these favorable technological changes [135,136]. It is impossible not to mention that the so-called systematic reviews of the literature on the subject [137,138] and on sterilization in endodontics [139] were published almost simultaneously. PRISMA recommendations [140] were used to develop them, formulating a set of questions concerning the population, intervention, comparison, and outcome (PICO) in the scope of interesting endodontic problems through bibliographic research on electronic databases [141]. After analyzing the obtained results by two independent experts and decisions made by the third expert in case of doubtful situations, the full texts of selected papers were analyzed in terms of the four-order classification of issues. The K-agreement between experts was established based on the formulas in the Cochrane Handbook for Systematic Reviews [142], also establishing Po as a proportion of agreement and Pe as agreement expected. The Newcastle–Ottawa scale for case–control studies was used to evaluate the risk of bias [143]. The Rev Manager software 5.3 (Cochrane Collaboration, Copenhagen, Denmark) was used for statistical analysis. These types of studies are prepared mainly by doctors. Both discussed as examples and relating to this matter, unfortunately, represent a low cognitive value in the field of materials science and are saturated with numerous substantive errors and glaring understatements, as a result of which, in fact, apart from the collection of lists of publications on the subject, they contain almost no valuable information. It should be noted that the methodology used and the procedures for selecting papers would certainly be avant-garde and could help in the proper selection of literature sources, provided that the authors firstly demonstrate adequate knowledge of the subject matter being developed and, after the selection procedures, are willing and able to discuss in detail the substantively cognitive and technological problems raised in papers selected in this way. Unfortunately, this did not happen. The authors wasted the opportunity to analyze real problems, dealing mainly with the description of formal IT aspects of handling metadata from databases collecting scientific papers in appropriate databases.

The attempts by dentists to perform laboratory engineering tests and draw conclusions that would serve dentists [144] as the results of scientific research must also be surprising. Such activities cannot serve well for the proper application of nitinol tools in endodontics. The work [144] did not familiarize itself with the chemical composition of the analyzed cases, making an erroneous assessment likely to be harmful if anyone were to take advantage of such suggestions. It is important to point out the errors and stereotypes disseminated in this way, some of which may even be harmful to patients and the treatment procedures performed, such as those indicated in the quoted work [144]. As dentists often assessed these works, their substantive deficiencies were not noticed most often. Yet, their information functions as if they were true, and they are freely disseminated among dentists. It is also important not to identify the so-called apparent relationships, which are extremely easy to find if the researcher is unaware of how many factors affect the final result of the research. In this case, there are still many circumstances related to various aspects of the manufacturing and heat treatment of nitinol alloys, of which the authors of cited work [144] are unaware. This aspect will be discussed in detail later in this paper.

The above argumentation, which also includes a critical evaluation of the exemplified works [137,138], leads to the obvious conclusion that the methodological errors made in this way should not be duplicated. Reasonable use of this methodology probably does not preclude a correct substantive analysis of the analyzed issues contained in a given literature review. The presented examples and several other works known to the authors of this paper, and concerning other issues, but also most often in the field of medicine, do not seem to confirm this assumption. For this reason, such a methodology was consciously departed from, despite the fact that, as described, it is known to the Authors of this article and apparently one might think that it speeds up the task if it were not for the fact that too often it causes falsification of the analyzed content. This fact met with criticism of the reviewer of this paper, which the Authors do not agree with, and for this reason, this commentary is included in the text of this paper. In the authors' opinion, it is an abuse to recognize the product of such work as the only possible method of a systematic review of the literature. Literally analyzing the meaning of the word systematic according to "The New Oxford Dictionary of English", systematic means "done or acting according to a fixed plan or system". "System", in turn, means "a set of connected things or parts forming a complex whole" or "set of principles or procedures according to which something is done; an organized scheme or method". The approach presented, inter alia, in works [137,138] fulfils these definitional meanings, but it is not the only possible approach, and hence the reviewer's expectation to perform each subsequent review work in this way is completely unjustified, especially because, as the examples show, it causes far-reaching simplifications along with the elimination of essential content, deciding on a very hasty analysis of the content of the articles included and, in fact, leads to the elimination of numerous substantively significant cognitive and technological problems, often not even noticed due to methodological simplifications. It is paradoxical to accuse the systematic review of several hundred published studies by the authors of the lack of systematic nature. In this paper, the systematic approach is based on the traditional methodology. The work consists of reading and understanding all analyzed works on the topic. For each work, a selection and excerpts of relevant information are made, formerly called flashcards, with the reference in each case of the literary source of such information, which may be many in each article read. Each of such individual pieces of information is provided with a lead slogan, only some of which can be considered keywords. Such information is collected in working texts containing similar entries, and after inserting such flashcards from the entire set of publications read, a fragment of the text of the entire literature review on a given sub-topic is compiled. Then, the individual descriptions are logically arranged according to the hierarchy of importance, and in this way, the table of contents of the entire literature review is built from below. It is painstaking and systematic work. Of course, one can easily use database software programs for this systematic composing of a huge amount of information prepared in this manner. While the approach criticized by the authors of this paper is based on the systematic elimination of problems contained in the literature, the systematics of the authors of this paper simply consists of collecting them and then taking into account all aspects in the literature review. Of course, in each fragment concerning a specific issue, generalizations are made if the same or similar information appears in several or many works, and the information that is individual is described as exceptions or even stated exceptions from the rules; due to the specific approach, or in such cases, doubts are raised as to the reliability or credibility of information formulated in this way. It would seem that such an approach is obvious and, as it should be assumed, is typical for many specialties, including in the field of the humanities. The information presented here fulfils the requirement to describe the methodological aspects, although for the Authors of this paper it is surprising that it requires description. As it is a necessary condition for the publication of this article, after reflection, the Authors decided to include these methodological explanations in this paper.

The issues of selecting the chemical composition and the technology of manufacturing tools used in endodontics, which are the subject of such works, go far beyond the professional competencies of the dentist. The dentist, however, has the right to expect optimal performance from the tools provided to him but still maintaining confidence in the engineering activities of the tool manufacturers and the results of scientific research carried out in compliance with all rules applicable in such cases. It does not mean that the results of all comparative studies of various endodontic tools to rank the properties of specific products available on the market [145] may be practically completely useless for doctors, even if the principles as mentioned above are not explicitly taken into account, as is also performed in technical-exploitation documentation of many products. A lot of such works have appeared even recently. It is impossible to ignore them in such a comprehensive review of the literature on endodontic tools made of nitinol alloys as this paper. However, it should be noted that they do not significantly increase scientific knowledge, although they cannot be deprived of some practical meaning. Therefore, in one of the following parts of this paper, they are reviewed in more detail. As such works are published in specialized dental journals addressed to endodontists, it is worth commenting on them. However, the often presented approach is purely practical, without any scientific references and a materiallographical analysis of the essence of the regularities noticed in them. It should also be noted that the manufacture of endodontic tools is only one of the numerous possible practical applications of nitinol alloys.

Each scientific work in the field of material engineering, including this one on endodontic tools, requires respect for the material engineering paradigm, i.e., in general, the study of cause–effect relationships between the type and chemical composition of the material, shaping the form and geometric features of the product, as well as its structure in the technological process and their influence on the physicochemical properties, including mechanical properties, to ensure the assumed operational functions of the product manufactured from a given material. It seems to be obvious to every materials science expert, but it may cause some surprise among dentists. Therefore, it should be remembered at this point in this paper that this paradigm comes down to the principle of six expectations, 6xE, expressed in octahedron and taking into account the basics of engineering design composed of three inseparable elements, including material and technological design [66,146–148] (Figure 4).

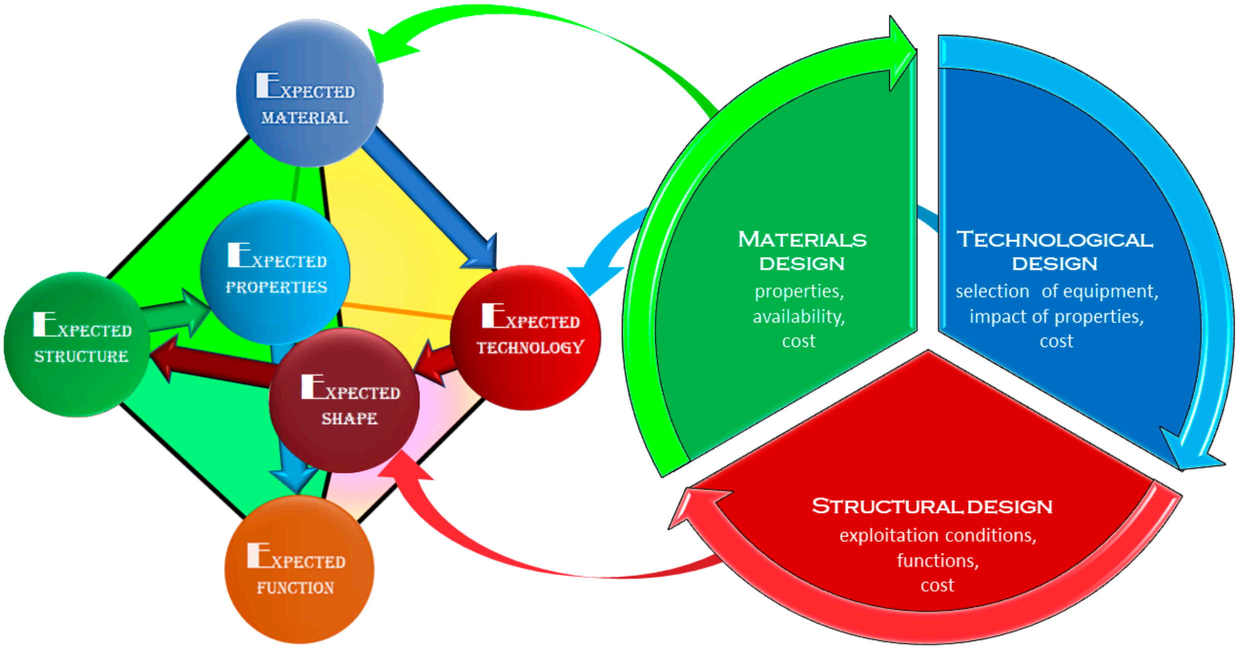

Figure 4. A diagram of the relationship between engineering design and the material engineering paradigm.

Given an example and the analysis carried out in connection with it, it is shown how important it is to make dentists realize how complex an engineering problem is to create a properly functioning endodontic tool not to harm the patient. It was this conclusion that was the basis for the development of this paper to broaden the analysis of the selection of the chemical composition and manufacturing technology and to discuss the set of properties of the alloys used for this purpose, to even discourage dentists from home-grown experiments in such a complex subject area, as well as formalistic preparation of literature reviews devoid of any substantive and practical analyzes and deliberations.

This paper aims to present a full material science characterization of the structure and properties of nitinol alloys as the most modern group of engineering materials used to prepare a root canal and to discuss all structural phenomena that determine the performance properties of these endodontic tools against the background of the basic elements of such dental treatment. Tools made of Ni–Ti alloys play a fundamental role in the implementation of endodontic treatment. Experimental studies were carried out, analyzing, among other things, variants of root canals preparation with the use of hand and rotary tools made of nitinol in endodontics, resulting from the literature review and the virtually performed analysis in the authors' work [47]. This paper presents a review of the literature on selecting the chemical composition and processing conditions of these alloys and their importance in endodontic treatment of teeth, which, of course, is beyond the dentist's control when buying a ready-made tool manufactured by the manufacturer. However, the results of laboratory tests concerning the analysis of changes occurring during sterilization necessary for sanitary and epidemiological reasons were also considered. In this regard, all decisions are made autonomously by the dentist who uses endodontic tools made of nitinol.

Nevertheless, the paper also reviews the results of various tests on the performance of tools made of nitinol made by dentists. Despite the lack of cognitive values, such a review may be useful for dentists, pointing to the functional properties of tools from different companies. It is worth adding that the main recipients of this paper are certain engineers, tool designers and manufacturers, PhD students, and students of materials and manufacturing engineering. Still, dentists will also certainly reach for it. It is this practical information that can be helpful to them in clinical practice. As each sterilization process causes irreversible degradation of each tool, the problem has been analyzed in detail in this paper, broadly illustrated by the results of experimental studies, including caused by sterilization necessary for clinical reasons. The mechanical preparation of root canals requires eliminating microorganisms and removing inorganic and organic debris from the root canals. Therefore, it is necessary to irrigate the root canals with appropriate rinsing fluids after each inserted instrument. However, these issues do not fall within the scope of this paper. The summary of all the conducted literature analyzes is an SWOT analysis of strengths, weaknesses, opportunities, and threats, and is a forecast of the development strategy of this material in a specific application, such as endodontics. The methodology used and described in earlier own work was used [66].

2. The Importance of Tools Made of Ni–Ti Alloy of the Nitinol Type in Endodontic Treatment

The success of endodontic treatment is influenced by several factors (Figure 2), including two directly dependent on the experience and practice of the dentist, which includes:

- ✓ Correct selection of filling material.
- ✓ Choosing the right obturation technique.

Another factor is the method of preparing the root canal, mainly depending on the choice of the tool. The way of using it by the dentist [110] has a significant influence on the wear or damage of the tool, including the one made of nitinol [110]. The risk of reducing the possibility of breaking the endodontic file inside the tooth during root canal treatment decreases with an increase in the dentist's experience, thus helping to improve patient safety. The "crown-down" technique from the group of crown-apical methods is appropriate when working with rotary tools and hand tools made of nitinol. This method generally reduces the risk of pushing dead pulp debris and dentine filings beyond the apical foramen [73,149]. In the first stage, the peripheral and middle parts are prepared for 2/3 of the root canal length or its straight part in the case of curved canals. In the second stage, the apical part is processed after measuring the working length.

The material and technological issues related to endodontic tools, in fact, largely go beyond the scope of professional dentists' interests. On the other hand, a mistake in selecting this material may determine the failure of endodontic treatment. Therefore, the general knowledge in this area is also useful for dentists. The aim is to avoid or even prevent iatrogenic errors during root canal preparation, consisting of breaking the tool and the necessity to leave its tip inside the root canal.

Regardless of the material from which they were made, endodontic tools are straightened inside curved root canals. Only by using nitinol endodontic tools with sufficient flexibility can the side forces that arise on the root canal walls be minimized [133,134]. In this case, even in the case of the use of rotary tools, the root canal transport associated with the evacuation of dentin filings and pulp debris from the root canal is significantly lower than when the root canals are prepared with hand tools made of corrosion-resistant steel. It also influences the reduction of errors related to this study [129–132]. Unfortunately, an even bigger problem that appears too often in clinical practice, even in the case of using nitinol endodontic instruments, is their fracture inside the root canal, which is one of the cardinal iatrogenic errors [78,79,150,151]. The cause of such damage may be insufficient torsional strength [151], which occurs when the working part of the tool becomes trapped in the root canal, and the handle continues to rotate until the torsional strength of the tool material is exceeded [152]. Most often, however, such damage occurs as a result of tool material fatigue [151]. As a measure of fatigue life, the time to fracture an endodontic tool during operation or the number of cycles to fracture this tool (NCF) may alternatively be taken. The reduction of the fatigue strength of endodontic tools is related to the increase in the amplitude of tensile stresses on the surface of these tools, which occurs at the root canal with the maximum curvature [153]. The reduction of the fatigue strength of endodontic tools also occurs due to the increase in temperature inside the root canal during its preparation compared to room temperature [154–157]. The fatigue life of both rotary and handheld nitinol endodontic tools can be increased by using the crown-down technique instead of the rotary motion [158,159]. As the torque decreases with the reduction of the diameter of the endodontic tool and the size of the taper, which is accompanied by an increase in the flexibility of endodontic tools [153,160], the fatigue life then increases with a simultaneous reduction in the amplitude of the tensile stress on the surface of the tool [161]. The cause of the damage, in this case, is, of course, fatigue phenomena, ranging from the initiation of cracks as a result of the impact of defects in the crystal structure, nonmetallic inclusions, and the precipitations of secondary phases, surface effects, and defects from the manufacturing process [162] through the propagation of cracks, to the fatigue scrap [162,163]. The fatigue properties of the nitinol alloy significantly depend not only on even slight changes in the chemical composition [164], but also on the metallurgical purity of the alloy [149,165,166], and especially on the method of manufacturing both the alloy [165,167,168] and tools.

The properties of nitinol determine the obvious advantages of tools used in endodontics, including the possibility of effective evacuation of dentin filings and pulp debris from the root canal thanks to its conical treatment, leaving a wide opening narrowing towards the apex. It is extremely important to ensure natural curves and the root canal's course and maintain its working length stably. In the case of rotary nitinol tools, compared to hand tools made of corrosion-resistant steel, much less dentine is removed from the root canal wall [150], so there are fewer cases of pushing the remains of pulp and cut canal dentine beyond the apical opening [169], as is a typical iatrogenic complication during root canal preparation. The advantage is a drastic reduction in the risk of breaking the tool during root canal preparation [170], the most common causes of which are the signs of damage to the structure of the prepared tooth invisible from the outside, with the necessary skill required by the dentist. The efficiency of cutting the root canal dentine is improved due to the shorter preparation time and the reduced number of used tools made of nitinol [171–173].

Thanks to the shape memory effect, endodontic nickel–titanium tools do not undergo permanent deformation. At the same time, under the influence of excessive stress or fatigue of the material, they could unexpectedly break [76,105–109,174,175], which requires a fixed rotational speed and also controlling the torque depending on the size and design of the tool [109]. The way the dentist uses it [109,110] also significantly influences the wear or damage of the tool. The possibility of breaking the endodontic file inside the tooth during root canal treatment is significantly reduced, thus improving the patient's safety. In the case of endodontic tools, high fatigue strength [74–76,105–128] and mechanical resistance to fractures [75] are some of their most important features (Figure 5).

Endodontic nitinol tools for preparing root canals can be adapted for manual or rotary preparation [73,104]. The geometrical features of these endodontic tools, including taper, radial contact surface, blade angle, and shear angle, varies [176]. The conicity reflects the increase in the diameter of the tool relative to the next millimeter of its length [177]. For example, for a tool with a 4% taper, its diameter increases by 0.04 mm for each additional millimeter of tool length. The conicity of nitinol tools can vary in value, e.g., 2, 4, 6, 8, 10, and 12% along the entire length, although they may also have variable taper along the length of the tool, e.g., from 3.5 to 19%, such as ProTaper [176]. The root canal can thus be shaped according to its natural course in the form of a cone. Rake angle can be neutral when 90°, positive when >90°, or negative when <90° [73].

For example, the K3 tools [176] have a positive cutting angle, promoting very effective cutting and evacuation of dentin from the root canal. On the other hand, ProTaper tools have a negative rake angle [176], which increases the risk of apical displacement of dentin scrapings due to their accumulation between the root canal wall and the tool. In both cases, the tip angle is <90°, which, despite the risk of distorting the original shape of the root canal, ensures its efficient and quick preparation. The K3 tools have an asymmetric shape of three faces, with a noncutting tip in the middle. The cross-sectional ProTaper tools have the shape of a convex triangle, also with a noncutting tip [73,171].

Figure 5. Examples of endodontic tools made of nitinol (commercial data available on the Internet).

3. Chemical Composition, Methods of Nitinol Manufacturing, and Conventional Technologies for the Endodontic Tools Manufacturing

The most suitable material for use in endodontic tools is a nitinol alloy with a chemical composition corresponding to the stoichiometric atomic concentration of the elements in the NiTi intermetallic phase with the lowest possible concentration of other elements that play the role of only impurities and reduce the physical properties of the material and endodontic tools made of it. Detailed requirements in this respect are included in the standard [178]. Most often, for the construction of endodontic tools, an alloy containing 56 wt.% Ni and 44 wt.% Ti is used, although it is not the only alloy composition currently used for this purpose [81–84,179–181] (Figure 6).

However, it should be noted that even slight changes in the chemical composition of the nitinol alloy, within the concentrations allowed by the standards, may cause significant changes in the functional properties of endodontic instruments and other medical devices made of them [164]. The company websites state that nitinol alloys contain 25–50% Ti and 50–75% Ni [182]. An exemplary chemical composition according to ASTM 2063 of Shape Memory Ni–Ti Alloy Nitinol 55 comprises 55.75% Ni; 0.038% C; 0.04% O; 0.012% Fe; not more than 0.005% each of Co, Cu, Cr, H, Nb, and the rest of titanium [183]. In these alloys, nickel and titanium are present in stoichiometric atomic concentrations corresponding to the NiTi intermetallic phase and are usually named according to the mass concentration of nickel, as, for example, Nitinol 55 and Nitinol 60 [183]. In some cases, a partial substitution of nickel by Co is possible, but in a mass concentration not exceeding 2% [123,184,185]. The manufacturing method is also essential [165,167,168]. Using the highest purity raw materials reduces the proportion of nonmetallic inclusions and improves fatigue properties [149,165,166].

Figure 6a shows a graph of the phase equilibrium of Ni–Ti, which comes, to this day from [186], with changes and additions introduced later [187–190] and then repeated in many other papers [191], often without specifying the source [191–193]. This figure (Figure 6b) also shows the effect of the mass concentration of nickel in a narrow range of approx. 48–51% on the value of the Ms temperature, derived from the comparison of the results from two classic studies [194,195]. For the stoichiometric chemical composition of Ni50Ti50, the Ms temperature is about 65 °C, and if the titanium concentration is slightly higher, it also slightly increases. On the other hand, increasing the nickel concentration above the equilibrium causes a radical reduction of the Ms temperature even to about −140 °C (Figure 6) [194]. These small fluctuations in the concentration of both elements affect significant changes in the physical properties of the Nitinol 55 alloy [164] because all the values discussed here relate to the alloy determined in this way (Table 1) according to the relevant standards [178].

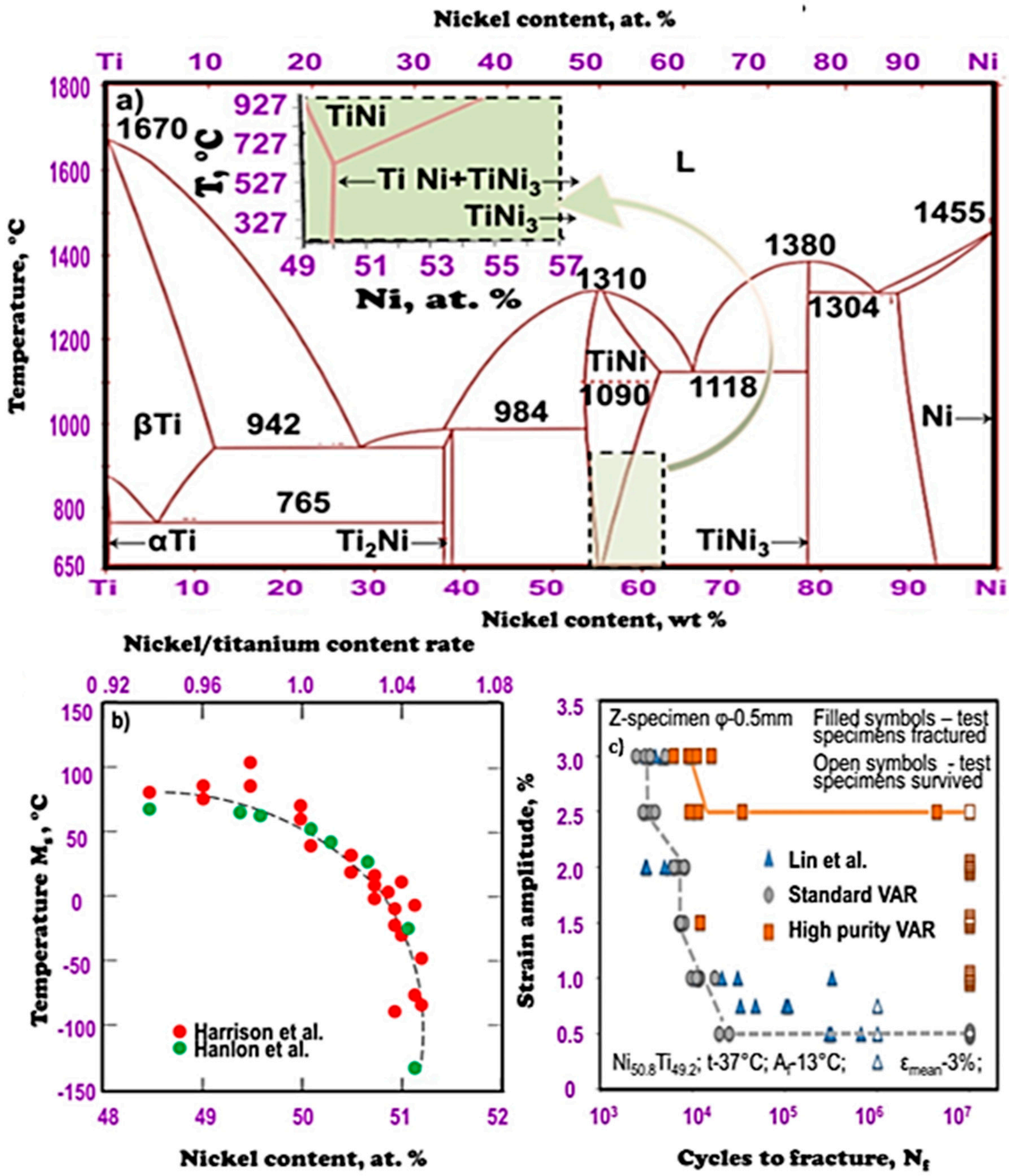

Figure 6. (**a**): Graph of phase equilibrium Ni–Ti; (**b**): the effect of mass concentration of nickel in the range of 48–52% on the value of temperature M_S; (**c**): and the dependence of strain amplitude and cycles of fatigue loads is the fracture Nf.

Table 2 compares the concentrations of elements in two exemplary heats of the Nitinol 55 alloy [165]. The tests were performed by faithfully repeating the experiments previously carried out on the same melt produced by the vacuum arc remelting (VAR) method as in the works of [167,168] and supplementing them.

Table 1. Physical properties of the Nitinol 55 alloy depending on the concentration of nickel and titanium.

Alloy No	**Weight Concentration, %**		**Temperature, °C**				**$\sigma_{0,2}$, MPa**
	Ni	**Ti**	**M_s**	**M_f**	**A_s**	**A_f**	
1	54.8	45.2	20	−20	39	77	115
2	55.5	44.5	−30	−53	−12	0	75

Table 2. Chemical composition of bars with a diameter of 25.4 mm from two heats of the Nitinol 55 alloy and their comparison with the requirements of ASTM F 2063-12.

Alloy	**Chemical Composition, wt. %**												
	Ni	**Ti**	**O + N max**	**C max**	**Al. max**	**Each of Co, Fe max**	**Each of Cu, Cr max**	**H max**	**Each of Mn, Mo, W max**	**Nb max**	**Si max**	**S max**	**Sn max**
Standard	55.6	Balance	0.0252	0.0020	0.0057	0.0050	0.0050	0.0015	0.0050	0.0050	0.0025	0.0010	0.0100
High purity	56.0		0.0060		0.0050			0.0012					
ASTM [178] requirement	54.5 - 57.0		0.050	0.050	-	0.050	0.010	-	-	0.025	-	-	-

These tests were compared with those obtained for the melt produced with the same method and within the concentration range established for the Nitinol 55 alloy in the standard [178] but characterized by high purity [165]. The much higher proportion of nonmetallic inclusions in the standard melt determines the fatigue strength several times lower (Figure 6c) [165] than in the high-purity alloy. Thus, produced high-purity nitinol has a 107-cycle fatigue stress limit of 2.5% with an average strain of 3%. Although falling within the requirements for the Nitinol 55 alloy specified in ASTM [178], both these heats undoubtedly differ substantially in structure and properties. In the standard alloy, the initiation of all cracks was due to nonmetallic near-surface inclusions, most likely $Ti_4Ni_2O_x$, which is also indicated by other reports [91,167,168,196]. In the case of high-purity melt, apart from the almost four-times lower volume fraction of nonmetallic inclusions (Table 2), their transverse dimensions are usually 5–10 times smaller than in the case of the standard melt (Table 3).

Table 3. Selected features of the structure of bars with a diameter of 25.4 mm from two heats of the Nitinol 55 alloy and their comparison with the requirements of ASTM F 2063-12.

Alloy	**Transformation Temperature [1], A_t, °C**	**Longitudinal Length, µm**	**Area Fraction, %**
Standard	−12	−11	-
High purity	35	17	≤39
ASTM [178] requirement	1.01	0.28	≤2.8

[1] Measured by differential scanning calorimetry (DSC) following ASTM F2004 (ASTM F2004-05) [197].

The technology of manufacturing the nitinol alloys [74,81,120,123,125,129,185,198–251] is therefore important due to the strong affinity of titanium for oxygen and carbon and the need to minimize the formation of nonmetallic inclusions in participation of this element. In addition to eliminating harmful nonmetallic inclusions, it is necessary to obtain an alloy with an exact stable chemical composition. Despite the very high affinity of this element for oxygen, preventing the oxidation of titanium is also intended to prevent an uncontrolled change in the ratio between the atomic concentrations of nickel and titanium, due to the involvement of its atoms in reactions with oxygen. Therefore, for nitinol manufacturing, it is necessary to use raw materials of high purity, i.e., containing 99.99 wt.% Ni and 99.8 wt.% Ti. As indicated, the vacuum arc remelting (VAR) method is preferred by igniting an electric arc in a water-cooled copper ladle under a high vacuum between the raw material and the water-cooled copper impact plate. If the highest purity raw materials are used, it is possible to reduce the proportion of nonmetallic inclusions and improve the fatigue properties [252]. It is judged that the most advantageous is the production of nitinol by the vacuum induction melting (VIM) method using alternating magnetic fields to melt the raw materials in a crucible under a high vacuum. In this case, the smallest possible proportion of nonmetallic inclusions is ensured [165], which increases the resistance to fatigue [166], although the works [165,253] indicate, on the contrary, that in the high-purity nitinol produced by the VIM method, there are more inclusions of both oxide and carbide type compared to the VAR method. The dependence of fatigue strength on the share, size, and distribution of nonmetallic inclusions was confirmed in [149]. Other methods of producing nitinol can also be used but are not of industrial importance, such as plasma arc melting, induction melting, and electron beam melting. On the other hand, the electric arc melting technology seems to be useless for nitinol alloys.

In the light of the information presented, it is obvious that slight changes in the chemical composition of the nitinol alloy within the concentrations allowed by the standards may cause significant changes in the functional properties of endodontic instruments and other medical devices made of them.

Technologies for manufacturing tools for the treatment of root canals made of nitinol alloys should ensure the highest possible tensile strength, ensured by the stoichiometric composition of the Ni–Ti alloy, and the significant elongation and associated elongation elasticity ensure high resistance to fatigue and the possibility of operating in curved canals. Nitinol is a material that is difficult to plasticize, so it is practically only subjected to hot plastic working, including rolling, swaging, drawing, and extrusion. Nitinol endodontic tools are made of rods or wires produced by drawing or extrusion. The manufacturing of endodontic tools for Nitinol is more complex than for corrosion-resistant steel because they cannot be made by twisting, as with corrosion resisted steel [233]. Due to the desired elasticity and the associated resistance to plastic deformation over a relatively wide deformation range, one must be aware that an attempt to impart the required geometrical features by twisting effectively would most likely lead to a scrap of the tool before the end of the technological process [233]. For this reason, the shape and geometrical features are provided by milling and subsequent grinding [120], eliminating surface irregularities and the resulting negative effects on fracture toughness, cutting efficiency and corrosion resistance [75,120,250,251,254–256]. The machining is carried out with the use of tools made of sintered carbides.

In the case of endodontic tools, mechanical resistance to fractures is one of the most important features [75]. Apart from grinding, among the various nontraditional manufacturing methods, it is also possible to use additive manufacturing technologies to produce elements from the nitinol alloy [257], laser and electrical discharge machining [164,258]. Electropolishing (EP) improves the surface roughness [75,259,260]. It even gains a gloss [259,261], which removes surface cracks and residual stresses and improves the efficiency of root canals preparation with their participation and the possibility of increasing deflection angle during root canal preparation and improvement of their corrosion resistance [255,259,262]. Electropolishing has a beneficial effect on the fracture resistance of nitinol endodontic tools, mainly by improving the fatigue life compared to untreated tools [75,256,263,264]. There is no evidence of suppression of crack propagation [265] as well as an increase in maximum scrap-determining torque compared to nonelectropolished endodontic tools [262]. Magnetoelectropolishing in a constant magnetic field (MEP) [24–26,105–108,174,175] is particularly advantageous, as it increases the fatigue strength [74–76,105–128]. Another innovative process is electrical discharge machining EDM [266], most commonly known by dentists as Hyflex EDM [267], which generates a unique, hardened surface that effectively improves superior fracture resistance and improved cutting efficiency [268]. It is particularly advantageous to combine this technology with the provision of a controlled memory nitinol structure known as CM, as discussed in the following sections of this paper. The process was implemented by Coltène/Whaledent Inc., Cuyahoga Falls, OH, USA [267] after the year 2011. EDM is a subtractive treatment that enables contactless and precise removal of the processed material using pulsed electrical discharge while eliminating any mechanical stresses [269]. The ionization of the dielectric liquid in which the process is carried out takes place after obtaining a sufficiently small gap between the material being processed and the electrode serving as a machining tool, provided that both of these elements are electrically conductive. Small particles of the processed object then evaporate under the influence of electric sparks, and after solidification in a dielectric liquid, they have washed away [270,271].

It is possible to reuse endodontic tools manufactured using this technology [268] without significant changes in the quality of their surface [272]. The type of material used determines the surface quality after developing strongly curved root canals and, hence, its differentiation depending on the examination of Hyflex CM and Hyflex EDM materials, to the benefit of the latter [272]. However, there is no convincing evidence showing an improvement in the cutting properties of Hyflex EDM tools compared to other tools made of nitinol [135]. Their hardness [273] and fatigue life [268,274,275] are higher. At the same time, the torque to be destroyed is lower [275], not only compared to Hyflex CM, but also to conventional nitinol and M-Wire tools whose phase compositions are described later in this paper.

4. Shape Memory Effect and Superelasticity of Nitinol

Controlling the properties of nitinol tools is ensured by a combination of heat treatment and cold working [23,276]. Endodontic tools with an equilibrium concentration of Ni and Ti [120] are characterized by an austenitic structure with an austenite finish temperature lower than the temperature of the human body [277,278].

In the case of endodontic tools, the unique features of the nitinol used in their manufacturing, defined as superelasticity and shape memory [120,279–283], are of crucial importance. The importance of homogenizing annealing, especially the cooling rate in this technological operation, was indicated [284–288]. Significant changes in the properties of nitinol alloys, including modulus of elasticity, yield point and electrical resistance, and the shape memory effect [81–84,179–181,250,289], occur as a result of cooling at the critical transformation temperature range (TTR). The TTR range is determined by the martensitic transformation's start (M_s) and end (M_f) temperatures.

The described changes in properties result from the course of the martensitic transformation of the simple cubic structure B2 of austenite (also known as the parent phase) (Figure 7a) [81–84,179–181,289,290], occurring above approx. 100 °C in twinned martensite, a monoclinic crystal structure of martensite B19′ (daughter phase) [44,81–84,179–181,289] according to scheme B2 $\rightarrow$ B19′. Martensite has better plastic properties than austenite [291–296]. The hysteresis loop of the martensitic transformation is shown in Figure 8a. The hysteresis loop's width depends on the alloy's exact chemical composition and the nitinol processing. The hysteresis loop of the martensitic transformation covers the range of 20–50 °C, although it can be reduced or increased by alloying additives [42] and the applied technological processes [43,81–84,179–181,289].

During subsequent heating, reverse martensitic transformation takes place into a reverse transformation of temperature range RTTR according to the scheme B19′ $\rightarrow$ B2 martensite into the mother phase high-temperature austenite with a stable energy state [81–84,179–181,289]. This phenomenon is referred to as the shape memory effect. The martensitic transformation in both directions is immediate [81–84,179–181,289].

The following mechanisms determine the shape-memory phenomenon [283] (Figure 9):

- One-way shape memory effect.
- Superelasticity.

- Bidirectional shape memory effect.

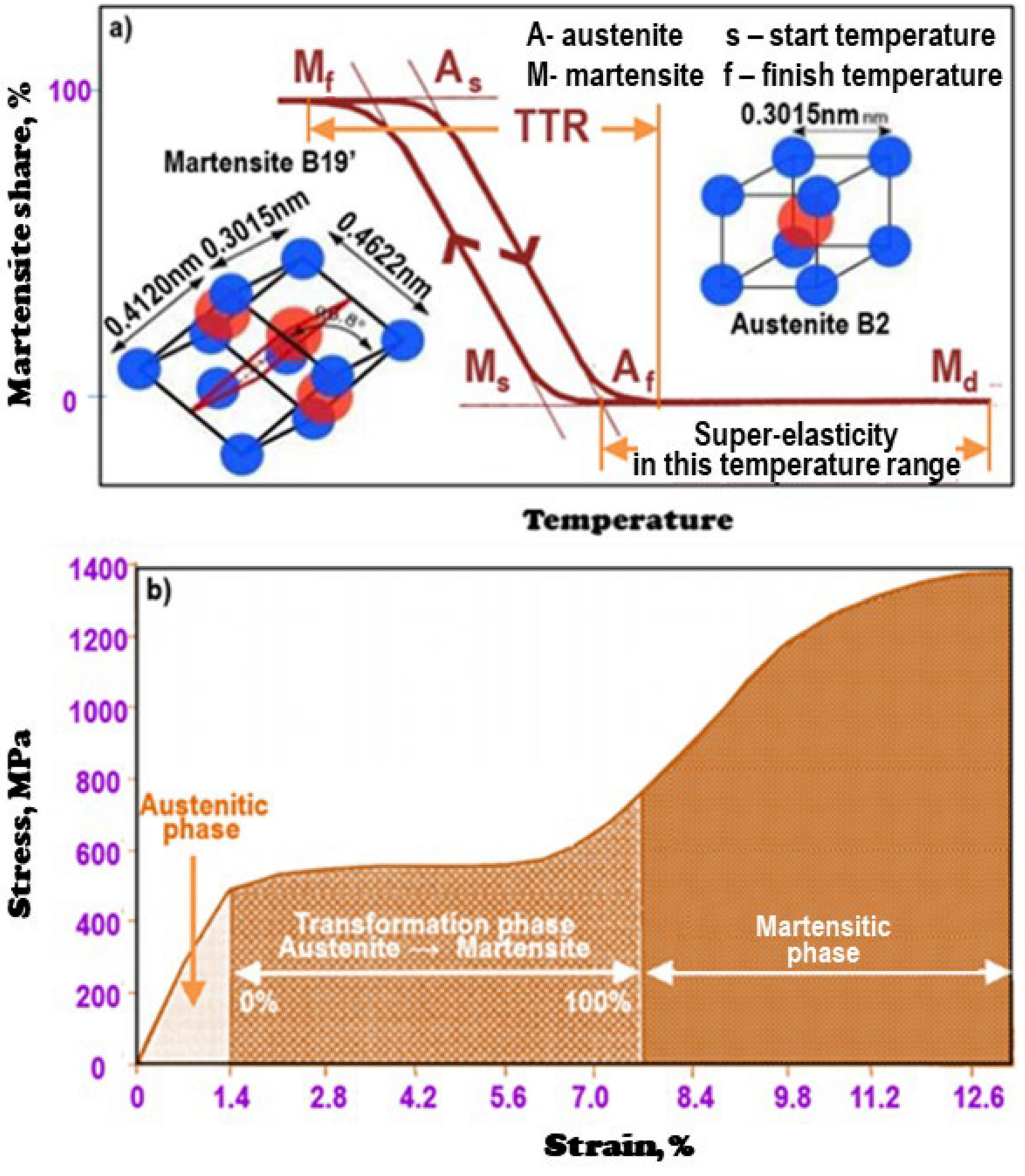

Figure 7. Schemes: (**a**) transformation of austenite by twinning into martensite in the RTTR temperature range, martensite reorientation through detwinning and reverse martensitic transformation in the RTTR temperature range; (**b**) stress–strain–temperature influence on the course of nitinol transformation.

Depending on the initial state, the unidirectional shape memory effect is a martensitic transformation caused by deformation or hardening and a subsequent reverse transformation into the parent phase when heated to the characteristic temperature. As a result, the workpiece returns to its original shape [283].

The phenomenon of superelasticity is related to the reversible martensitic transformation under the influence of external stress. As a result of the formation of martensite at a temperature higher than A_r, elastic deformation of the object occurs by several to dozen per cent, which completely disappears after unloading. In this case, the recovery to its original shape occurs during heating. No change in shape occurs during cooling, so only the shape of the high-temperature parent phase is remembered. As a result, the shape of the object returns to its original state.

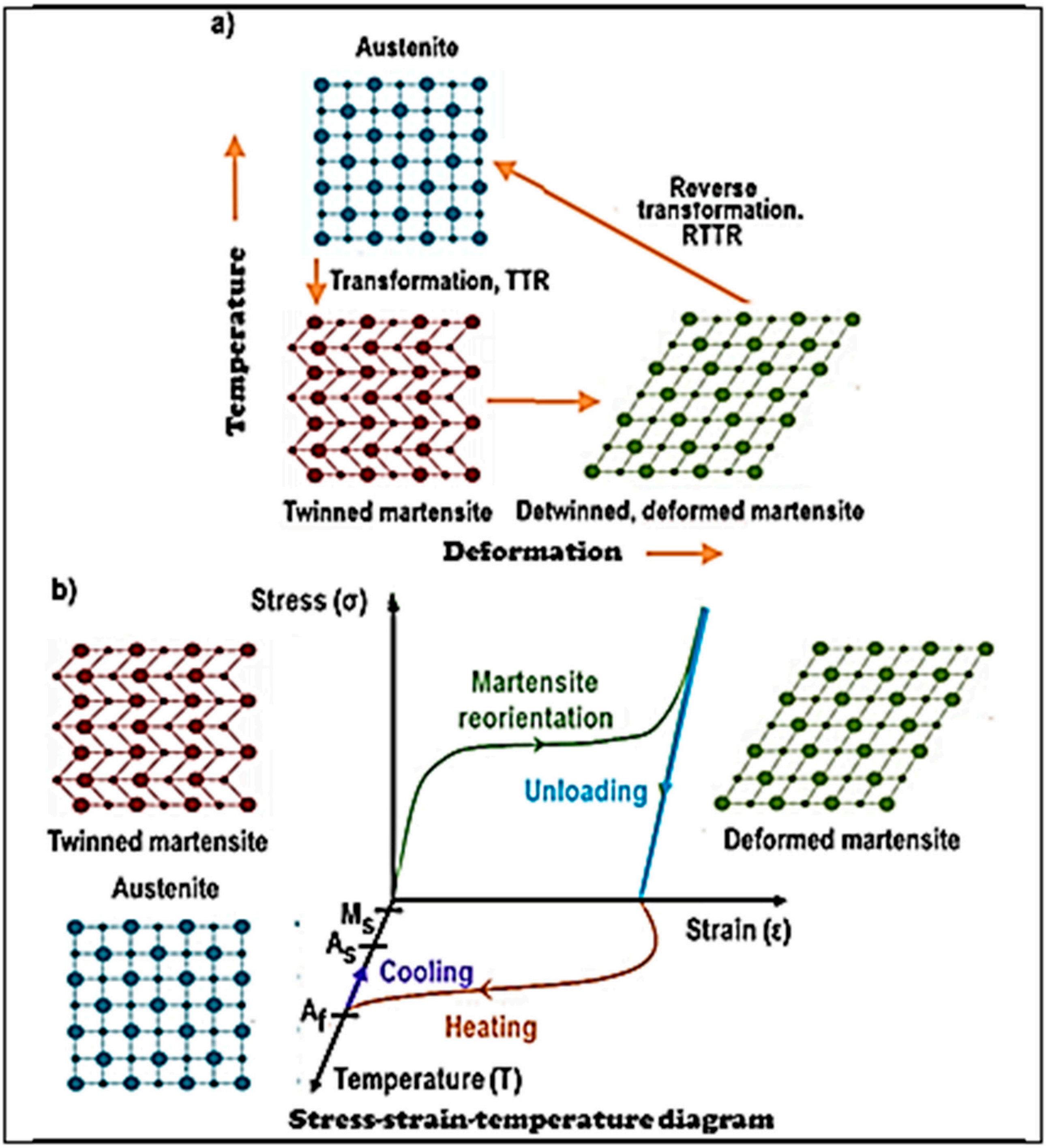

Figure 8. (**a**): The hysteresis loop of the martensitic transformation; (**b**): The dependence of the structure of nitinol alloys on changes in stress and strain.

The bidirectional shape memory effect of the alloy is based on the preservation of shape memory [44,81–84,179–181,289] of both the high-temperature parent phase and the low-temperature martensitic phase. As a result of the two-way shape memory effect, in the temperature range M_f-A_f, respectively, of the end of martensitic transformation and the end of austenite formation, changes occur cyclically, causing reversible changes in the shape of the object, without external stress. As the martensitic transformation usually results in the formation of martensite laths of different orientations during cooling, apart from a volume change, usually there is no macroscopic change in shape. The privileged orientation of martensite seeds limits the variants of the lath orientation, causing anisotropic, macroscopic changes in shape. The transformations causing shape changes may be repeated cyclically by cooling and heating, provided that during the reversible transformation into the parent phase or as a result of high-temperature annealing, the martensite nuclei are not removed [283].

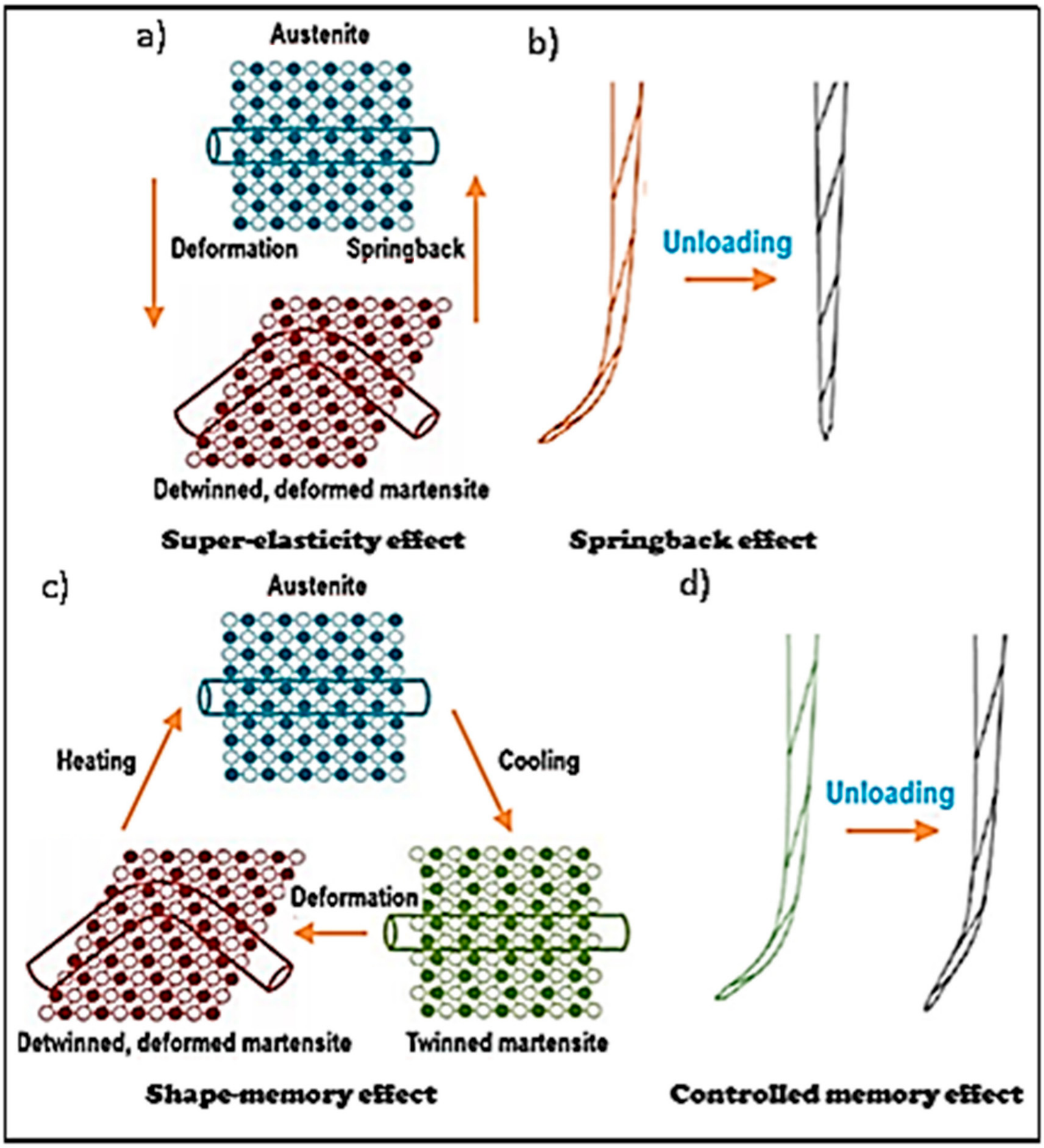

Figure 9. Schemes: (**a**): superelasticity effect; (**b**): springback effect; (**c**): shape-memory effect; (**d**): controlled memory effect.

The source of shape memory and superelasticity effects is thermoelasticity and reversible martensitic transformation in nearly stoichiometric Ni–Ti alloys, even if their composition differs relatively slightly from the stoichiometric one towards the advantage of nickel [297]. The properties of nitinol alloys significantly depend on the conditions of heat treatment [298,299] and the structure that arises as a result of technological processes, especially the refinement of the austenitic matrix grain [300,301], including as a result of drawing [302] or cold rolling [303], as well as high-pressure torsion (HPT) [304] and equal channel angular pressing (ECAP) [305]. The course of the dispersion precipitation processes of Ni_4Ti_3 [306–308] in austenite and the course of the martensitic transformation [308,309] are important.

The transformation according to the scheme B2 $\rightarrow$ B19′ takes place as one stage in almost stoichiometric Ni–Ti alloys [65], or with a relatively slight advantage of Ni [297], but in austenite with relatively large grains with a size of 6.6 to 21.7 μm [297]. It requires heating to a relatively high temperature of >800 °C, which results in grain growth, directly determining the uneven release of the metastable Ni_4Ti_3 phase [310]. Among the remedial methods counteracting this unfavorable influence, one can mention the modern technology of electric pulse treatment (EPT) [311–313]. Multiple heating in millisecond cycles, with appropriately selected frequency and time of the impulse, current density, especially peak current [313–315], provides the desired structure, causing diffusion of atoms, as well as generation and annihilation of dislocations [316–318] and plastic deformation processes [313,316,317]. The use of the annealing sequence, stretch–bending deformation (SBD), and electric pulse treatment (EPT) ensure obtaining the optimal grain size of the bound austenite, control of the release of the metastable Ni4Ti3 phase, and improvement of the martensitic transformation plateau [311], which was confirmed by the tests of the nitinol Ni50.8Ti49.2 alloy (at.%).

The annealing processes, stretch–bending deformation (SBD), and electric pulse treatment (EPT) proceed sequentially. They are associated with obtaining the optimal grain size of the bound austenite and the extraction of the metastable Ni_4Ti_3 phase. Stage I shows the coarse structure of B2 austenite, indicating the grain boundary zone and the grain interior zone. Annealing causes the precipitation of Ni_4Ti_3 phases near the grain boundaries and the depletion of nickel in these regions. On the other hand, in stage II, dislocations are generated as a result of the repeated SBD process, and their concentration and tangles occur in some places [319], and the size of austenite grains varies. Due to the combination of thermal and athermal effects, EPT causes homogenization and refinement of austenite grains from 9.1 μm after annealing to 5.4 μm as an effect of EPT. High pulse frequency EPT treatment reduces the recrystallization temperature of the NiTi alloy. Subsequent ageing at a relatively low temperature for a long time and an increase in the equivalent current density causes an increase in dispersion and fragmentation of the separated phases. The combination of the mentioned technological operations is an effective method of shaping the desired structure of nitinol alloys [311]. With the increase of the pulse frequency from 150 Hz to 400 Hz, a two-stage martensitic transformation B2 $\rightarrow$ R $\rightarrow$ B19′ takes place with the participation of the R phase. After ageing at 250 °C for 48 h, the sizes of Ni_4Ti_3 precipitations are in the range of 20–40 nm and show high dispersion in the matrix. The combination of SBD, EPT, and ageing processes affects the fragmentation of the structure and gives favorable effects in terms of properties. Figure 9a illustrates the evolution of the structure of this alloy as a result of various technological operations.

During cooling, the course of phase transformations is significantly influenced by precipitation processes in the austenitic matrix with the B2 network structure. When analyzing this problem, it should be noted that in Ti–Ni alloys with a predominance of Ni, there are two stable phases, TiNi and $TiNi_3$, according to the equilibrium system [186]. During ageing, the austenite of the B2 structure of nitinol alloys with a predominance of Ni concentration, on the other hand, emits dispersive precipitations of the metastable phases Ti_3Ni_4 and Ti_2Ni_3 [179,320,321]. The morphological features of these precipitations largely depend on the ageing conditions, both temperature and treatment time. The analysis of the time–temperature–transformations TTT diagram of the nitinol Ti48Ni52 alloy [320] shows that, e.g., as a result of isothermal annealing at the temperature of 600 °C, depending on the annealing time, the processes of separation of the mentioned phases take place in a sequence. Initially, after short annealing, the Ti_3Ni_4 phase is precipitated. After about 10 h, Ti_2Ni_3 is precipitated, while for the stable TiNi3 phase to precipitate, it is necessary to heat it for about 4650 h [320,322]. The sequence of precipitation processes in austenite with structure B2 systematically depleted in alloying elements under such conditions can therefore be written as follows [320]:

$$B2 \rightarrow Ti_3Ni_4 \rightarrow Ti_2Ni_3 \rightarrow TiNi_3$$

Alternatively, during adequately fast cooling from the homogenizing annealing temperature, e.g., in water, the sequence of changes B2 → R and R → B19′ [323–326] occurs. The transformation of B2 → R [290] into the R phase is also martensitic and takes place through sheer. It is also reversible and determines the shape memory and pseudoelasticity effects [327,328]. The R phase was discovered in 1965 [329], and its similarity to the Au–Cd equilibrium phase [330] suggests $P^{-}31m$ as a possible space group, which was confirmed in [331], but it was finally established that it is a structure P3 [332]. The differences between the two lattice structures are not significant but, in the case of the R phase, much smaller than in the Au–Cd alloy [332]. The essence of these differences concerns only the distance in the z-direction [191] (Figure 10c). The R phase is martensite, and it has been accepted to have a rhombohedral lattice structure, from which it is even named. The R phase designation used, however, does not correspond to its actual lattice structure because the R phase has a trigonal structure and should be marked as the T phase [179,191]. The transformation should be written according to the B2 → T scheme. However, it was decided to keep the traditional term R phase to avoid unnecessary confusion. The transformation of R → B19′ consists of reconstructing the martensite lattice [191], which was not realized before.

It is estimated that the formation of the R phase is favorable due to the properties and behavior of nitinol alloys [65,333]. The control of its course, especially the temperature range, is essential for a quick response to temperature changes [179,328,334–336] and considerable stability at cyclic changes in temperature and loads [165,336–339]; it causes a narrowing of the hysteresis loop [179,340], and most importantly, it increases the fatigue strength of nitinol [165,334,341]. While the mechanism of B2 → R transformation is known [179,191,342], the conditions for controlling its course still require research interest, especially in the scope of annealing temperature [343], as well as temperature [344] and ageing time [345], despite that the available literature data collection is quite extensive [65]. The factors favoring the activation of the B2 → R transformation include, among other things, annealing after plastic deformation [284,323,346] and ageing of alloys with a relatively small advantage of the atomic nickel concentration in the Ni–Ti nitinol alloys [297–299,342,347–350], as well as cyclic temperature changes [337,338,351,352] and stresses [353,354].

According to the scheme B2 → R [290], the martensitic transformation into the R phase usually results from the previous ageing associated with precipitating Ti_3Ni_4 phase particles in the B2 matrix [189]. The issues of Ni_4Ti_3 phase precipitation have been discussed in numerous publications [308,355–363].

The precipitation processes of Ni4Ti3 in the parent phase with the B2 structure, which determine the formation of the R phase, cause the precipitation hardening of the matrix according to the Orowan mechanism [299]. The boundaries of the Ti_3Ni_4 phase precipitations with the B2 matrix are coherent or semicoherent [364], which was also investigated in [365–367], mainly due to their importance for the course of the martensitic transformation [368–370] and the formation of the martensitic R phase [299]. The precipitations of Ti_3Ni_4 have an oval and disc-like shape and a rhombohedral lattice structure with the lattice parameter a = 0.670 nm and the apex angle $\alpha = 113.9°$ [189]. The habitus plane of the precipitations is parallel to the planes of the {111} B2 family matrix of the B2 austenite matrix [189]. The crystallographic relationships of M. Nishida's, C.M. Wayman's, R. Kainuma's, and T. Honma's between-phase B2 and these precipitations [371] are in the following two variants:

$$(1\bar{1}0)_{Ti_3Ni_4} // (\bar{3}21)_{B2};\ [111]_{Ti_3Ni_4} // [111]_{B2},$$

$$(1\bar{1}0)_{Ti_3Ni_4}//(\bar{3}12)_{B2};\ [111]_{Ti_3Ni_4}//[111]_{B2}.$$

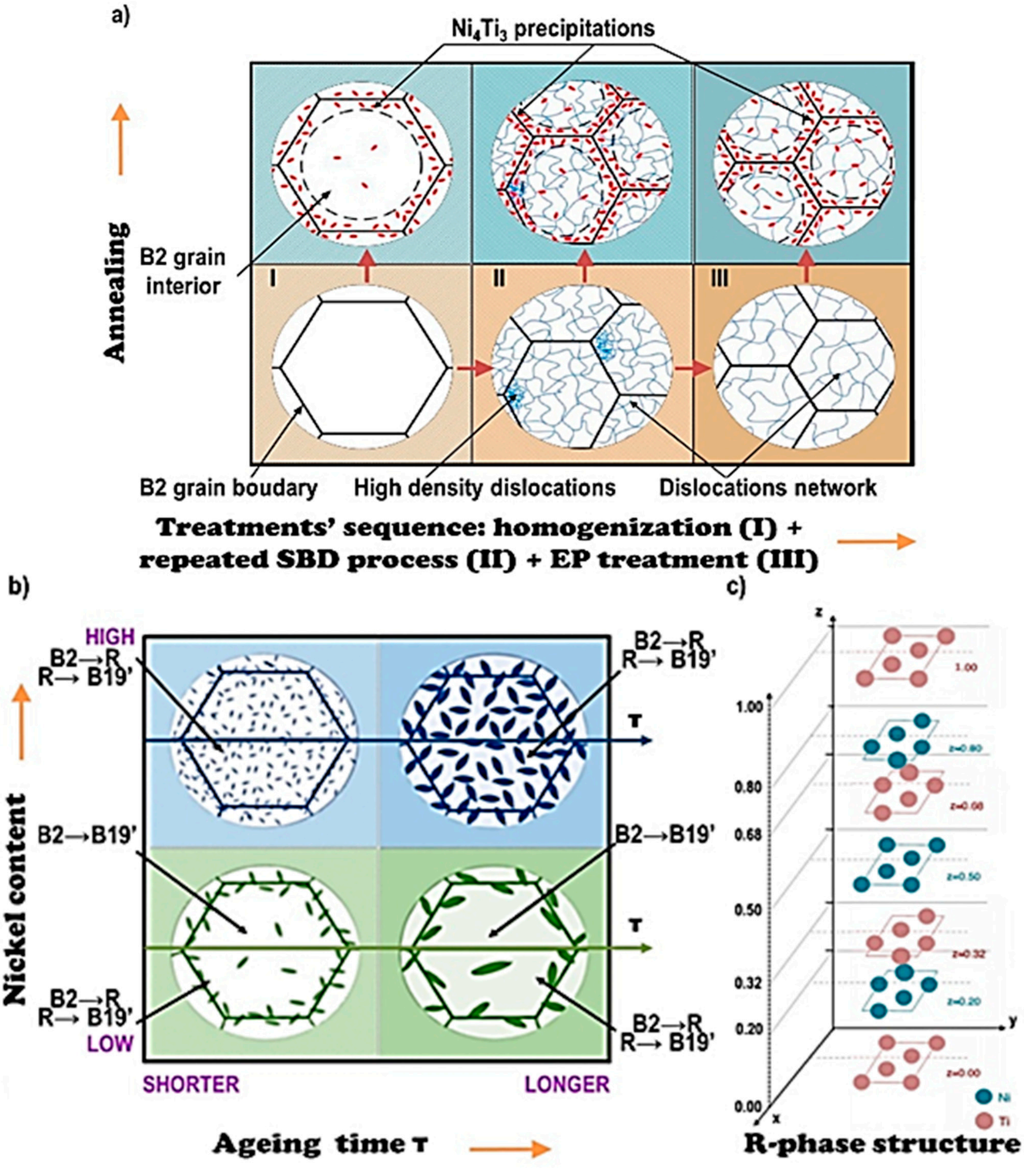

Figure 10. Schemes: (**a**): the annealing sequence, stretch–bending deformation (SBD), and electric pulse treatment (EPT) on obtaining the optimal grain size of the bound austenite and the extraction of the metastable Ni_4Ti_3 phase; (**b**): the influence of the nickel concentration of the annealing time on the precipitation processes of the metastable Ni_4Ti_3 phase and the course of transformations B2 → B19′ and B2 → R and R → B19′; (**c**): the crystallographic structure of R phase.

The processes of dispersion precipitation of the Ti3Ni4 phase and the state of internal stresses resulting from their coherence with the austenitic matrix of the B2 structure [372] have a critical influence on the course of the martensitic transformation [189]. The dispersion precipitation of this Ti_3Ni_4 phase occurs during ageing at a lower temperature and in a relatively short time near the grain boundaries of the B2 austenitic matrix [366,368]. The release of the Ti_3Ni_4 phase causes changes in the temperature of the beginning and end of the martensitic transformation M_s and M_f adequately [297,350]. The stresses around these precipitations strongly counteract the direct transformation of B2 → B19′ when their lack of significant reduction favors the transformation of B2 → R [373]. The growth of Ti3Ni4 precipitations with time influences the generation of dislocations with the Burgers (111) B2 and (200) B2 vectors that eliminate coherence stresses while maintaining coherence in other areas [372]. Such conditions favor the transformation of B2 → R during cooling [368–370].

The deformation related to the B2 → R transformation is small as it reaches 0.5–3% [165,328]. The transformation of B2 → R is activated, e.g., as a result of annealing after plastic deformation [284,323,346] and ageing of alloys with a predominance of nickel atomic concentration in Ni–Ti alloys [298,299,342,347–349], as well as a result of cyclic temperature changes [337,338,351,352]. The B2 → R transformation implies significant application possibilities, and the use of its advantages requires precise control of its course [297], especially the temperature range, as well as the suppression of the direct transformation into martensite B19′ according to the scheme B2 → B19′ [374]. The main application advantages of the B2 → R transformation related to its course include the already described increased fatigue strength [165,334,341], considerable stability under cyclic changes in temperature and loads [165,336–339], quick reaction to temperature changes [179,328,334–336], and a narrow hysteresis loop [179,340]. Although the above-described mechanism of the B2 → R transformation is now well recognized [179,191,342], the information on how to control the temperature of this transformation, associated with the annealing temperature [343] and the temperature [344] and ageing time [345], is still incomplete. If the R phase is formed, it is still possible to form B19′ martensite, but this requires even greater supercooling [297]. After the B2 → R transformation, in these conditions, a direct transformation of B2 → B19′ [372] takes place. The consequence of the B2 → R transformation is the course of the two-stage B2 → R → B19′ transformation [297,373,375,376], involving the R phase [297,375], but initiated by the precipitation processes of the Ti3Ni4 phase. The transformation of R → B19′ consists of reconstructing the martensite lattice [191], which was previously not present, and the view that in each stage of transformation B2 → R → B19′ the martensitic transformation takes place sequentially is not true. According to the B2 → R → B19′ mechanism, the transformation is two-stage when the grain is fine, and its size is ≤5.6 μm. However, it should be noted that the grinding of grains after cold plastic deformation increases the probability of obtaining nonuniform austenite grains in terms of size, and this, in turn, may cause a weakening of the stress-induced martensitic transformation plateau [377]. The transformation of B2 → R → B19′ can only take place in polycrystals [297], regardless of the nickel concentration [297], and also with the predominance of the atomic concentration of titanium [378] and cannot take place in monocrystals.

It was shown in work [297] that in one part made of the nitinol alloy, the direct B2 → B19′ transformation and the two-stage B2 → R → B19′ transformation can occur in parallel. The differentiation of the nickel concentration at the grain boundaries and inside the Ni–Ti alloys associated with the differentiation of the intensity of successive growth and coagulation of Ti_3Ni4 phase particles at the grain boundaries associated with the local decrease in nickel concentration (Figure 10b) [297] as the ageing time lengthens, causes the course of the two-stage B2 transformation → R → B19′ [297]. Inside the grains with a relatively higher concentration of nickel in the alloy [297], the direct transformation B2 → B19′ [297] takes place. It is related to the explanation of the essence of this phenomenon only in the first decade of this century [297], despite the long-standing information about a three-stage martensitic transformation in aged Ni-enriched polycrystalline Ni–Ti alloys, as opposed to alloys with a stoichiometric composition [348,373,379–390]. No new type of martensite has been diffractionally confirmed to be induced by such a conversion. The abnormal multistage martensitic transformation in aged Ni–Ti alloys, as revealed by the presence of three peaks on the differential scanning calorimeter DSC curves during the two-step conversion [297], was explained by testing two alloys with different atomic nickel concentrations of 50.6 and 51.5%. As described, the cause of this phenomenon is the differentiation of nickel concentration at the boundaries and inside the grains of

Ni–Ti alloys and the resulting heat flow effects on the temperature axis. Therefore, in the border areas of grains, a two-stage transformation takes place according to the scheme B2 → R → B19′, while inside the grains, a direct transformation takes place according to the scheme B2 → B19′, as a result of which the DSC curves noticed not a pair, but a larger number of peaks, apparently indicating how it was thought before: the three stages of change. With the higher nickel concentration among the test, there are conditions for the homogeneous separation of Ti_3Ni_4 phase particles during ageing in the volume of the entire grains, and with a relatively longer ageing time, the growth and coagulation processes of the precipitations also take place. It is the reason for the normal one-step transformation of B2 → B19′ [297].

A crystallographic relationship of R. Kainuma's, M. Matsumoto's, and T. Honma's was found between martensite B19′ and the other phases confirmed on the stereographic projection [366], given below:

$$[\bar{1}01]_{B19'}//[111]_R//[111]_{Ti_3Ni_4}//[111]_{B2}.$$

The significant stress field generated in this way enables a two-variant course of the directly or two-stage transformation [365,366] associated with increasing the temperature of the R phase transformation [368]. The necessary condition to ensure the course of the B2 → R transformation is the damping of the direct transformation according to the scheme B2 → B19′ [374]. The opposite is the case with the precipitation of coarse-grained precipitations of the Ti_3Ni_4 phase, which has little effect on the formation of the R phase in the absence of coherence. Therefore, the growth and coagulation of Ti3Ni4 precipitations and the related loss of coherence favor the direct transformation B2 → B19′ [189,391,392]. Therefore, with the extension of the ageing time and the increase in the ageing temperature, the precipitation hardening mechanism by Ti_3Ni_4 phases is less effective [299], which reduces the hardness [299]. Under such conditions, the proportion of Ni_4Ti_3 decreases, or this phase decomposes into a mixture of Ni_3Ti_2 and Ni_3Ti [393]. The distinctive parabolic character of hardness changes with the extension of the annealing time is related to the ageing effect [299]. Under these conditions, nitinol exhibits only a one-sided shape memory effect [372].

During reheating, the B19′→ R conversion takes place in a relatively short time. In contrast, after lengthening the time, the direct formation of austenite B19′ → B2 dominates, and most probably R → B2, because the differential scanning calorimeter DSC peaks corresponding to both coincide transformations of B19 ′→ B2 and R → B2 [345].

5. The Importance of Heat Treatment and Other Technological Processes of Shaping the Structure and Properties of Nitinol Alloys Used in the Production of Endodontic Tools

This chapter presents numerous examples of detailed information taken from the literature on applying various structure-shaping processes in technological operations of heat, thermomechanical, and surface treatment aimed at changing functional properties. Tests of various materials' mechanical properties are often carried out, especially products manufactured by different manufacturers, but without properly documented dependence of these properties on the state of the structure and chemical and phase composition of the materials from which endodontic instruments were made. As a result, many of the works cited in this chapter take a piecemeal approach. In many of the cited publications, there is no proper material science interpretation of the properties of various endodontic tools tested for mechanical properties, including fatigue. Products of different companies with well-known brand names are often compared without knowing the exact chemical composition and without researching the structure, or only with a very rough estimation of it. Usually, there is no analysis of the share of nonmetallic inclusions and no knowledge of the exact technological history of the tested element. Simplified tests of mechanical and fatigue properties are often performed in workshop conditions simulating real working conditions.

Nevertheless, despite these obvious methodological flaws in many of these works, the results obtained, as a rule by authors directly or indirectly related to dental practice and not to material science research, may have some practical significance. Despite many reported results, it is very difficult to generalize them, because in general, no attempts were made to plan the experiments statistically. These results are, therefore, mainly of the so-called swift trying. In this chapter, therefore, an effort has been made to provide the correct interpretation of the observed regularities with the use of this numerous residual information, often taken from the mentioned sources, and the essence of phase changes and structural phenomena described in detail in Section 4 of this paper. However, this information is missing in the most frequently quoted literature sources. The interpretation mentioned above is the contribution of the authors of this paper to the organization of the complex material science knowledge concerning endodontic tools etched from nickel–titanium alloys of the nitinol type.

Endodontic tools made of nitinol alloys, similar to all other metal materials, to be practically available for any practical application, require technological processes of shaping their structure and properties [146–148,162]. Regardless of the material manufacturing processes and the processes shaping their geometric features, these processes include conventional heat treatment and thermomechanical treatment and surface treatment processes. At the turn of the first and second decades of the current 21st century, several new technological solutions were implemented, which increased producers' offer of nitinol alloys and endodontic tools made of them and improved their functional properties. The essence of the actions taken in this respect is the differentiation of the phase composition of the matrix of nitinol alloys, starting from austenitic B2 through mixtures of austenite, martensite, and R phase B2 + B19′ + R, with a different proportion of individual phases or without the participation of some of them, as noted in this chapter. It shapes the differentiated transformation temperature range (TTR) of the initiation and the end of individual phases, i.e., A_s, A_f, M_s, M_f, R_s, R_f, respectively. The structure of nitinol subjected to various shaping processes may also include the dispersion of the metastable phases Ti_3Ni_4 and Ti_2Ni_3 [179,320,321]. All these issues are described in detail in Section 4. Due to the significant differentiation in hardness and plastic properties of individual phases, especially austenite, martensite, and R phase, it is possible to differentiate the properties of endodontic tools, especially their fatigue life and suitability for the preparation of curved root canals without excessive risk of iatrogenic errors related to instrument fracture inside the root canal. Hitherto known technological solutions in this field are described in detail in the further part of this chapter.

Annealing is a commonly used technological operation of the heat treatment of nitinol alloys. In order to investigate the significance of annealing, the Ni54.5Ti45.5 alloy (wt.%) was tested in static tensile tests [284] under standard conditions under ASTM E8M-91 [394] after annealing at 400, 600, and 800 °C for 30 and 45 min, followed by cooling in water to room temperature. DSC methods found that only one-stage transformation B2 → B19′ [284] takes place in this case. The intensity of the transformation is greater at the annealing temperature of 600 and 800 °C than in the as-received state and after annealing at 400 °C, which results from the field of internal stresses, point defects, and deformations generated in plastic working processes during the production of Ni–Ti bars [286]. On the other hand, increasing the annealing temperature above the recrystallization temperature makes the defects mentioned above of the crystal structure disappear, but grain growth and precipitation processes occur [287,288]. Local stresses related to these coherent and semicoherent precipitations increase the M_s temperature after annealing during the martensitic transformation [286]. The A_s and A_f temperatures also increases, while the M_f temperature decreases [284]. The flow stress during static tension and the shape of the tension curves depend on the annealing temperature (Figure 11a). Immediately in the delivered condition, after plastic deformation after annealing at 400 °C, the proportion of plastic deformation is insignificant, and the elongation slightly exceeds 14%. After annealing at 600, 800, and 900 °C, the elongation is at least 45%, even 60%. In the first stage, the stress increases linearly due to the elastic deformation of martensite. In the second stage, a stress plateau occurs despite an increase in strain, after a slight decrease in stress, resulting from the initial blocking of the B19′ martensite reorientation [395] and subsequent martensite detwinning [396,397]. In the third stage, there is a significant increase in detwinning processes in martensite B19′, and a significant increase in stress and elongation [284], generation of dislocations [398], and reorientation of martensite B19′ [398,399] continues. The last stage is characterized by plastic deformation of nitinol with intensified dislocation slip [284]. The dislocations generated influence the immobilization of the twin boundaries in martensite B19′ [400], although the link with the detwinning mechanism is difficult to demonstrate [401].

Cyclic temperature changes have a significant influence on the structure of nitinol alloys. Properly prepared samples from the Ni50.5Ti49.5 (at.%) alloy with a temperature of M_s and A_f, respectively approx. 1 °C and 23 °C, were subjected to thermal cycles, starting from room temperature (RT), followed by immersion in liquid nitrogen (LN), and then in boiling water (BW) according to the scheme of each cycle RT → LN → BW → RT [337]. By DSC with an interpretation under ASTM 2004-05 [197], it was found that the temperature of M_s and M_f and A_s and A_f respectively decreased with an increase in the number of heat cycles, although the temperature of A_s and A_f decreased at a much slower rate (Figure 11b) [337]. The temperature range of $M_s - M_f$ is around 4.5 °C in the first two cycles and stabilizes at 5.5 °C in the following cycles. The temperature range A_s and A_f of the austenite transformation also decreases with increasing the number of thermal cycles from about 6.5 °C after one cycle to about 3 °C. With an increase in the number of cycles, the B2 → R transformation occurs, and the temperature Rs and Rf increases strongly by ~21 °C and ~16 °C, respectively, after 100 cycles. Therefore, the peak width for the R phase increases from 6.6 K after the fourth cycle to 15.7 K after 100 cycles [337].

The thermodynamic treatment of thermoelastic martensite [402–406] emphasized the importance of the change of the free elastic energy accompanying the transformation and the frictional work required for propagation between the martensite–parent phase during transformation. As the number of thermal cycles increases, the temperature M_s decreases faster than the temperature A_s, which causes the friction work ΔE^{a-m} to increase almost logarithmically with the increasing number of cycles. ΔE^{a-m} is calculated based on the width of the hysteresis loop of the transformation B2 → B19′, where the indices (a–m) refer to the transformation in the direction of B2 → B19′ austenite into martensite. The increase in ΔE^{a-m} results from the domination of the friction energy Δ Ef, determined by the density of dislocations counteracting the migration of the martensite interface and the increase in the friction energy by two orders of magnitude. Along with the increase in the number of cycles, there is an almost logarithmic increase in the reversible elastic energy $\Delta E^{a-m\ eo}$, related to the initial nucleation of martensite at the M_s temperature [402–405]. The stored elastic energy $\Delta E^{a-m\ eo}$ is estimated on the basis of the measurements of the temperature M_s and M_f [402,403,407].

The heat treatment temperature is an important factor influencing the properties of nitinol alloys. Ni 50.7Ti 49.3 (at.%) alloy was aged at temperature of 300, 350, 400, 450, 500, and 550 °C for 2, 10, 20, 30, 60, 120, and 180 min, followed by air cooling [349]. It is accompanied by the precipitation of the Ti_3Ni_4 phase influencing the M_s and M_f phase transition temperatures and the associated stress levels, as shown in Figure 11c [297,350]. Ageing in the range of 300–500 °C systematically reduces the temperature of the upper and lower plateau of the hysteresis loop—ageing at 550 °C results in an initial stress reduction that quickly decreases as the ageing time increases. Ageing at 500 and 550 °C for 120 and 180 min significantly increases the residual deformation of the permanent set.

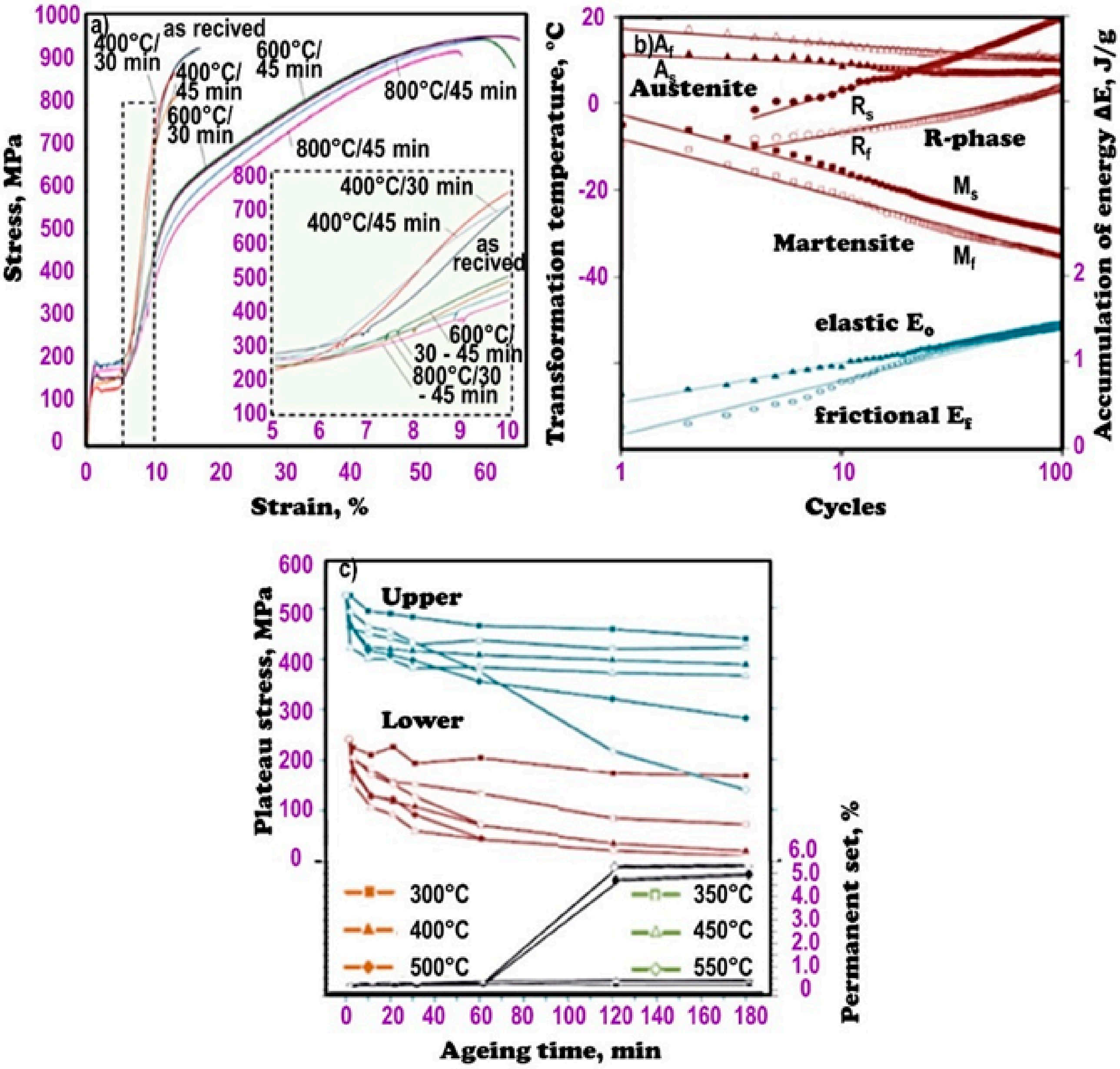

Figure 11. Schemes: (**a**): he influence of annealing conditions on the form of the tensile curves of the nitinol alloy; (**b**): the influence of cyclic temperature changes on the characteristic temperature of the beginning and end of the martensitic transformation, the formation of the R phase and the reverse martensitic transformation, and the change of the free energy of elasticity accompanying the transformation; (**c**): the influence of ageing time and temperature on the stress plateau range of the hysteresis loop of the martensitic transformation and increasing the residual permanent set deformation.

The tests of the Ni55Ti45 alloy (wt.%) were performed after aging at the temperature of 500 °C in the range from 10 min to 5 h using the DSC method [298]. During cooling, the transformation of austenite into the R phase B2 → R and the R phase into martensite R → B19′ [323–326] was identified. During heating, the inverse conversion of B19′→ R occurs sequentially after ageing for 30 min or less and after ageing for more than 40 min, which indicates that most martensite is formed by the transformation of B19′ → B2 directly into austenite, although R → B2 cannot be excluded as the peak corresponding to this transformation may be hidden inside the main peak [345]. At the beginning and end of the phase transformation, the temperatures increase with the ageing time (Figure 12a). It was found to be related to an increase in the volume fraction of Ni_4Ti_3 precipitations in the parent phase [298]. The precipitation effects during ageing have a very significant influence on the mechanical properties of nitinol alloys. Several nitinol alloys with the following composition Ni58Ti42, Ni57Ti43, Ni56Ti44, Ni55Ti45, Ni54Ti46, and Ni53Ti47, (at.%) [299], cast and remelted several times under argon atmosphere, were tested, which were then homogenized in vacuum at 1050 °C for 24 h and cooled in the furnace to be hot rolled, followed by annealing at ~980 °C for 150 min and cooling in quench oil. They were again annealed by soaking at 1050 °C for 10 h with cooling in water. Then, the ageing was performed at 400, 625, and 750 °C for various times, from 10 min to 200 h. In any case, where the ageing time is greater than 24 h, the specimens were wrapped with a tantalum foil and treated under an argon atmosphere to eliminate oxidation. After cooling with the furnace, coarse-grained, stable, and metastable precipitations of nickel-rich phases were formed, resulting in the alloy's low hardness [393]. Water cooling of the Ni57Ti43, Ni56Ti44, and Ni55Ti45 alloys causes the precipitation of Ni_4Ti_3 in the matrix with the B2 structure, decisive for obtaining the maximum hardness in the range of 634–649 VHN, respectively [299] (Figure 12b,c), by precipitation hardening according to the Orowan mechanism. The hardness is significantly reduced [299] as the volume fraction of the metastable Ni_4Ti_3 phase decreases, and when it decomposes into larger Ni_3Ti_2 and Ni_3Ti particles at higher ageing temperatures when cooling with the furnace is slower [393]. The ageing of Ni54Ti46, and Ni53Ti47 alloys at the temperature of 400 °C, for several hours shows a characteristic parabolic character of changes in hardness (Figure 12b), while alloys with a higher concentration of Ni do not show significant changes in hardness as the ageing time is extended to at least 100 h. In the Ni58Ti42, Ni57Ti43, and Ni56Ti44 alloys, along with the increase in Ni concentration in the alloy, as well as the temperature and ageing time, the Ni_4Ti_3 phase precipitates quickly decompose into coarse Ni_3Ti_2 and/or Ni_3Ti phases, which causes a significant reduction in hardness (Figure 12c).

Phase transitions accompanying temperature changes and deformations presented in Figure 10 constitute the basis for using endodontic tools in heat treatment. Nitinol alloys with B2 austenitic structure make it possible to use the superelasticity effect only due to changing the stress state and even without changing the temperature [408]. Stress-induced martensite (SIM) transformation ensures the formation of a martensitic structure according to the scheme B2 $\rightarrow$ B19′, described in detail in Section 4 of this paper. It may take place, for example, when inserting an endodontic tool into a curved root canal, and it allows to increase the maximum deformation by up to 8% [120] and to lower the elastic modulus without increasing the stress compared to corrosion-resistant steels [134]. As a result, the flexibility of Ni–Ti endodontic tools is also increased [134]. Withdrawal of the tool from the curved root canal and the associated reduction of the stress level causes the reverse transformation of the structure of the nitinol alloy according to the B19′$\rightarrow$ B2 martensite scheme into the austenitic phase and the restoration of the original shape of the tool. It is accompanied by a transformation of twin martensite into deformed one, defined as martensite reorientation MR. The mechanism of the relevant phase transformations has been described previously. The described changes related to the shape memory effect of SME and the martensite reorientation MR temporarily occur in nitinol alloys under the influence of external factors, while the permanent achievement of the B19′ martensitic structure by endodontic tools is of fundamental importance. The martensitic structure undergoes reverse transformation according to the B19′$\rightarrow$ B2 scheme into austenite, showing the shape memory effect during heating (e.g., autoclaving) by returning to its original shape, which is described in detail in Section 4 of this paper. The properties of nitinol with the martensitic structure B19′, i.e., lower hardness and greater plastic properties than those characteristic for the austenitic structure B2 [291–296], ensure increased fatigue life and fracture toughness [409,410]. It was also confirmed that the two-phase austenitic–martensitic structure B2 + B19′ provides better fatigue life than the single-phase austenitic structure of nitinol B2, regardless of the previously indicated methods of increasing the martensitic transformation temperature according to the scheme B2 → B19′ (Figure 9) by alloying additives [42] and the applied technological processes [43,81–84,179–181,289].

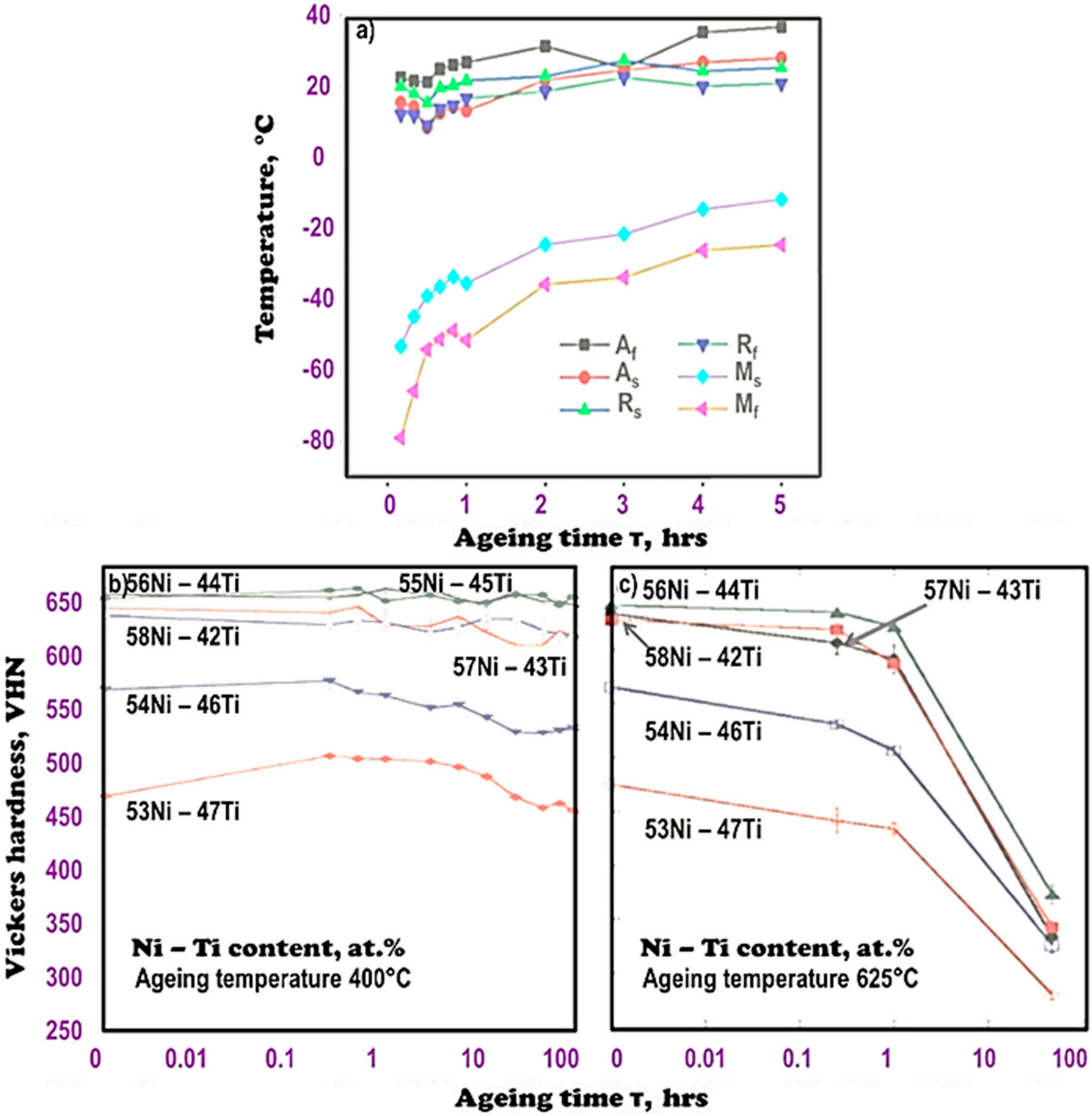

Figure 12. The influence of ageing time on (**a**): the temperature of the beginning and end of phase transformations of martensite formation, R phase, and austenite in reverse martensitic transformation in the Ni55Ti45 alloy (wt.%); (**b**,**c**) changes in the hardness of Ni58Ti42, Ni57Ti43, Ni56Ti44, Ni55Ti45, Ni54Ti46, and Ni53Ti47 alloys (at.%); (**c**) at a temperature of (**b**) 400 °C, (**c**) 625 °C.

Marketing activities are also accompanied by improvements or only changes in technological processes concerning tools made of nitinol alloys. Undoubtedly, a manifestation of such activities is the implementation of gold and blue heat-treated tools. In 2011, Dentsply Tulsa Dental (Tulsa, OK, USA) developed the ProFile Vortex Blue and ProTaper Gold rotary endodontic tools and the Reciproc Blue, VDW, and WaveOne Gold reciprocating endodontics [411]. Said tools after manufacture are then subjected to complementary post-production heat treatment [412,413]. The thin surface layer of titanium oxide produces a distinctive surface contrast of blue color [414]. In the so-called gold heat-treated endodontic instruments, the surface layer is also responsible for the characteristic color [415]. After such heat treatment, the nitinol matrix is predominantly the R phase or B19′ martensite, whereby the alloy is more flexible [413] and has significantly improved fatigue life [416–418], conventionally treated nitinol with austenitic B2 matrix.

Heat treatment of nitinol is, therefore, one of the methods of improving the mechanical properties of nitinol, by regulating its transformation temperature and controlling its structure by cooling in the critical transformation temperature range (TTR) between the temperature of the beginning and end of the transformation of austenite into martensite B19′ and the R phase, respectively [412]. For example, the temperature A_f = 38.5 °C of austenite in the case of nitinol Vortex Blue is close to the temperature of the human body, while the temperature M_s = approx. 31 °C, and therefore it is lower than this temperature [419]. Due to the high proportion of soft and malleable martensite B19′, heat-treated blue endodontic instruments show lower surface hardness than other nitinol tools [420,421]. The so-called gold endodontic instruments subjected to post-production heat treatment reduce the technological defects of heat treatment [415,422,423] and have a temperature of A_f = about 50 °C; therefore, at the temperature of the oral cavity, their structure consists mainly of martensite B19′ and/or phase R [415]. The desirable structure of nitinol so shaped provides greater flexibility and fatigue life than untreated nitinol alloys [415,422,423]. Due to the martensitic structure of B19′ and/or R, respectively, all the so-called heat-treated gold and blue endodontic tools exhibit increased flexibility and fatigue life compared to other nitinol instruments [157,274,415,417,418,420,421,423–431]. However, blue and gold endodontic tools are inferior in terms of fatigue life to tools subjected to EDM processes [274,432]. The torque, however, remains greater in this case, even though the maximum twist-break angle was smaller [274].

All of these heat-treated endodontic tools ensure good centering when preparing even strongly curved root canals [433–437]. The so-called gold and blue endodontic tools are more effective in lateral root canal preparation [438], due to the relatively harder surface layer after post-production heat treatment, which can compensate for even the lower hardness of the martensitic substrate B19″ and/or R or B19′ + R, respectively [421]. Recently, even newer TruNatomy endodontic instrument systems (TRN, Dentsply Sirona) have been developed, employing post-production heat treatment [412]. According to the manufacturer, they show greater flexibility and effective shaping while removing the dentin itself where clinically required [439,440].

A very similar structural concept to the so-called gold and blue endodontic instruments are demonstrated by the MaxWire technology (Martensite–Austenite-electropolish-fileX) by FKG Dentaire [441]. Thanks to thermomechanical treatment, the structure of martensite B19′ at room temperature is obtained, which undergoes reverse transformation according to the B19′ → B2 scheme into the austenitic phase, which restores the original curved shape of the tool under the influence of intracanal temperature. Therefore, these tools show a shape memory effect after insertion into the root canal and, during production, superelasticity. The curved shape of the tools produced in this way makes it possible to develop a curved root canal.

The use of thermomechanical treatment for nitinol, first used in 2007 by Sportswire LLC (Langley, OK, USA) to the so-called M-Wire bars [135,442] containing 55.8 ± 1.5 wt.% Ni, 44.2 ± 1.5% Ti and <1 wt.% trace elements [443]. This alloy is characterized by a higher temperature A_f = 43–50 °C than in the case of conventional nitinol [278,416,444–446], which results, at human body temperature, in the structure B2 + B19′+ R of the austenite mixture with a relatively small share of martensite and R phases [278,444,446]. This phase composition provides a superelastic state [447] and increased flexibility compared to conventional nitinol [278,421,448,449]. In the case of nitinol subjected to the mentioned thermomechanical treatment, there is a reduction in initial elastic modulus compared to conventional nitinol due to the stress-plateau occurring due to stress-induced martensite (SIM) transformation [278,448]. The induction of B19′ martensite transformation requires less stress than conventional nitinol [278,448]. Nitinol produced by the mentioned technology is also characterized by better fatigue life than conventionally produced [163,445,447,448,450,451], with increased resistance to fatigue crack initiation [163] and torsional strength comparable to conventionally produced alloys [163,447,452].

A similar structure of the B2 + B19′ + R mixture of austenite and martensite with a relatively small proportion of the R phase at room temperature is shown by CM Wire [273,416,453], which was introduced in 2010. The structure of unused Hyflex CM tools provides a temperature of A_f = 32–37 °C, and after use, it rises to A_f = 54–61 °C, when the intracanal temperature is lower, i.e., 47–55 °C [273,416,453]. The temperature of M_s, A_s, and A_f for unused CM Wire tools is lower than for tools made with EDM technology, which is a consequence of different phase structures [273]. In the case of nitinol produced by the EDM method, the structure of nitinol is a mixture of martensite with a significant share of the R phase, i.e., B19′ + R [268,273]. In this case, the lack of austenite B2 at room or body temperature is related to the temperature A_s = 42 °C [273,416]. In the structure of nitinol produced by the EDM method, the precipitation of the Ti3Ni4 phase was also found [273] as an ageing effect of the austenitic matrix accelerating the martensitic transformation according to the B2 → R scheme, which is described in Section 4 of this paper, e.g., in work [179]. In the case of CM Wire, the temperature As = 21 °C [273,453], therefore the structure is a mixture of austenite and martensite B2 + B19′ [273]. CM Wire shows no superelasticity at both room temperature and oral temperature [454]. As a result, endodontic tools produced in this way do not straighten during the preparation of curved root canals [455–457]. In many cases, in clinical practice, the reduction in the transport of dentine removed from the root canal wall was not confirmed compared to other nitinol endodontic tools [455–459], despite the improvement in this respect indicated by the manufacturer [460]. Hyflex CM tools are also characterized by increased cutting efficiency, especially inside action [461,462]. Due to the reduction of the martensite reorientation MR temperature, the SIM mechanism requires less critical stress [454], which directly justifies the increased flexibility of CM Wire concerning other nitinol tools [160,413,463–467], as well as increased fatigue life [157,463,465,468–470]. There was no significant effect on the maximum torque, but the twist angle leading to the scrap was greater [471–473].

Further search for an improvement in fatigue life [159,442,451,474–482] and an increase in endodontic tools' flexibility compared to conventional non-heat-treated nitinol tools [483–487]. They were led to the development in 2008 by the company SybronEndo (Orange, CA, USA) of the production process of the so-called twisted file TF. The TF process involves heat treatment to obtain the R phase structure by twisting the raw wire with a B2 austenitic structure in the required temperature range with controlled cooling, ensuring the stabilization of the R phase according to the B2 → R scheme, which is described in detail in Section 4 of this paper and the subsequent surface conditioning of this wire [451]. Nitinol with the R phase structure shows a lower shear strength modulus, and the deformation required for the transformation into the R phase according to the scheme B2 → R is about ten times smaller than that corresponding to the transformation into martensite B19′ according to the scheme B2 → B19′ [488,489]. It is technologically advantageous as it requires much less stress to induce the transformation to R phase according to scheme B2 → R [484]. In the TF process, after twisting, the reverse transformation of the R phase into austenite occurs according to the R → B2 scheme, which requires controlled methods of lowering the temperature [484]. Subsequent modifications of this approach to obtain the R phase according to the B2 → R scheme include the TF adaptive process similar to TF, also marked as TFA, also by SybronEndo, as well as another, marked as K3XF, in which the tools are produced by grinding nitinol with austenitic structure B2, and only subsequent heat treatment allows them to obtain the R phase structure according to the scheme B2 → R [135]. Formation of stress-induced martensite SIM requires less stress for significant advancement of the course of the transformation according to the B2 → R scheme [490]. In the case of TF technology tools, the stress-plateau occurring due to SIM transformation and martensite reorientation MR are reduced, as mentioned in Section 4 of this paper. The stress hysteresis loop is narrowed compared to conventionally processed nitinol [484,485]. The described structural mechanisms, inherent in the essence of the TF technological process, have a close impact on the functional properties of endodontic tools, thanks to the increased flexibility, allowing dentists to center the tool during the preparation of the root canal and reduce the transport of the dentine removed from the root canal wall and the risk of pushing the remains of pulp and cut canal dentine beyond the apical hole compared to when using conventional rotary tools made of nitinol [491–494]. On the other hand, nitinol tools produced in the TFA process allow the dentist to adapt the tool during the preparation of the root canal, being a superposition of rotational and/or reciprocating movement depending on intracanal torsional forces [135]. Because in the discussed cases, when the structure of the tool is the R phase, temperature A_f = 18–25 °C [416,484,485,495] under working conditions in the oral cavity, they show the structure of superelastic austenite as a result of the reverse transformation of the R phase into austenite under these conditions according to the scheme R $\rightarrow$ B2 [484]. All details regarding the sequence of such structural changes to nitinol are explained in Section 4 of this paper. The fatigue life of nitinol tools with the R phase structure is similar to that exhibited by tools made with the use of thermomechanical treatment in the M-Wire process [474,496], while the maximum torque is reduced, with a greater twist angle to scrap compared to M-Wire and conventionally-made Ni–Ti nitinol tools [471,483,497,498].

6. The Influence of Sterilization on the Possibility of Using Nitinol Endodontic Tools

An important factor determining the effectiveness of the dentist's work in the performance of endodontic procedures and the suitability of tools for this work in subsequent procedures are the phenomena occurring in the tools during sterilization in the dentist's office, necessary due to the maintenance of obvious sanitary and epidemiological conditions [137,499–501]. While all the aforementioned structural phenomena described in the previous chapters and the previously cited works [137,499–501] are related to the manufacturing of the material, and the manufacturing of tools, and the dentist receives ready tools in the same condition as provided by the manufacturer, his decisions have a direct impact on the phenomena occurring in tools during sterilization in their clinic. General guidelines in this regard are given in [502–507]. At the same time, in [139], the so-called systematic review, which, as stated earlier, does not provide valuable substantive information on this issue, despite using a very avant-garde approach to developing the collected information. For this reason, these issues are discussed a bit more in this chapter.

The sterilization of endodontic tools made of nitinol alloys has been analyzed in numerous publications [137,471,475,499–501,508–542]. A very important issue for solving this problem is the selection of an appropriate research methodology, which consists of measuring the cutting efficiency [513] with the use of linear "push and pull" movement [514,516], rotational movement concerning the long axis of the tool [513,515], and also with irrigation [511,512]. Acting as the processed material simulating clinical conditions, is the dentin of extracted natural human [516,518] or bovine [517] teeth and bovine bones [514,515,517], as well as blocks of polymeric materials [511], phenolic resin [512], and poly (methyl) methacrylate PMMA [510,513] with cylindrical canals symbolizing curved root canals [499,508,510,513]. Surface changes of tools were observed after cutting tests with the SEM scanning electron microscope [519,520,523,524] and atomic force microscope [521,522].

In general, it can be concluded that tools made of nitinol alloys show lower cutting efficiency [510], and, at the same time, greater flexibility than those made of other metal materials, including corrosion-resistant steels [499]. When corrosion-resistant steel is used for endodontic tools, sterilization processes do not have a significant effect [511,512], although it is not confirmed by the work results [502], which makes this statement ambiguous. Compared to conventional tools made of corrosion-resistant steel, it was unequivocally found that sterilization influences a significant decrease in cutting ability and efficiency [499,508,509]. Table 4 compares, for example, the results of the assessment of cutting efficiency using tools made of corrosion-resistant steels and nitinol alloys subjected to sterilization under various conditions.

An original experimental technique was developed that simulated clinical conditions [513] to measure the impact of sterilization impact assessment. This method is based on the assessment of the effectiveness of cutting tools on their full working length of 16 mm in properly profiled poly (methyl) methacrylate PMMA plates with a hardness of 33 VHN inclined to follow the taper of 2% of the tools. Four series of 25 cuts were made with each tool, and each cut was made on a new flat, smooth surface of the PMMA plate. Prior to each cut, water was irrigated at 85 mL/s. A quarter-turn clockwise rotation was made, followed by a 16 mm/s pull action at 16 mm/s. The constant load was 325 g. The cutting efficiency was determined by measuring the weight of the cut PMMA plate with an accuracy of 3×10^{-5} g for the unit of energy used during cutting in Mg/J. The research allowed for the formulation of a ranking of various tools from different materials [513]. There are new variants of the measurement of cut mass in PMMA concerning the energy used in the standard number, e.g., 50 linear cutting cycles [510]. In vitro tests of endodontic tools used to develop 1, 5, and 10 molars were also carried out, showing significant differences between the properties when processing one tooth compared to those used for processing 5 or 10 teeth [512]. Treatment efficiency decreased when one to five teeth was used. Its decrease is due to the sterilization of tools [512].

A significant decrease in the cutting efficiency of nitinol rotary tools with a taper of 0.04 or 0.06 was found under the influence of repeated 14 or 7 sterilization cycles for 30 min compared to those not sterilized at all (Figure 13) [499]. Repeated autoclaving changes the surface structure of endodontic tools [499]. In the case of the highest number of 14 sterilization cycles, there are significant changes in the distribution of the surface chemical composition compared to nonsterilized tools, mainly due to the increased proportion of titanium oxide on the surface [499], which resulted in the loss of properties of these tools.

Table 4. The cutting efficiency of endodontic tools concerning sterilization procedures.

No.	Material	Type of Autoclave	Time and Temperature	Autoclave Cycles Number	Reduction of Cutting Efficiency	Comments	Reference
1	Stainless steel	Steam autoclave	15 min, 121 °C	5, 10, and 15	No results	No significant differences in cutting efficiency.	[512]
2		Autoclave bags	30 min, 132 °C	10	No results	Autoclave sterilization resulted in a small but significant decrease in cutting ability of the files.	[511]
3		Chemiclave	30 min, 131 °C	5 10	63.9–77% 50.4–73%	A cutting efficiency reduction in range of 50% to 77%.	[502]
4	Nitinol	Euroclave	30 min, 121 °C	7 14	20% 50%	The number of sterilization cycles is a determining factor as to cutting efficiency.	[499]
5		Aesculap Automat 356	30 min, 134 °C	5 10	16.1% 50.6%	Sterilization resulted in a significant decrease in cutting ability.	[508]
6		STATIM 5000	6 min, 132 °C	2,3,7,8, and 9	No results	A statistically significant decrease in cutting efficiency.	[509]

Assessment of the effect of repeated simulated clinical use and successively after 1–10 sterilization cycles on the cutting performance and flexibility of rotary tools in a three-point bending test is performed by measuring the load required to maintain a constant feed rate during the development of simulated root canals. In cases where the sample size was statistically sufficient, a significant decrease in cutting efficiency was found with an increase in the number of sterilization processes [509]. After treatment with sodium hypochlorite NaOCl for 12 or 48 h or not at all, the cutting performance was assessed compared to a conventional K-type tool in corrosion-resistant steel. Treatment by chemical disinfection in NaOCl has no significant effect on the cutting performance of endodontic tools [510]. This aspect has been extensively studied by chemical disinfection in NaOCl (2.5%) for 12 and 48 h and NH4 (5%) for 1 and 4 h, ultrasonic cleaning for 4 and 16 cycles of 15 min, and sterilization methods using chemiclave for 5 and 10 cycles of 20 min, thermal sterilization (Poupinel) for 5 and 10 cycles of 120 min at 180 °C, and glass bead for 10 and

40 cycles at 250 °C. Cutting efficiency was assessed as the mass of PMMA cut per unit of energy expended by the tool. Cutting efficiency decreased from 1 to 77%, depending on the type of tool, while thermal sterilization (Poupinel) did not change the cutting efficiency, and the decrease in cutting efficiency was independent of the frequency and time of treatments [502]. Multiple autoclave sterilization in combination with the initial exposure to sodium hypochlorite NaOCl does not increase the efficiency of tools made of nitinol coated with TiN surface in the physical vapor deposition PVD process [508].

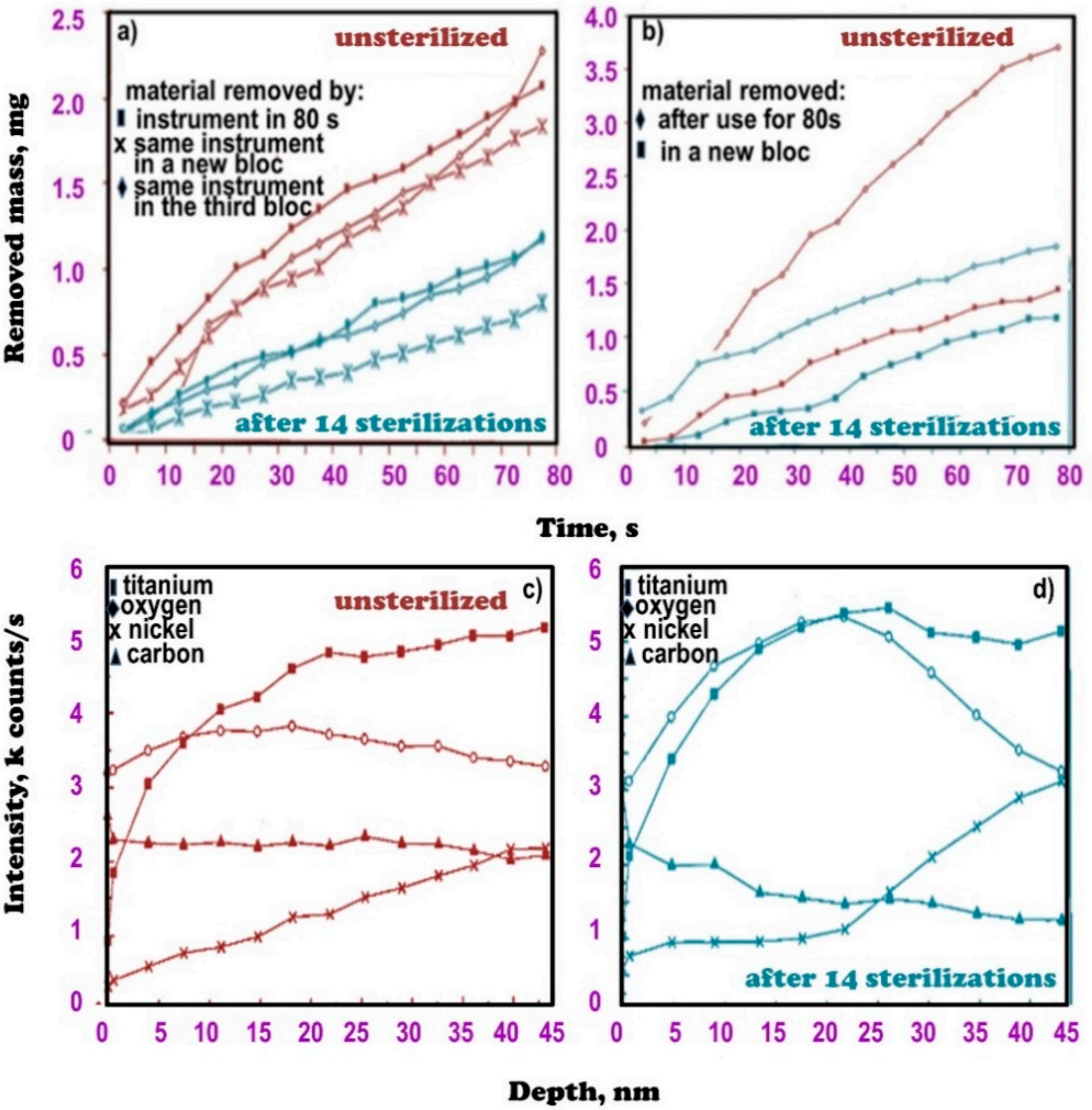

Figure 13. Dependence of the cutting efficiency of nitinol rotary tools (**a**,**b**) or changes in the concentration of Ti, O, Ni, and C in the surface layer of these tools (**c**,**d**) under the influence of repeated 14 sterilization cycles for 30 min (**a**,**b**,**d**) compared to nonsterilized (**a**–**c**).

7. SWOT Analysis of Strengths and Weaknesses as Well as Opportunities and Threats of Using Nitinol Tools in Endodontics and Forecast of Their Strategic Development

This chapter of the paper contains an SWOT point analysis, including a comparative analysis of the strengths and weaknesses of endodontic tools made of nitinol, as well as a list of key opportunities and threats that may affect the development and market success of tools made of this type of Ni–Ti alloy for the preparation of root canals. SWOT analysis is an integrated method that compiles and compares the key internal and external factors, both positive and negative, that most significantly affect the current market position of the subject of the analysis and determine its future development [66]. The SWOT analysis results constitute the base information for formulating a strategy aimed at indicating the best way to strengthen the diagnosed market position in the long term.

As part of the performed work, an expert evaluation of nitinol as a material used in endodontics was performed, taking into account twenty key factors. A universal scale of relative states was used to assess the impact of each of them. It is a ten-step unipolar positive interval scale with no zero, with 1 being the minimum value and 10 being the maximum value that can be assigned (Figure 14).

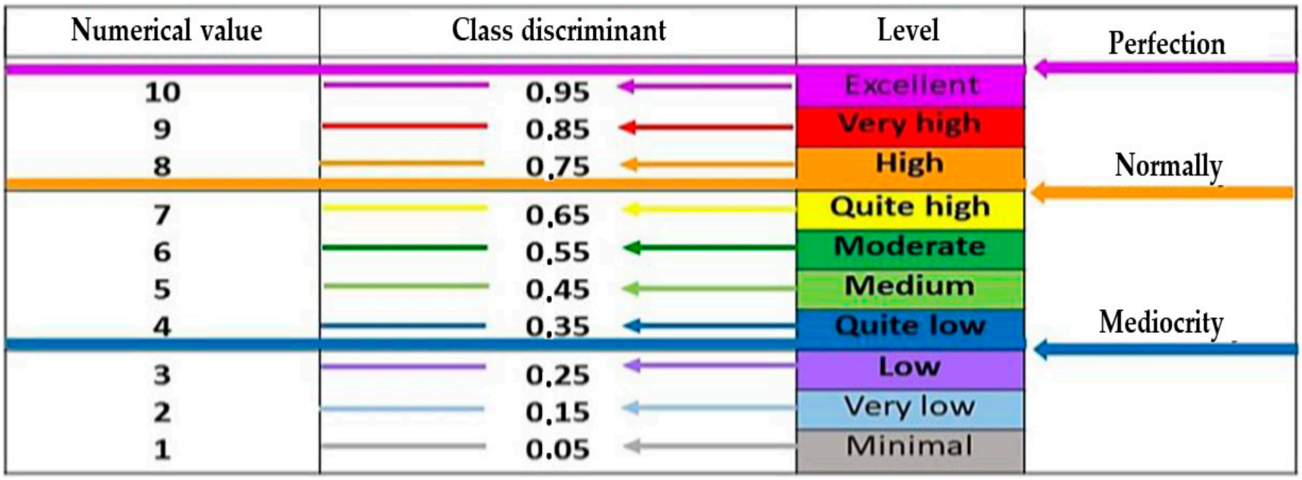

Figure 14. The universal scale of relative states.

Five key internal positives (strengths) and negative (weaknesses) factors, as well as positive (opportunities) and negative (threats) external factors, were defined. In this way, four groups of factors of the most important and the greatest influence on the development of endodontic tools made of nitinol were created, and assigned weights reflecting their importance (Figure 15).

The most important strengths of endodontic instruments made of nitinol include the mechanical resistance to breaking (S1) inside the root canal, which was assessed as quite high, corresponding to 7 points on the universal scale of relative states. The awarded assessment is related to the fact that, although endodontic tools made of nitinol are characterized by higher torsional strength than tools made of corrosion-resistant steels, it is difficult to avoid incidental fracture during clinical practice in their case as well. One of the reasons for this type of iatrogenic error during root canal preparation may be the insufficient torsional strength, which occurs when the working part of the tool becomes trapped in the root canal. The handle continues to rotate until the torsion strength of the tool material is exceeded. The second possible cause of tool breakage, which has to leave its tip inside the prepared canal, is tool material fatigue even more often. Therefore, among the strengths of nitinol tools, the material fatigue life (S2) is distinguished, which can be optionally measured as the time to fracture during operation or the number of cycles to fracture (NCF) of the tool. Another strength of the tools made of nitinol is these tools working efficiency (S5). Nitinol tools, as the only ones on the market, are suitable for working in curved canals. Their use provides the possibility of a conical preparation of the root canal with a wide mouth tapering towards the apex. Thus, effective evacuation of dentin filings and pulp remains from the root canal and their absence pushing past the apex. The use of nitinol tools also allows for the natural curvature of the prepared canal and its natural course. One of the key properties of the alloy, which makes it possible for a dentist to undertake these works, is its springiness (S3) (which is greater than in the case of tools made of other metal materials) and the associated resistance to plastic deformation over a relatively wide range of deformation. In addition, tools made of nitinol can be characterized by shape memory and superelasticity (S4), which requires the use of additional technological processes, including heat treatment and cold working.

Indicator	Strengths	Impact force	Rating	Weighted average	Indicator	Weaknesses	Impact force	Rating	Weighted average
S1	Mechanical resistance to breaking	0.25	7	1.75	W1	The harmful effects of nickel on human health	0.20	3	0.60
S2	Fatigue life	0.22	8	1.76	W2	Root canals disinfection	0.10	7	0.70
S3	Springiness	0.16	9	1.44	W3	Reduction in cutting effectiveness due to sterilization	0.25	10	2.50
S4	Shape memory and super elasticity	0.16	9	1.44	W4	Difficulty mastering the technique of root canal preparation	0.20	6	1.20
S5	Tools working efficiency	0.21	8	1.68	W5	Unit cost of the endodontic procedure	0.25	8	2.00
	Strengths index			8.07		Weaknesses index			7.00

Indicator	Opportunities	Impact force	Rating	Weighted average	Indicator	Threats	Impact force	Rating	Weighted average
O1	Increasing the share of rotary nitinol tools in the total endodontic tools market	0.15	7	1.05	T1	Intensive development and reduction of costs of manufacturing tools from competitive materials	0.30	9	2.70
O2	Improving the crown-down method and its popularization	0.15	8	1.20	T2	Invention of a completely new material for endodontic tools	0.15	8	1.20
O3	Optimizing the chemical composition of the tool material	0.20	9	1.80	T3	Significant improvement of the existing or introduction of a completely new technique of root canal preparation	0.10	5	0.50
O4	Improving the most effective technologies of manufacturing nitinol tools	0.30	10	3.00	T4	Promotion of competitive materials and techniques through the industrial lobby	0.25	8	2.00
O5	Reduction of manufacturing costs of nitinol tools	0.20	8	1.60	T5	Introduction of standards and/or legal regulations limiting the use of Ni-based tools	0.20	5	1.00
	Opportunities index			8.65		Threats index			7.40

Figure 15. Analysis of strengths, weaknesses, opportunities, and threats of nitinol as a material used to develop root canals in endodontics (the color markings correspond to that adopted in previous publications [47,65–67]).

The most significant weaknesses of nitinol endodontic instruments include reducing cutting effectiveness due to sterilization (W3), which is necessary because of the obvious sanitary and epidemiological conditions. Multiple autoclave sterilization changes the surface structure of nitinol endodontic tools, regardless of the type of autoclave used. During this process, significant changes in the distribution of the surface chemical composition occur, mainly in the form of an increased proportion of titanium oxide on the surface. A weakness of the tools made of nitinol is also the relatively high unit cost of the endodontic procedure (W5) performed with their use, which includes the market price of these tools and the need to use irrigators and lubricants, as well as high labor costs because high-class specialists perform the procedures. It is directly related to another disadvantage associated with the practical use of nitinol endodontic tools, which is the difficulty mastering the root canal preparation technique (W4), requiring theoretical training and great skill and experience of the dentist and their assistant. Among the disadvantages of tools made of nitinol, the harmful effect of nickel on human health (W1) cannot be ignored. However, this weakness was assessed as low (3 points) because the carcinogenic and allergenic effects of nickel ions mainly concern medical devices that remain in the human body for a long time. Their harmful effects in the case of temporary-use devices with a very limited time of contact with human tissue are certainly much smaller or negligible and not yet supported by scientific evidence. The last weakness regarding the use of nitinol endodontic tools is the need for root canals disinfection (W2), which should ideally include irrigation of the root canals in combination with the use of lubricants containing, in addition to glycerin, urea peroxide or sodium edetate, thanks to which the synergy effect is obtained. These actions complicate the performance of the procedure, and they are not always effective enough to prevent postoperative complications.

Among the positive external factors, the greatest chance was the improving the most effective technologies of manufacturing nitinol tools (O4), i.e., those during which thermoelastic reversible martensitic transformation takes place in almost stoichiometric Ni–Ti alloys, thanks to which the shape memory effect occurs, and the accompanying phenomenon appears to be superelasticity. Obtaining these desired properties of nitinol alloys is significantly dependent on the heat treatment conditions and the structure that arises as a result of technological processes, in particular, the fining of austenitic matrix grain, dispersion precipitation Ni_4Ti_3 in austenite, and the course of martensitic transformation. A complementary action, offering a chance for further development, is optimizing the chemical composition of the tool material (O3). The most suitable material for endodontic tools is the nitinol alloy with a chemical composition corresponding to the stoichiometric atomic concentration of the elements in the NiTi intermetallic phase with the lowest possible concentration of the remaining elements admixtures are undesirable and only reduce the properties of the final products. It is necessary to use high-purity raw materials containing 99.99% weight of Ni and 99.80% by weight of Ti to manufacture high-quality nitinol. Purely practical aspects also determine the future market success of nitinol endodontic tools. Therefore, improving the most effective manufacturing technologies and optimizing the chemical composition of the tool material should be accompanied by the reduction of manufacturing costs of nitinol tools (O5). Higher production volume is a chance for scale effect. It means a lower unit cost of manufacturing a single endodontic tool. Another chance for a systematic increase in the importance of nitinol tools used in endodontics is the improving the crown-down method and its popularization (O2). This two-step technique for elaborating root canals involves preparing the papillary and medial parts for 2/3 of the root canal length or its straight part in the case of curved canals (step 1) and preparing the apical part after measuring the working length (step 2). Improving this method should minimize the risk of pushing the remains of dead pulp and dentine filings beyond the apical opening. At the same time, its popularization should include extensive training and marketing activities, increasing the interest of direct (dentists) and indirect (patients) customers. Due to the greater efficiency and lower number of postoperative complications, one should strive to increase the share of rotary nitinol tools in the total endodontic tools market (O1). As part of the old generation, hand tools should be gradually withdrawn from the market and replaced by more modern rotary counterparts.

The most important factors that may hinder the development of tools made of nitinol in the market of class I medical devices for endodontics in the future is the intensive development and reduction of costs of manufacturing tools from competitive materials (T1). The undoubted advantages of nitinol tools compared to corrosion-resistant steels, such as springiness, flexibility, or fatigue life, alternatively used in mechanical techniques for the development of root canals, can be overcome if these properties are significantly improved for steel tools or the difference is increased price between steel and nitinol tools, to the disadvantage of the latter. Promoting competitive materials and techniques through industry lobby (T4) may become a significant threat in this area. It should be remembered that, statistically, customers most often choose a product with a favorable quality to price ratio. Therefore, sophisticated advantages may not compensate for the benefits of acquiring a relatively good product at an affordable price, especially when it is backed up by a good promotional campaign targeted at properly selected market segments. According to the current proecological trends, there is a high probability that in the near future, there will be the introduction of standards and/or legal regulations limiting the use of Ni-based tools (T5). However, it is unlikely that it is the case for class I medical devices, including endodontic tools. The harmful effects of nickel ions in the case of instantaneous devices with a very limited contact time with human tissue are slight or negligible and not supported by scientific evidence at the moment. Another potential external threat is the invention of completely new materials for endodontic tools (T2). It is not excluded due to the intensive development of materials engineering in recent decades, especially in bio- and nanomaterials. Endodontic tools made of nitinol may also be threatened by the significant improvement of the existing or introduction of a completely new technique of root canal preparation (T3). Currently, competing with the mechanical techniques of root canal preparation, laser and ultrasonic methods do not show any significant advantages, hampering the development of mechanical techniques, which is reflected in the assessment. However, a breakthrough in their development in the future cannot be ruled out, especially in the emergence of more sophisticated laser devices used in more and more new areas and industries.

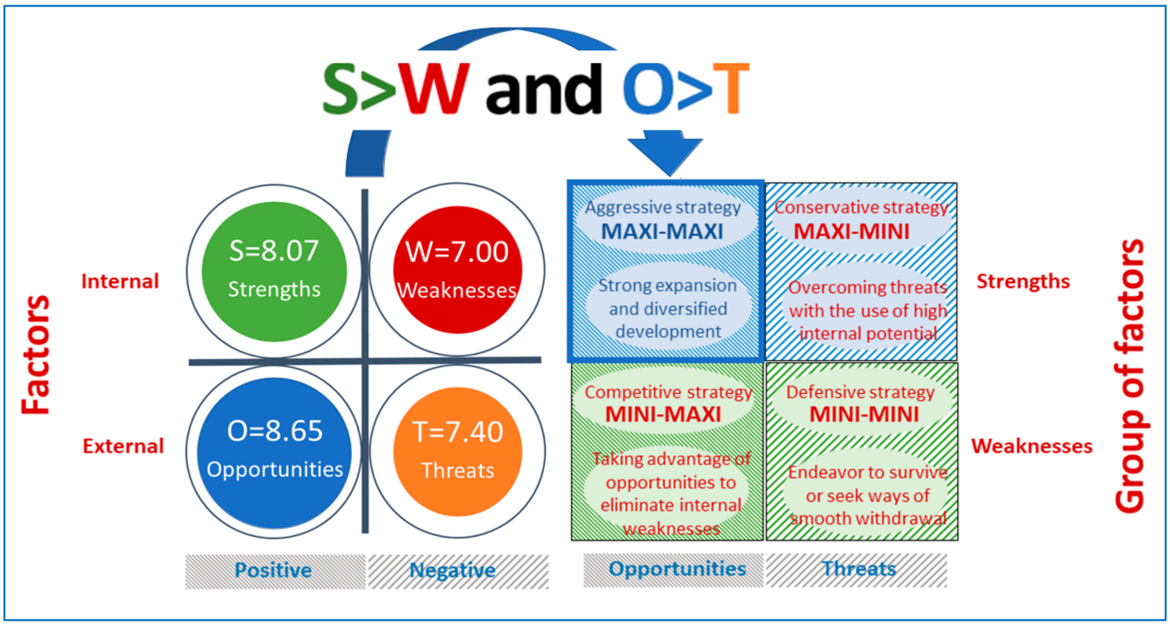

Figure 16. Scheme of an aggressive MAXI-MAXI strategy for the development of nitinol as a material for tools in endodontics in the face of the advantage of strengths over the weaknesses and opportunities over threats.

The next step of the SWOT analysis is a multicriteria analysis, the result of which is the award of four scores expressing strengths numerically (8.07), and weaknesses (7.00), of endodontic tools made of nitinol, as well as opportunities (8.65) and threats (7.40) carried by their surroundings (Figure 16). The strengths of the nitinol tools outweigh their weaknesses, and the difference between their weighted averages is 1.07 points. In the case of external factors, the difference between the weighted averages is slightly larger and amounts to 1.25 points, favoring positive environmental factors. Therefore, an aggressive strategy, called MAXI-MAXI, is adequate for developing endodontic tools made of nitinol. The application of this strategy in practice consists of diversification by searching for new geographic markets and new groups of recipients, combined with a strong expansion based on numerous opportunities that arise from the immediate and further environment and continuous and systematic monitoring of identified threats.

8. Recapitulation and Final Conclusions

Dental caries is the most common contagious disease globally, affecting 3–5 billion people. Caries causes numerous systemic diseases, and the resulting toothlessness causes further serious health complications, a significant deterioration of wellbeing, and a decrease of quality and length of human life. Generally, good health of the population is closely related to oral hygiene, prevention, and effective treatment of oral diseases at the earliest possible stage of the disease, according to the Authors' Dentistry Sustainable Development (DSD) model. Depending on the stage of the disease, the method used is conservative treatment and endodontic treatment in the case of more advanced disease. It is possible to successfully avoid tooth extraction by keeping it as a natural pillar, leaving a healthy marginal and periapical periodontium. Among the factors influencing effective endodontic treatment, apart from the correct selection of filling material and obturation methods, the root canal is properly prepared. Among the various techniques of preparation of the dentine of the root canal for connection with the filling material, the classical methods of mechanical preparation and disinfection by cutting the dentine using hand or rotary tools are of great importance. When using classic corrosion-resistance steel tools, an increase in their size reduces the tool's flexibility. It thus increases the risk of iatrogenic treatment error related to the breaking of the tool inside the root canal, especially in curved canals. An alternative is tools made of nickel–titanium alloys, known as nitinol, which significantly reduces the likelihood of incidental fracture in the course of clinical practice.

The paper presents a complete material science characterization of the structure of nitinol alloys. It discusses all structural phenomena and phase transformations that determine the functional properties of endodontic tools made of this alloy. Attention was paid to the importance of even small changes in the chemical composition around the equilibrium atomic concentration of Ni and Ti and the processing conditions of these alloys. The various variants of heat and thermomechanical treatment and surface treatment used by various tool manufacturers and the importance of the participation of B2, B19′, and R phases and their share in the nitinol alloys matrix structure for application in endodontic tooth treatment were indicated. The importance of sanitary and epidemiological sterilization has also been taken into account, as each sterilization process causes irreversible degradation of each endodontic tool.

To sum up, in full, the prepared literature review gives the possibility of an SWOT analysis of the strengths and weaknesses and the opportunities and threats of using this material for endodontic tools. The strengths include mechanical resistance to fracture, fatigue life, springiness, shape memory, and superelasticity, as well as the cutting effectiveness of the tools, when the opportunities include increasing the share of rotary nitinol tools in the total market, improvement of the crown-down root canal preparation method and its popularization, optimization of the chemical composition material for tools, improvement of the most effective technologies for the manufacturing of tools from nitinol, and reduction of manufacturing costs of these tools. It provides an appropriately decisive advantage over the weaknesses characterized by the harmful effects of nickel on human health, disinfection of root canals, reduced cutting efficiency as a result of sterilization, difficulty in mastering the technique of using nitinol tools and increasing the unit cost of the treatment in the endodontic procedure when the threats include intensive development and lowering the costs of manufacturing tools from competing materials, the possibility of inventing a completely new material for endodontic tools, significant improvement of the existing or completely new technique of root canal preparation, promotion of competitive materials and techniques by the industrial lobby, and the possibility of introducing standards and/or legal regulations limiting the use of tools based on nickel, harmful to human health.

The extensive literature studies performed, and the SWOT analysis carried out, indicate the conclusion that the numerical superiority of strengths (8.07) over weaknesses (7.00) and opportunities (8.65) over threats (7.40) in the case of endodontic tools made of nitinol requires application of an adequate and aggressive development strategy of MAXI-MAXI. This strategy consists of diversification related to the search for new recipients and geographic markets and strong expansion to take advantage of numerous opportunities brought by the environment, both closer and further, and requires constant monitoring of the existing threats. Due to the specific fields of application in clinical practice, this places endodontic tools in an unbeatable position compared to those made of corrosion-resistant steel, although they are undoubtedly complementary.

Author Contributions: Conceptualization, literature review, presentation, design, resources, data curation and analysis, software, formal analysis, writing, original draft preparation, visualization, practical verification, L.A.D., L.B.D., A.D.D.-D. and J.D.; writing—review and editing, L.A.D., L.B.D. and A.D.D.-D.; supervision, project administration, funding acquisition, L.A.D. and L.B.D. All authors have read and agreed to the published version of the manuscript.

Funding: This paper was prepared to actually implement Project POIR.01.01-00-0485/16-00 on "IMSKAMAT Innovative dental and maxillofacial implants manufactured using the innovative additive technology supported by computer-aided materials design ADD-MAT" realized by the Medical and Dental Engineering Centre for Research, Design, and Production (ASKLEPIOS) in Gliwice, Poland. The project was implemented in 2017–2021 and was cofinanced by the Operational Program for Intelligent Development of the European Union.

Institutional Review Board Statement: Not applicable.

Informed Consent Statement: Not applicable.

Conflicts of Interest: The authors declare no conflict of interest.

References

1. Oxilia, G.; Peresani, M.; Romandini, M.; Matteucci, C.; Debono Spiteri, C.; Henry, A.G.; Schulz, D.; Archer, W.; Crezzini, J.; Boschin, F.; et al. Earliest evidence of dental caries manipulation in the Late Upper Palaeolithic. *Sci. Rep.* **2015**, *5*, 12150. [CrossRef] [PubMed]
2. Dobrzański, L.A.; Dobrzański, L.B.; Dobrzańska-Danikiewicz, A.D.; Dobrzańska, J. The Concept of Sustainable Development of Modern Dentistry. *Processes* **2020**, *8*, 1605. [CrossRef]
3. Allen, J.P. *The Art of Medicine in Ancient Egypt*; The Metropolitan Museum of Art: New York, NY, USA, 2005.
4. Frayer, D.W.; Gatti, J.; Monge, J.; Radovčic, D. Prehistoric dentistry? P4 rotation, partial M3 impaction, toothpick grooves and other signs of manipulation in krapina dental person 20. *Bull. Int. Assoc. Paleodont.* **2017**, *11*, 1–10.
5. Caldas, A.F., Jr. Reason for tooth extraction in a Brazilian population. *Int. Dent. J.* **2000**, *50*, 267–273. [CrossRef] [PubMed]
6. Chestnutt, I.G.; Binnie, V.I.; Taylor, M.M. Reason for tooth extraction in Scotland. *J. Dent.* **2000**, *28*, 295–297. [CrossRef]
7. Morita, M.; Kimura, T.; Kanegae, M.; Ishikawa, A.; Watanobe, T. Reasons for extraction of permanent teeth in Japan. *Community Dent. Oral. Epidemiol.* **1994**, *22*, 303–306. [CrossRef] [PubMed]
8. Angelillo, I.F.; Nobile, C.G.A.; Pavia, M. Survey of reasons for extraction of permanent teeth in Italy. *Community Dent. Oral. Epidemiol.* **1996**, *24*, 336–340. [CrossRef]
9. Al-Shammari, K.F.; Al-Arsari, J.M.; Al-Melh, M.A.; Al-Khabhaz, A.K. Reasons for tooth extraction in Kuwait. *Med. Princ. Pract.* **2006**, *15*, 417–422. [CrossRef]
10. Hollandra, A.C.B.; de Alencar, A.H.G.; de Estrela, C.R.A.; Bueno, M.R.; Estrela, C. Prevalance of Endodontically Trale Teeth in a Brazilian Adult Population. *Braz. Dent. J.* **2008**, *19*, 313–317. [CrossRef]
11. Fejerskov, O. Concepts of dental caries and their consequences for understanding the disease. *Community Dent. Oral Epidemiol.* **1997**, *25*, 5–12. [CrossRef]

12. Reisine, S.; Litt, M. Social and psychological theories and their use for dental practice. *Int. Dent. J.* **1993**, *43* (Suppl. 1), 279–287. [PubMed]
13. Selwitz, R.H.; Ismail, A.I.; Pitts, N.B. Dental caries. *Lancet* **2007**, *369*, 51–59. [CrossRef]
14. Yu, C.; Abbott, P.V. An overview of the dental pulp: Its functions and responses to injury. *Aust. Dent. J.* **2007**, *52*, S4–S16. [CrossRef]
15. Harumi Miyagi, S.P.; Kerkis, I.; da Costa Maranduba, C.M.; Gomes, C.M.; Martinis, M.D.; Marques, M.M. Expression of extracellular matrix proteins in human dental pulp stem cells depends on the donor tooth conditions. *J. Endod.* **2010**, *36*, 826–831. [CrossRef] [PubMed]
16. Vieira, C.L.Z.; Caramelli, B. The history of dentistry and medicine relationship: Could the mounth finally return to the body? *Oral Dis.* **2009**, *15*, 538–546. [CrossRef]
17. Pallasch, T.J.; Wahl, M.J. Focal infection: New age or ancient history? *Endod. Top.* **2003**, *4*, 32–45. [CrossRef]
18. Mueller, A.A.; Saldami, B.; Stübinger, S.; Walter, C.; Flückiger, U.; Merlo, A.; Schwenzer-Zimmerer, K.; Zeilhofer, H.F.; Zimmerer, S. Oral bacterial cultures in nontraumatic brain abscesses: Results of a first line study. *Oral Surg. Oral Med. Oral Pathol. Oral Radiol. Endod.* **2009**, *107*, 469–476. [CrossRef]
19. Buset, S.L.; Walter, C.; Friedmann, A.; Weiger, R.; Borgnakke, W.S.; Zitzmann, N.U. Are periodontal diseases really silent? A systematic review of their effect on quality of life. *J. Clin. Periodontol.* **2016**, *43*, 333–344. [CrossRef]
20. Sierpinska, T.; Golebiewska, M.; Dlugosz, J.W.; Kemona, A.; Laszewicz, W. Connection between masticatory efficiency and pathomorphologic changes in gastric mucosa. *Quint. Int.* **2007**, *38*, 31–37.
21. Al-Nawas, B.; Maeurer, M. Severe versus local odontogenic bacterial infections: Comparision of microbial isolates. *Eur. Surg. Res.* **2008**, *40*, 220–224. [CrossRef]
22. De Pablo, P.; Dietrich, T.; McAlindon, T.E. Association of periodontal disease and tooth loss with rheumatoid arthritis in the US population. *J. Rheumatol.* **2008**, *35*, 70–76. [PubMed]
23. Felton, D.A. Edentualism and comorbid factors. *J. Prosthodont.* **2009**, *18*, 88–96. [CrossRef]
24. Volzke, H.; Schwahn, C.; Hummel, A.; Wolff, B.; Kleine, V.; Robinson, D.M.; Dahm, J.B.; Felix, S.B.; John, U.; Kocher, T. Tooth loss is independently associated with the risk of acquired aortic valve sclerosis. *Am. Heart J.* **2005**, *150*, 1198–1203. [CrossRef]
25. Bagchi, S.; Tripathi, A.; Tripathi, S.; Kar, S.; Tiwari, S.C.; Singh, J. Obstructive sleep apnea and neurocognitive dysfunction in edentulous patients. *J. Prosthodont.* **2019**, *28*, e837–e842. [CrossRef] [PubMed]
26. Nagpal, R.; Yamashiro, Y.; Izumi, Y. The two-way association of periodontal infection with systemic disorders: An overview. *Mediat. Inflamm.* **2015**, *2015*, 793898. [CrossRef] [PubMed]
27. Abnet, C.C.; Qiao, Y.L.; Dawsey, S.M.; Dong, Z.W.; Taylor, P.R.; Mark, S.D. Tooth loss is associated with increased risk of total death and death from upper gastrointestinal cancer, heart disease, and stroke in a Chinese population-based cohort. *Int. J. Epidemiol.* **2005**, *34*, 467–474. [CrossRef]
28. Burzyńska, B.; Mierzwińska-Nastalska, E. Rehabilitacja protetyczna pacjentów bezzębnych. *Nowa Stomatol.* **2011**, *4*, 167–199.
29. Bui, F.Q.; Almeida-da-Silva, C.L.C.; Huynh, B.; Trinh, A.; Liu, J.; Woodward, J.; Asadi, H.; Ojcius, D.M. Association between periodontal pathogens and systemic disease. *Biomed. J.* **2019**, *42*, 27–35. [CrossRef]
30. Holmlund, A.; Holm, G.; Lind, L. Number of teeth as a predictor of cardiovascular mortality in a cohort of 7674 subjects followed for 12 years. *J. Periodontol.* **2010**, *81*, 870–876. [CrossRef]
31. Takata, Y.; Ansai, T.; Matsumura, K.; Awano, S.; Hamasaki, T.; Sonoki, K.; Kusaba, A.; Akifusa, S.; Takehara, T. Relationship between tooth loss and electrocardiographic abnormalities in octogenarians. *J. Dent. Res.* **2001**, *80*, 1648–1652. [CrossRef]
32. Felton, D.A. Complete edentulism and comorbid diseases: An update. *J. Prosthodont.* **2016**, *25*, 5–20. [CrossRef] [PubMed]
33. Chen, H.; Iinuma, M.; Onozuka, M.; Kubo, K.-Y. Chewing maintains hippocampus-dependent cognitive. *Int. J. Med. Sci.* **2015**, *12*, 502–509. [CrossRef]
34. Stein, P.S.; Desrosiers, M.; Donegan, S.J.; Yepes, J.F.; Kryscio, R.J. Tooth loss, dementia and neuropathology in the Nun study. *J. Am. Dent. Assoc.* **2007**, *138*, 1314–1322. [CrossRef]
35. Henke, K. A model for memory systems based on processing modes rather than consciousness. *Nat. Rev. Neurosci.* **2010**, *11*, 523–532. [CrossRef] [PubMed]
36. Lexomboon, D.; Trulsson, M.; Wårdh, I.; Parker, W.G. Chewing ability and tooth loss: Association with cognitive impairment in an elderly population study. *J. Am. Geriatr. Soc.* **2012**, *60*, 1951–1956. [CrossRef] [PubMed]
37. Hirano, Y.; Obata, T.; Takahashi, H.; Tachibana, A.; Kuroiwa, D.; Takahashi, T.; Ikehira, H.; Onozuka, M. Effects of chewing on cognitive processing speed. *Brain Cognit.* **2013**, *81*, 376–381. [CrossRef]
38. Onishi, M.; Iinuma, M.; Tamura, Y.; Kubo, K.Y. Learning deficits and suppression of the cell proliferation in the hippocampal dentate gyrus of offspring are attenuated by maternal chewing during prenatal stress. *Neurosci. Lett.* **2014**, *560*, 77–80. [CrossRef]
39. Kawahata, M.; Ono, Y.; Ohno, A.; Kawamoto, S.; Kimoto, K.; Onozuka, M. Loss of molars early in life develops behavioral lateralization and impairs hippocampus-dependent recognition memory. *BMC Neurosci.* **2014**, *15*, 4. [CrossRef]
40. Li, X.; Tornstad, L.; Olsen, I. Brain abscesses caused by oral infection. *Dent. Traumatol.* **1999**, *15*, 95–101. [CrossRef]
41. Scannapieco, F.A.; Bush, R.B.; Paju, S. Associations between periodontal disease and risk for nosocomial bacterial pneumonia and chronic obstructive pulmonary disease. A systemic review. *Ann. Periodontol.* **2003**, *8*, 54–69. [CrossRef]

42. Dobrzański, L.A.; Dobrzański, L.B.; Dobrzańska-Danikiewicz, A.D.; Dobrzańska, J.; Rudziarczyk, K.; Achtelik-Franczak, A. Non-antagonistic contradictoriness of the progress of advanced digitized production with SARS-CoV-2 virus transmission in the area of dental engineering. *Processes* **2020**, *8*, 1097. [CrossRef]
43. Aleksander, M.; Krishnan, B.; Shenoy, N. Diabetes mellitus and odontogenic infections-an exaggerated risk? *Oral Maxillofac. Surg.* **2008**, *12*, 129–130. [CrossRef]
44. Scannapieco, F.A. Role of oral bacteria in respiratory infection. *J. Periodontol.* **1999**, *70*, 793–802. [CrossRef]
45. Tan, H.; Peres, K.G.; Peres, M.A. Retention of teeth and oral health-related quality of life. *J. Dent. Res.* **2016**, *95*, 1350–1357. [CrossRef]
46. Murray, C.J.L.; Lopez, A.D. *The Global Burden of Disease: A Comprehensive Assessment of Mortality and Disability from Diseases, Injuries, and Risk Factors in 1990 and Projected to 2020*; University Press on behalf of the World Health Organization and The World Bank: Boston, MA, USA; Harvard: Cambridge, MA, USA, 1996. Available online: https://apps.who.int/iris/handle/10665/41864 (accessed on 17 August 2021).
47. Dobrzańska, J.; Dobrzański, L.B.; Gołombek, K.; Dobrzański, L.A.; Dobrzańska-Danikiewicz, A.D. Virtual approach to the comparative analysis of biomaterials used in endodontic treatment. *Processes* **2021**, *9*, 926. [CrossRef]
48. Castellucci, A. *Endodontics*; Il Tridente Edizioni Odontolatriche: Bologna, Italy, 2005; Volume 1.
49. Alwadani, M.; Mashyakhy, M.H.; Jali, A.; Hakami, A.O.; Areshi, A.; Daghriri, A.A.; Shaabi, F.I.; Al Moaleem, M.M. Dentists and Dental Intern's Preferences of Root Canal Treatment with Restoration Versus Extraction then Implant-Supported Crown Treatment Plan. *Open Dent. J.* **2019**, *13*, 93–100. [CrossRef]
50. Estrela, C.; Holland, R.; Estrela, C.R.; Alencar, A.H.; Sousa-Neto, M.D.; Pécora, J.D. Characterization of successful root canal treatment. *Braz. Dent. J.* **2014**, *25*, 3–11. [CrossRef]
51. Dental Consumables Market by Product [Dental Implants (Root Form Dental Implants and Plate Form Dental Implants), Dental Prosthetics (Crowns, Bridges, Dentures, Abutments, Veneers, and Inlays & Onlays), Endodontics (Endodontic Files, Obturators, and Permanent Endodontic Sealers), Orthodontics (Brackets, Archwires, Anchorage Appliances, and Ligatures), Periodontics (Dental Sutures and Dental Hemostats), Retail Dental Care Essentials (Specialized Dental Pastes, Dental Brushes, Dental Wash Solutions, Whitening Agents, and Dental Floss), and Other Dental Consumables (Dental Splints, Dental Sealants, Dental Burs, Dental Impression Materials, Dental Disposables, Bonding Agents, Patient Bibs, and Aspirator Tubes & Saliva Ejectors)]—Global Opportunity Analysis and Industry Forecast, 2017–2023. Available online: https://www.alliedmarketresearch.com/dental-consumables-market (accessed on 7 May 2021).
52. Endodontic Devices Market Size, Share & Trends Analysis Report by Type (Instruments, Consumables), by End Use (Hospitals, Clinics, Dental Academic & Research Institutes), and Segment Forecasts, 2019–2026. Available online: https://www.grandviewresearch.com/industry-analysis/endodontic-devices-market (accessed on 7 May 2021).
53. Dental Endodontics Market (Product—Instruments (Endodontic Scalers & Lasers, Motors, Apex Locators, and Machine Assisted Obturation Systems) and Consumables (Obturation, Shaping and Cleaning, and Access Cavity Preparation); End User: Dental Hospitals, Dental Clinics, and Dental Academic & Research Institutes)—Global Industry Analysis, Size, Share, Growth, Trends, and Forecast 2017–2025. Available online: https://www.transparencymarketresearch.com/dental-endodontics-market.html (accessed on 7 May 2021).
54. Dobrzański, L.A.; Dobrzańska-Danikiewicz, A.D.; Dobrzański, L.B. Effect of Biomedical Materials in the implementation of a long and healthy life policy. *Processes* **2021**, *9*, 865. [CrossRef]
55. Dobrzański, L.A.; Dobrzańska-Danikiewicz, A.D.; Dobrzański, L.B.; Dobrzańska, J. The Importance of Synthesis and Characterization of Biomedical Materials for the Current State of Medicine and Dentistry. *Processes* **2021**, *9*, 978. [CrossRef]
56. Dobrzański, L.A.; Dobrzański, L.B. Dentistry 4.0 Concept in the Design and Manufacturing of Prosthetic Dental Restorations. *Processes* **2020**, *8*, 525. [CrossRef]
57. Dobrzański, L.A.; Dobrzański, L.B.; Achtelik-Franczak, A.; Dobrzańska, J. Application Solid Laser-Sintered or Machined Ti6Al4V Alloy in Manufacturing of Dental Implants and Dental Prosthetic Restorations According to Dentistry 4.0 Concept. *Processes* **2020**, *8*, 664. [CrossRef]
58. Peres, M.A.; Macpherson, L.M.D.; Weyant, R.J.; Daly, B.; Venturelli, R.; Mathur, M.R.; Listl, S.; Celeste, R.K.; Guarnizo-Herreño, C.C.; Kearns, C.; et al. Oral diseases: A global public health challenge. *Lancet* **2019**, *394*, 249–260. [CrossRef]
59. Watt, R.G.; Daly, B.; Allison, P.; Macpherson, L.M.D.; Venturelli, R.; Listl, S.; Weyant, R.J.; Mathur, M.R.; Guarnizo-Herreño, C.C.; Celeste, R.K.; et al. Ending the neglect of global oral health: Time for radical action. *Lancet* **2019**, *394*, 261–272. [CrossRef]
60. Carrotte, P. Endodontics: Part 1. The modern concept of root canal treatment. *Br. Dent. J.* **2004**, *197*, 181–183. [CrossRef]
61. Siqueira, J.F.; Rocas, I.N.; Lopes, H.P.; de Uzeda, M. Coronal leakage of two root canal sealers containing calcium hydroxide after exposure to human saliva. *J. Endod.* **1999**, *25*, 14–16. [CrossRef]
62. Hirsch, J.M.; Ahlstrom, U.; Henrikson, P.A.; Peterson, L.E. Periapical surgery. *Int. J. Oral Surg.* **1979**, *8*, 173–185. [CrossRef]
63. Sundqvist, G.; Figdor, D.; Persson, S.; Sjörgren, U. Microbiological analysis of teeth with failed endodontic treatment and the outcome of conservative re-treatment. *Oral Surg. Oral Med. Oral Pathol. Oral Radiol. Endod.* **1998**, *85*, 86–93. [CrossRef]
64. Ǿstravik, D. Materials used for root canal obturation: Technical, biological and clinical testing. *Endod. Top.* **2005**, *12*, 25–38. [CrossRef]
65. Dobrzańska, J.; Dobrzański, L.B.; Gołombek, K.; Dobrzański, L.A. Is gutta-percha still the "gold standard" among filling materials in endodontic treatment? *Processes* **2021**, *9*, 1467. [CrossRef]

66. Dobrzański, L.A.; Dobrzańska, J.; Dobrzański, L.B.; Dobrzańska-Danikiewicz, A.D.; Gołombek, K. Development Strategy of Endodontic Filling Materials Based on Engineering and Medical Approaches. *Processes* **2021**, *9*, 2014. [CrossRef]
67. Dobrzańska, J.; Dobrzański, L.B.; Dobrzański, L.A.; Dobrzańska-Danikiewicz, A.D.; Gołombek, K. What Are the Chances of Resilon to Dominate the Market Filling Materials for Endodontics? *Metals* **2021**, *11*, 1744. [CrossRef]
68. Stabholz, A.; Sahar-Helft, S.; Moshonov, J. Lasers in endodontics. *Dent. Clin. N. Am.* **2004**, *48*, 809–832. [CrossRef]
69. Kimura, Y.; Wilder-Smith, P.; Matsumoto, K. Lasers in endodontics: A review. *Int. Endod. J.* **2000**, *33*, 173–185. [CrossRef]
70. Van der Sluis, L.W.M.; Versluis, M.; Wu, M.K.; Wasserlink, P.R. Passive ultrasonic irrigation of the root canal: A review of the literature. *Int. Endod. J.* **2007**, *40*, 415–426. [CrossRef] [PubMed]
71. Roy, R.A.; Ahmad, M.; Crum, L.A. Physical mechanisms governing the hydrodynamic response of an oscillating ultrasonic file. *Int. Endod. J.* **1994**, *27*, 197–207. [CrossRef]
72. Huque, J.; Kota, K.; Yamaga, M.; Iwaku, M.; Hoshino, E. Bacterial eradication from root dentine by ultrasonic irrigation with sodium hypochloride. *Int. Endod. J.* **1998**, *31*, 242–250. [CrossRef]
73. Hülsmann, M.; Paters, O.A.; Dummer, P.M.H. Mechanical preparation of root canals: Shaping goals, techniques and means. *Endod. Top.* **2005**, *10*, 30–76. [CrossRef]
74. Walia, H.M.; Brantley, W.A.; Gerstein, H. An initial investigation of the bending and torsional properties of Nitinol root canal files. *J. Endod.* **1988**, *14*, 346–351. [CrossRef]
75. Anderson, M.E.; Price, J.H.W.; Parashos, P. Fracture resistance of electropolished rotary Nickel-Titanium endodontic instruments. *J. Endod.* **2007**, *33*, 1212–1216. [CrossRef]
76. Duerig, T.; Pelton, A.; Stöckel, D. An overview of nitinol medical applications. *Mater. Sci. Eng. A* **1999**, *273–275*, 149–160. [CrossRef]
77. Fife, D.; Gambarini, G.; Britto, L.R. Cyclic fatigue testing of ProTaper NiTi rotary instruments after clinical use. *Oral Surg. Oral Med. Oral Pathol. Oral Radiol. Endod.* **2004**, *97*, 251–256. [CrossRef] [PubMed]
78. Gutmann, J.L.; Gao, Y. Alteration in the inherent metallic and surface properties of nickel-titanium root canal instruments to enhance performance, durability and safety: A focused review. *Int. Endod. J.* **2012**, *45*, 113–128. [CrossRef]
79. Pruett, J.P.; Clement, D.J.; Carnes, D.L., Jr. Cyclic fatigue testing of nickel-titanium endodontic instruments. *J. Endod.* **1997**, *23*, 77–85. [CrossRef]
80. Metallurgy: The Alloy That Remembers. Available online: http://content.time.com/time/subscriber/article/0,33009,838687,00.html (accessed on 10 May 2021).
81. Buehler, W.J.; Gilfrich, J.W.; Wiley, R.C. Effects of Low-Temperature Phase Changes on the Mechanical Properties of Alloys Near Composition TiNi. *J. App. Phys.* **1963**, *34*, 1475–1477. [CrossRef]
82. Wang, F.E.; Buehler, W.J.; Pickart, S.J. Crystal Structure and a Unique Martensitic Transition of TiNi. *J. App. Phys.* **1965**, *36*, 3232–3239. [CrossRef]
83. Kauffman, G.B.; Mayo, I. The Story of Nitinol: The Serendipitous Discovery of the Memory Metal and Its Applications. *Chem Edu.* **1997**, *2*, 1–21. [CrossRef]
84. Withers, N. Nitinol. Available online: https://www.chemistryworld.com/podcasts/nitinol/6710.article (accessed on 10 May 2021).
85. Ölander, A. An Electrochemical Investigation of Solid Cadmium-Gold Alloys. *J. Am. Chem. Soc.* **1932**, *54*, 3819–3833. [CrossRef]
86. Hornbogen, E.; Wassermann, G. Über den Einfluβ von Spannungen und das Auftreten von Umwandlungsplastizität bei β1-β-Umwandlung des Messings. *Z. Metalkd.* **1956**, *47*, 427–433.
87. Tamburrino, F.; Apicella, A.; Aversa, R.; Petrescu, F.I.T. Advanced Manufacturing for Novel Materials in Industrial Design Applications. *Am. J. Eng. Appl. Sci.* **2018**, *11*, 932–972. [CrossRef]
88. Cao, H.; Wu, M.H.; Zhou, F.; McMeeking, R.M.; Ritchie, R.O. The influence of mean strain on the high-cycle fatigue of Nitinol with application to medical devices. *J. Mech. Phys. Solids* **2020**, *143*, 104057. [CrossRef]
89. Stoeckel, D.; Pelton, A.; Duerig, T. Self-expanding nitinol stents: Material and design considerations. *Eur. Radiol.* **2004**, *14*, 292–301. [CrossRef]
90. Lanz, J.; Kim, W.-K.; Walther, T.; Burgdorf, C.; Möllmann, H.; Linke, A.; Redwood, S.; Thilo, C.; Hilker, M.; Joner, M.; et al. Safety and efficacy of a self-expanding versus a balloon-expandable bioprosthesis for transcatheter aortic valve replacement in patients with symptomatic severe aortic stenosis: A randomised non-inferiority trial. *Lancet* **2019**, *394*, 1619–1628. [CrossRef]
91. Pelton, A.R.; Schroeder, V.; Mitchell, M.R.; Gong, X.Y.; Barney, M.; Robertson, S.W. Fatigue and durability of Nitinol stents. *J. Mech. Behav. Biomed. Mater.* **2008**, *1*, 153–164. [CrossRef]
92. Grassi, C.J. Inferior vena caval filters: Analysis of five currently available devices. *AJR Am. J. Roentgenol.* **1991**, *156*, 813–821. [CrossRef]
93. Hull, J.E.; Robertson, S.W. Bard Recovery filter: Evaluation and management of vena cava limb perforation, fracture, and migration. *J. Vasc. Interv. Radiol.* **2009**, *20*, 52–60. [CrossRef]
94. Robertson, S.W.; Pelton, A.R.; Ritchie, R.O. Mechanical fatigue and fracture of Nitinol. *Int. Mater. Rev.* **2012**, *57*, 1–37. [CrossRef]
95. Suresh, S. *Fatigue of Materials*, 2nd ed.; Cambridge University Press: Cambridge, UK, 1998; pp. 1–704. [CrossRef]
96. Cheng, C.P.; Wilson, N.M.; Hallett, R.L.; Herfkens, R.J.; Taylor, C.A. In vivo MR angiographic quantification of axial and twisting deformations of the superficial femoral artery resulting from maximum hip and knee flexion. *J. Vasc. Interv. Radiol.* **2006**, *17*, 979–987. [CrossRef]

97. Murphy, E.H.; Johnson, E.D.; Arko, F.R. Evaluation of wall motion and dynamic geometry of the inferior vena cava using intravascular ultrasound: Implications for future device design. *J. Endovasc. Ther.* **2008**, *15*, 349–355. [CrossRef]
98. Milnor, W.R. *Hemodynamics*; Williams & Wilkins: Baltimore, MD, USA, 1982; pp. 1–390.
99. Laborda, A.; Sierre, S.; Malvé, M.; De Blas, I.; Ioakeim, I.; Kuo, W.T.; De Gregorio, M.A. Influence of breathing movements and Valsalva maneuver on vena caval dynamics. *World J. Radiol.* **2014**, *6*, 833–839. [CrossRef]
100. Dobrzański, L.A.; Dobrzański, L.B.; Dobrzańska-Danikiewicz, A.D.; Dobrzańska, J.; Kraszewska, M. The synergistic ethics interaction with nanoengineering, dentistry, and dental engineering. In *Ethics in Nanotechnology; Emerging Technologies Aspects*; Van de Voorde, M., Jeswani, G., Eds.; De Gruyter: Berlin, Germany, 2021; Volume I, pp. 119–189.
101. Brantley, W.A. Evolution, clinical applications, and prospects of nickel-titanium alloys for orthodontic purposes. *J. World Fed. Orthod.* **2020**, *9*, S19–S26. [CrossRef]
102. Harshavardhan, J.M.; Dhanavel, C.; Vijayaraja, S.; Manoj, K.T.; Bakkiyalakshmi, A.; Kavimalar, S. Metallurgy of Rotary Files—A Review. *J. Curr. Med. Res. Opin.* **2021**, *4*, 975–980. [CrossRef]
103. Jordan, L.; Bronnec, F.; Machtou, P. Endodontic Instruments and Canal Preparation Techniques. In *Endodontic Materials in Clinical Practice*; Camilleri, J., Ed.; Wiley: Hoboken, NJ, USA, 2021; pp. 81–131. [CrossRef]
104. Pawlicka, H.; Ebert, J.; Prociów, A. Systematyka rotacyjnych narzędzi niklowo-tytanowych. *Czas. Stomatol.* **2005**, *58*, 709–713.
105. Hryniewicz, T.; Rokosz, K.; Rokicki, R. Magnetoelectropolishing process improves characteristics of finished metal surfaces: Intensity of externally applied magnetic field, plus oxygen control, manipulates rate of dissolution in electropolishing. *Met. Finish.* **2006**, *104*, 26–31, 33. [CrossRef]
106. Hryniewicz, T. *Wstęp do Obróbki Powierzchniowej Biomateriałów Metalowych*; Wyd. Politechniki Koszalińskiej: Koszalin, Poland, 2007; pp. 1–155.
107. Rokicki, R.; Hryniewicz, T. Nitinol Surface Finishing by Magnetoelectropolishing. *Trans. Inst. Met. Finish.* **2008**, *86*, 280–285. [CrossRef]
108. Hryniewicz, T.; Rokicki, R.; Rokosz, K. Modifying Metallic Implants with Magnetoelectropolishing. *Med. Dev. Diagn. Indust.* **2008**, *30*, 102–111.
109. Mtwo. The Efficient NiTi Sytem. Available online: https://www.vdw-dental.com/en/products/detail/mtwo/ (accessed on 7 May 2021).
110. Hryniewicz, T.; Rokosz, K. On the wear inspection and endurance recovery of Nitinol endodontic files. *PAK* **2009**, *55*, 247–250.
111. Shi, P.; Cheng, F.T.; Man, H.C. Improvement in corrosion resistance of NiTi by anodization in acetic acid. *Mater. Lett.* **2007**, *61*, 2385–2388. [CrossRef]
112. Ibris, N.; Rosca, J.C.M. EIS study of Ti and its alloys in biological media. *J. Electroanal. Chem.* **2002**, *526*, 53–62. [CrossRef]
113. Tan, L.; Dodd, R.A.; Crone, W.C. Corrosion and wear-corrosion behaviour of NiTi modified by plasma source implantation. *Biomaterials* **2003**, *24*, 3931–3939. [CrossRef]
114. Cheng, F.T.; Shi, P.; Man, H.C. A preliminary study of TiO_2 deposition on NiTi by a hydrothermal method. *Surf. Coat. Technol.* **2004**, *187*, 26–32. [CrossRef]
115. Figueira, N.; Silva, T.M.; Carmezim, M.J.; Fernandes, J.C.S. Corrosion behaviour of NiTi alloy. *Electrochim. Acta* **2009**, *54*, 921–926. [CrossRef]
116. Shabalovskaya, S.A. Surface, corrosion and biocompatibility aspects of Nitinol as an implant material. *Biomed. Mater. Eng.* **2002**, *12*, 69–109. [PubMed]
117. Venugopalan, R.; Trépanier, C. Assessing the corrosion behaviour of Nitinol for minimally-invasive device design. *Min. Invas. Therap. Allied Technol.* **2000**, *9*, 67–74. [CrossRef]
118. Rondelli, G.; Brunella, M.F.; De Nardo, L.; Cigada, A. Corrosion Behaviour of Nitinol Vascular Stents. *Adv. Sci. Technol.* **2006**, *49*, 252–257. [CrossRef]
119. McInnes, P.M.; Wendt, S.L., Jr.; Retief, D.H.; Weinberg, R. Effect of dentin surface roughness on shear bond strength. *Dent. Mater.* **1990**, *6*, 204–207. [CrossRef]
120. Thompson, S.A. An overview of nickel–titanium alloys used in dentistry. *Int. Endod. J.* **2000**, *33*, 297–310. [CrossRef] [PubMed]
121. Himel, V.T.; Ahmed, K.M.; Wood, D.M.; Alhadainy, H.A. An evaluation of nitinol and stainless steel files used by dental students during a laboratory proficiency exam. *Oral Surg. Oral Med. Oral Pathol. Oral Radiol. Endod.* **1995**, *79*, 232–237. [CrossRef]
122. Pelton, A.R.; Stöckel, D.; Duerig, T.W. Medical Uses of Nitinol. *MSF* **2000**, *327–328*, 63–70. [CrossRef]
123. Civjan, S.; Huget, E.F.; DeSimon, L.B. Potential applications of certain nickel-titanium (nitinol) alloys. *J. Dent. Res.* **1975**, *54*, 89–96. [CrossRef]
124. Karacay, S.; Akin, E.; Olmez, H.; Gurton, A.U.; Sagdic, D. Forsus Nitinol Flat Spring and Jasper Jumper corrections of Class II division 1 malocclusions. *Angle Orthod.* **2006**, *76*, 666–672. [CrossRef] [PubMed]
125. Lee, D.H.; Park, B.; Saxena, A.; Serene, T.P. Enhanced surface hardness by boron implantation in Nitinol alloy. *J. Endod.* **1996**, *22*, 543–546. [CrossRef]
126. Wadood, A. Brief Overview on Nitinol as Biomaterial. *Adv. Mater. Sci. Eng.* **2016**, *2016*, 4173138. [CrossRef]
127. Cutright, D.E.; Bhaskar, S.N.; Perez, B.; Johnson, R.M.; Cowan, G.S., Jr. Tissue reaction to nitinol wire alloy. *Oral Surg. Oral Med. Oral Pathol.* **1973**, *35*, 578–584. [CrossRef]
128. Jensen, O.T.; Jansen, C.E.; Seo, Y.; Yellich, G. Guided Nitinol-Retained (Smileloc) Single-Tooth Dental Restorations. *Oral Maxillofac. Surg. Clin. N. Am.* **2019**, *31*, 437–446. [CrossRef]

129. Glossen, C.R.; Haller, R.H.; Dove, S.B.; del Rio, C.E. A comparison of root canal preparations using Ni-Ti hand, Ni-Ti engine-driven, and K-Flex endodontic instruments. *J. Endod.* **1995**, *21*, 146–151. [CrossRef]
130. Short, J.A.; Morgan, L.A.; Baumgartner, J.C. A comparison of canal centering ability of four instrumentation techniques. *J. Endod.* **1997**, *23*, 503–507. [CrossRef]
131. Schäfer, E. Shaping ability of Hero 642 rotary nickel-titanium instruments and stainless steel hand K-Flexofiles in simulated curved root canals. *Oral Surg. Oral Med. Oral Pathol. Oral Radiol. Endod.* **2001**, *92*, 215–220. [CrossRef] [PubMed]
132. Schäfer, E.; Lohmann, D. Efficiency of rotary nickel-titanium FlexMaster instruments compared with stainless steel hand K-Flexofile—Part 1. Shaping ability in simulated curved canals. *Int. Endod. J.* **2002**, *35*, 505–513. [CrossRef] [PubMed]
133. Craig, R.G.; McIlwain, E.D.; Peyton, F.A. Bending and torsion properties of endodontic instruments. *Oral Surg. Oral Med. Oral Pathol.* **1968**, *25*, 239–254. [CrossRef]
134. Viana, A.C.; Chaves Craveiro de Melo, M.; Guiomar de Azevedo Bahia, M.; Lopes Buono, V.T. Relationship between flexibility and physical, chemical, and geometric characteristics of rotary nickel-titanium instruments. *Oral Surg. Oral Med. Oral Pathol. Oral Radiol. Endod.* **2010**, *110*, 527–533. [CrossRef] [PubMed]
135. Zupanc, J.; Vahdat-Pajouh, N.; Schäfer, E. New thermomechanically treated NiTi alloys—A review. *Int. Endod. J.* **2018**, *51*, 1088–1103. [CrossRef]
136. Tabassum, S.; Zafar, K.; Umer, F. Nickel-Titanium Rotary File Systems: What's New? *Eur. Endod. J.* **2019**, *4*, 111–117. [CrossRef]
137. Dioguardi, M.; Laneve, E.; Di Cosola, M.; Cazzolla, A.P.; Sovereto, D.; Aiuto, R.; Laino, L.; Leanza, T.; Alovisi, M.; Troiano, G.; et al. The Effects of Sterilization Procedures on the Cutting Efficiency of Endodontic Instruments: A Systematic Review and Network Meta-Analysis. *Materials* **2021**, *14*, 1559. [CrossRef] [PubMed]
138. Dioguardi, M.; Sovereto, D.; Aiuto, R.; Laino, L.; Illuzzi, G.; Laneve, E.; Raddato, B.; Caponio, V.C.A.; Dioguardi, A.; Zhurakivska, K.; et al. Effects of Hot Sterilization on Torsional Properties of Endodontic Instruments: Systematic Review with Meta-Analysis. *Materials* **2019**, *12*, 2190. [CrossRef]
139. Dioguardi, M.; Sovereto, D.; Illuzzi, G.; Laneve, E.; Raddato, B.; Arena, C.; Caponio, V.C.A.; Caloro, G.A.; Zhurakivska, K.; Troiano, G.; et al. Management of Instrument Sterilization Workflow in Endodontics: A Systematic Review and Meta-Analysis. *Int. J. Dent.* **2020**, *2020*, 5824369. [CrossRef] [PubMed]
140. Moher, D.; Liberati, A.; Tetzlaff, J.; Altman, D.G.; PRISMA Group. Preferred reporting items for systematic reviews and meta-analyses: The PRISMA statement. *PLoS Med.* **2009**, *6*, e1000097. [CrossRef]
141. Lo Russo, G.; Spolveri, F.; Ciancio, F.; Mori, A. Mendeley: An easy way to manage, share, and synchronize papers and citations. *Plast. Reconstr. Surg.* **2013**, *131*, 946e–947e. [CrossRef]
142. Higgins, J.P.T.; Green, S. *Cochrane Collaboration. Cochrane Handbook for Systematic Reviews of Interventions*; Wiley-Blackwell: Chichester, UK; Hoboken, NJ, USA, 2008; p. 649.
143. Lo, C.K.-L.; Mertz, D.; Loeb, M. Newcastle-Ottawa Scale: Comparing reviewers' to authors' assessments. *BMC Med. Res. Methodol.* **2014**, *14*, 45. [CrossRef]
144. La Rosa, G.R.M.; Shumakova, V.; Isola, G.; Indelicato, F.; Bugea, C.; Pedullà, E. Evaluation of the Cyclic Fatigue of Two Single Files at Body and Room Temperature with Different Radii of Curvature. *Materials* **2021**, *14*, 2256. [CrossRef]
145. Gu, Y.; Kum, K.-Y.; Perinpanayagam, H.; Kim, C.; Kum, D.J.; Lim, S.-M.; Chang, S.-W.; Baek, S.-H.; Zhu, Q.; Yoo, Y.-J. Various heat-treated nickel–titanium rotary instruments evaluated in S-shaped simulated resin canals. *J. Dent. Sci.* **2017**, *12*, 14–20. [CrossRef]
146. Dobrzański, L.A. *Materiały Inżynierskie i Projektowanie Materiałowe: Podstawy Nauki o Materiałach i Metaloznawstwo*, 2nd ed.; WNT: Warszawa, Poland, 2006.
147. Dobrzański, L.A. Significance of materials science for the future development of societies. *J. Mater. Proc. Technol.* **2006**, *175*, 133–148. [CrossRef]
148. Dobrzański, L.A. *Podstawy Metodologii Projektowania Materiałowego*; Wydawnictwo Politechniki Śląskiej: Gliwice, Poland, 2009.
149. Rahim, M.; Frenzel, J.; Frotscher, M.; Pfetzing-Micklich, J.; Steegmüller, R.; Wohlschlögel, M.; Mughrabi, H.; Eggeler, G. Impurity levels and fatigue lives of pseudoelastic NiTi shape memory alloys. *Acta Mater.* **2013**, *61*, 3667–3686. [CrossRef]
150. Bergmans, L.; van Cleynenbreugel, J.; Wevers, M.; Lambrechts, P. Mechanical root canal preparation with NiTi rotary instruments: Rationale, performance and safety. Status report for the American Journal of Dentistry. *Am. J. Dent.* **2001**, *14*, 324–333.
151. Sattapan, B.; Nervo, G.J.; Palamara, J.E.; Messer, H.H. Defects in rotary nickel-titanium files after clinical use. *J. Endod.* **2000**, *26*, 161–165. [CrossRef]
152. Martín, B.; Zelada, G.; Varela, P.; Bahillo, J.G.; Magán, F.; Ahn, S.; Rodríguez, C. Factors influencing the fracture of nickel-titanium rotary instruments. *Int. Endod. J.* **2003**, *36*, 262–266. [CrossRef]
153. Melo, M.C.; Pereira, E.S.; Viana, A.C.; Fonseca, A.M.; Buono, V.T.; Bahia, M.G. Dimensional characterization and mechanical behaviour of K3 rotary instruments. *Int. Endod. J.* **2008**, *41*, 329–338. [CrossRef] [PubMed]
154. De Vasconcelos, R.A.; Murphy, S.; Carvalho, C.A.; Govindjee, R.G.; Govindjee, S.; Peters, O.A. Evidence for Reduced Fatigue Resistance of Contemporary Rotary Instruments Exposed to Body Temperature. *J. Endod.* **2016**, *42*, 782–787. [CrossRef] [PubMed]
155. Dosanjh, A.; Paurazas, S.; Askar, M. The Effect of Temperature on Cyclic Fatigue of Nickel-titanium Rotary Endodontic Instruments. *J. Endod.* **2017**, *43*, 823–826. [CrossRef]
156. Grande, N.M.; Plotino, G.; Silla, E.; Pedullà, E.; DeDeus, G.; Gambarini, G.; Somma, F. Environmental Temperature Drastically Affects Flexural Fatigue Resistance of Nickel-titanium Rotary Files. *J. Endod.* **2017**, *43*, 1157–1160. [CrossRef]

157. Plotino, G.; Grande, N.M.; Mercadé Bellido, M.; Testarelli, L.; Gambarini, G. Influence of Temperature on Cyclic Fatigue Resistance of ProTaper Gold and ProTaper Universal Rotary Files. *J. Endod.* **2017**, *43*, 200–202. [CrossRef]
158. Pedullà, E.; Grande, N.M.; Plotino, G.; Gambarini, G.; Rapisarda, E. Influence of continuous or reciprocating motion on cyclic fatigue resistance of 4 different nickel-titanium rotary instruments. *J. Endod.* **2013**, *39*, 258–261. [CrossRef]
159. Pérez-Higueras, J.J.; Arias, A.; de la Macorra, J.C. Cyclic fatigue resistance of K3, K3XF, and twisted file nickel-titanium files under continuous rotation or reciprocating motion. *J. Endod.* **2013**, *39*, 1585–1588. [CrossRef] [PubMed]
160. Ninan, E.; Berzins, D.W. Torsion and bending properties of shape memory and superelastic nickel-titanium rotary instruments. *J. Endod.* **2013**, *39*, 101–104. [CrossRef] [PubMed]
161. Bahia, M.G.; Buono, V.T. Decrease in the fatigue resistance of nickel-titanium rotary instruments after clinical use in curved root canals. *Oral Surg. Oral Med. Oral Pathol. Oral Radiol. Endod.* **2005**, *100*, 249–255. [CrossRef] [PubMed]
162. Dobrzański, L.A. *Podstawy Nauki o Materiałach*; Wydawnictwo Politechniki Śląskiej: Gliwice, Poland, 2012.
163. Gao, Y.; Shotton, V.; Wilkinson, K.; Phillips, G.; Johnson, W.B. Effects of raw material and rotational speed on the cyclic fatigue of ProFile Vortex rotary instruments. *J. Endod.* **2010**, *36*, 1205–1209. [CrossRef] [PubMed]
164. Bojarski, Z.; Morawiec, H. *Metale z Pamięcią Kształtu*; PWN: Warsaw, Poland, 1989.
165. Launey, M.; Robertson, S.W.; Vien, L.; Senthilnathan, K.; Chintapalli, P.; Pelton, A.R. Influence of microstructural purity on the bending fatigue behavior of VAR-melted superelastic Nitinol. *J. Mech. Behav. Biomed. Mater.* **2014**, *34*, 181–186. [CrossRef]
166. Urbano, M.F.; Coda, A.; Beretta, S.; Cadelli, A.; Sczerzenie, F. The Effect of Inclusions on Fatigue Properties for Nitinol. In *Fatigue and Fracture Metallic Medical Materials and Devices*; Mitchell, M., Smith, S., Woods, T., Berg, B., Eds.; ASTM International: West Conshohocken, PA, USA, 2013; pp. 18–34. [CrossRef]
167. Lin, Z.; Pike, K.; Schlun, M.; Zipse, A.; Draper, J. Nitinol Fatigue Life for Variable Strain Amplitude Fatigue. *J. Mater. Eng. Perform.* **2012**, *21*, 2628–2632. [CrossRef]
168. Lin, Z.; Pike, K.; Zipse, A.; Schlun, M. Nitinol Fatigue Investigation on Stent-Finish Specimens Using Tension-Tension Method. *J. Mater. Eng. Perform.* **2011**, *20*, 591–596. [CrossRef]
169. Tanalp, J.; Kaplan, F.; Sert, S.; Kayahan, B.; Bayirl, G. Quantitative evaluation of the amount of apically extruded debris using 3 different rotary instrumentation systems. *Oral Surg. Oral Med. Oral Pathol. Oral Radiol. Endod.* **2006**, *101*, 250–257. [CrossRef]
170. Zuolo, M.L.; Walton, R.E. Instrument deterioration with usage: Nickel-titanium versus stainless steel. *Quint. Int.* **1997**, *28*, 397–402.
171. Guelzow, A.; Stamm, O.; Martus, P.; Kielbassa, A.M. Comparative study of six rotary nickel-titanium systems and hand instrumentation for root canal preparation. *Int. Endod. J.* **2005**, *38*, 743–752. [CrossRef] [PubMed]
172. Bechelli, C.; Orlandini, S.Z.; Colafranceschi, M. Scanning electron microscope study on the efficacy of root canal wall debridement of hand versus Lightspeed instrumentation. *Int. Endod. J.* **1999**, *32*, 484–493. [CrossRef] [PubMed]
173. Tucker, D.M.; Wenckus, C.S.; Bentkover, S.K. Canal wall planning by engine-driven nickel-titanium instruments, compared with stainless steel hand instrumentation. *J. Endod.* **1997**, *23*, 170–173. [CrossRef]
174. Hryniewicz, T.; Rokicki, R. Improved surface properties of nitinol after magnetoelectropolishing. In Proceedings of the 16th Annual International Conference on Composites/Nano-Engineering "ICCE-16", Kunming, China, 20–26 July 2008.
175. Hryniewicz, T. Biomaterials surface improvement by magnetoelectropolishing. In Proceedings of the BIT Life Sciences' 1st Annual World Congress of IBIO2008, New Starting Line for Decision Makers in Bioeconomy Era, Hangzhou, China, 18–22 May 2008.
176. Product Catalog Dentsply Maillefer. Available online: https://www.maillefer.com/wp-content/uploads/2016/10/2016-Maillefer-Catalog.pdf (accessed on 31 May 2021).
177. Schrader, C.; Ackermann, M.; Barbakow, F. Step-by-step description of a rotary root canals preparation technique. *Int. Endod. J.* **1999**, *32*, 312–320. [CrossRef]
178. ASTM F2063-18. *Standard Specification for Wrought Nickel-Titanium Shape Memory Alloys for Medical Devices and Surgical Implants*; ASTM International: West Conshohocken, PA, USA, 2018.
179. Otsuka, K.; Ren, X. Physical Metallurgy of Ti-Ni-based Shape Memory Alloys. *Prog. Mater. Sci.* **2005**, *50*, 511–678. [CrossRef]
180. Chluba, C.; Ge, W.; Lima de Miranda, R.; Strobel, J.; Kienle, L.; Quandt, E.; Wuttig, M. Shape memory alloys. Ultralow-fatigue shape memory alloy films. *Science* **2015**, *348*, 1004–1007. [CrossRef]
181. Spini, T.S.; Valarelli, F.P.; Cançado, R.H.; Freitas, K.M.; Villarinho, D.J. Transition temperature range of thermally activated nickel-titanium archwires. *J. Appl. Oral. Sci.* **2014**, *22*, 109–117. [CrossRef]
182. GT Rotary Files 20/.06 Yellow 25 mm. Available online: https://www.dentsplysirona.com/en-ca/products/endodontics/glide-path-shaping.html/Endodontics/Glide-Path-%26-Shaping/Rotary-%26-Reciprocating-Files/Shaping/GT-Rotary-Files/p/TUL-GTR0602025/c/1000671.html (accessed on 7 May 2021).
183. ASTM 2063 Shape Memory Ni Ti Alloy Nitinol 55 Nitinol 60 Wire. Available online: https://www.nitinolcn.com/showroom/astm-2063-shape-memory-ni-ti-alloy-nitinol-55-nitinol-60-wire.html (accessed on 7 May 2021).
184. Andreasen, G.F.; Barrett, R.D. An evaluation of cobalt-substituted nitinol wire in orthodontics. *Am. J. Orthod.* **1973**, *63*, 462–470. [CrossRef]
185. Andreasen, G.F.; Hilleman, T.B. An evaluation of 55 cobalt substituted Nitinol wire for use in orthodontics. *J. Am. Dent. Assoc.* **1971**, *82*, 1373–1375. [CrossRef]
186. Massalski, T.B.; Okamoto, H.; Subramanian, P.R.; Kacprzak, L. (Eds.) *Binary Alloy Phase Diagrams*, 2nd ed.; ASM International: Cleveland, OH, USA, 1990; Volume 3, pp. 1–2875.

187. Honma, T.; Matsumoto, T.; Shugo, Y.; Nishida, M. Annual Research Report. *Res. Rep. Nucl. Sci. Lab. Tohoku Univ.* **1979**, *12*, 183–190.
188. Nishida, M.; Wayman, C.M.; Honma, T. Electron microscopy studies of the $Ti_{11}Ni_{14}$ phase in an aged Ti-52.0at%Ni shape memory alloy. *Scr. Metall.* **1985**, *19*, 983–987. [CrossRef]
189. Tadaki, T.; Nakata, Y.; Shimizu, K.; Otsuka, K. Crystal Structure, Composition and Morphology of a Precipitate in an Aged Ti-51 at%Ni Shape Memory Alloy. *Trans. JIM* **1986**, *27*, 731–740. [CrossRef]
190. Saburi, T.; Nenno, S.; Fukuda, T. Crystal structure and morphology of the metastable X phase in shape memory Ti-Ni alloys. *J. Less Com. Met.* **1986**, *125*, 157–166. [CrossRef]
191. Otsuka, K.; Ren, X. Martensitic transformations in nonferrous shape memory alloys. *Mater. Sci. Eng. A* **1999**, *273–275*, 89–105. [CrossRef]
192. Batalu, D.; Guoqiu, H.; Aloman, A.; Cosmeleata, G.; Xiaoshan, L.; Zhihua, Z. A Review on TiNi Shape Memory Alloys (SMA) Used for Medical Applications. Recycling Aspects. Available online: https://www.researchgate.net/profile/Dan_Batalu/publication/268338951_A_review_on_TiNi_shape_memory_alloys_SMA_used_for_medical_applications_Recycling_aspects/links/5471047a0cf216f8cfad0bd7/A-review-on-TiNi-shape-memory-alloys-SMA-used-for-medical-applications-Recycling-aspects.pdf (accessed on 10 May 2021).
193. Cascadan, D.; Grandini, C.R. Structure, Microstructure, and Some Selected Mechanical Properties of Ti-Ni Alloys. In *Recent Advancements in the Metallurgical Engineering and Electrodeposition*; Al-Naib, U.B., Vikraman, D., Karuppasamy, K., Eds.; IntechOpen: Rijeka, Croatia, 2020; pp. 1–14. [CrossRef]
194. Hanlon, J.E.; Butler, S.R.; Wasilewski, R.J. Effect of martensitic transformation on the electrical and magnetic properties of NiTi. *Trans. Metall. Soc. AIME* **1967**, *239*, 1323–1327.
195. Harrison, J.D.; Hodgson, D.E. Use of TiNi in Mechanical and Electrical Connectors. In *Shape Memory Effects in Alloys*; Perkins, J., Ed.; Plenum Press: New York, NY, USA, 1975; pp. 517–523. [CrossRef]
196. Schaffer, J.E.; Plumley, D.L. Fatigue Performance of Nitinol Round Wire with Varying Cold Work Reductions. *J. Mater. Eng. Perform.* **2009**, *18*, 563–568. [CrossRef]
197. ASTM F2004-05. *Standard Test Method for Transformation Temperature of Nickel-Titanium Alloys by Thermal Analysis*; ASTM International: West Conshohocken, PA, USA, 2005.
198. Andreasen, G.F.; Morrow, R.E. Laboratory and clinical analyses of nitinol wire. *Am. J. Orthod.* **1978**, *73*, 142–151. [CrossRef]
199. Andreasen, G.; Wass, K.; Chan, K.C. A review of superelastic and thermodynamic nitinol wire. *Quint. Int.* **1985**, *16*, 623–626.
200. Bryant, S.T.; Thompson, S.A.; al-Omari, M.A.; Dummer, P.M. Shaping ability of Profile rotary nickel-titanium instruments with ISO sized tips in simulated root canals: Part 1. *Int. Endod. J.* **1998**, *31*, 275–281. [CrossRef]
201. Bryant, S.T.; Thompson, S.A.; al-Omari, M.A.; Dummer, P.M. Shaping ability of ProFile rotary nickel-titanium instruments with ISO sized tips in simulated root canals: Part 2. *Int. Endod. J.* **1998**, *31*, 282–289. [CrossRef]
202. Buehler, W.J.; Wang, F.E. A summary of recent research on the Nitinol alloys and their potential application in ocean engineering. *Ocean Eng.* **1968**, *1*, 105–120. [CrossRef]
203. Buehler, W.J.; Cross, W.B. 55-Nitinol unique wire alloy with a memory. *Wire J.* **1969**, *2*, 41–49.
204. Burstone, C.J.; Goldberg, A.J. Beta titanium: A new orthodontic alloy. *Am. J. Orthod.* **1980**, *77*, 121–132. [CrossRef]
205. Burstone, C.J. Variable-modulus orthodontics. *Am. J. Orthod.* **1981**, *80*, 1–16. [CrossRef]
206. Clinard, K.; von Fraunhofer, J.A.; Kuftinec, M.M. The corrosion susceptibility of modern orthodontic spring wires. *J. Dent. Res.* **1981**, *60A*, 628–Abstract 1277.
207. Drake, S.R.; Wayne, D.M.; Powers, J.M.; Asgar, K. Mechanical properties of orthodontic wires in tension, bending, and torsion. *Am. J. Orthod.* **1982**, *82*, 206–210. [CrossRef]
208. Duerig, W. Applications of shape memory. *Mater. Sci. Forum* **1990**, *56–58*, 679–692. [CrossRef]
209. Edie, J.; Andreasen, G. Surface corrosion of Nitinol and stainless wires. *J. Dent. Res.* **1980**, *59A*, 528.
210. Edie, J.W.; Andreasen, G.F.; Zaytoun, M.P. Surface corrosion of nitinol and stainless steel under clinical conditions. *Angle Orthod.* **1981**, *51*, 319–324. [CrossRef]
211. Esposito, P.T.; Cunningham, C.J. A comparison of canal preparation with nickel-titanium and stainless steel instruments. *J. Endod.* **1995**, *21*, 173–176. [CrossRef]
212. Evans, T.J.; Durning, P. Aligning archwires, the shape of things to come?—A fourth and fifth phase of force delivery. *Br. J. Orthod.* **1996**, *23*, 269–275. [CrossRef]
213. Gould, J.V. *Machinability of Nickel–Titanium Alloys*; Metcut Research Associates, Report No. 573–4062–1, Report No. AD-419009; Office of Technical Services, U.S. Deptartment of Commerce: Washington, DC, USA, 1963.
214. Hamanaka, H.; Doi, H.; Kohno, O.; Miura, I. Dental castings of NiTi alloys. Part 2. New casting techniques for NiTi alloys. *J. Dent. Mater.* **1985**, *4*, 573–579.
215. Hasegawa, K. Ti-Ni shape memory alloy for dental use. Trial production of prefabricated straight-slit type posts by electric discharge machining. *J. Dent. Mater.* **1989**, *8*, 388–409. [CrossRef]
216. Hasegawa, K. The studies of Ti-Ni shape memory alloy for dental use—The influence of shape memory alloy post on the stress of post hole. *J. Dent. Mater.* **1991**, *10*, 509–517.
217. Kapila, S.; Haugen, J.W.; Watanabe, L.G. Load-deflection characteristics of nickel-titanium alloy wires after clinical recycling and dry heat sterilization. *Am. J. Orthod. Dentofacial Orthop.* **1992**, *102*, 120–126. [CrossRef]

218. Kimura, H.; Sohmura, T. Pure Ti thermal spray coating on Ti-Ni shape memory alloys and Ti. *J. Osaka Univ. Dent. School* **1987**, *6*, 672–678.
219. Kimura, H.; Sohmura, T. Improvement in corrosion resistance of Ti-Ni shape memory alloy by oxide film coating. *J. Dent. Mater.* **1988**, *7*, 106–110.
220. Kuo, P.; Yang, P.; Zhang, Y.; Yang, H.; Yu, Y.; Dai, K.; Hong, W.Q.; Ke, M.Z.; Cai, T.D.; Tao, J.C. The use of nickel–titanium alloy in orthopaedic surgery in China. *Orthopaedics* **1989**, *12*, 111–116. [CrossRef]
221. Kusy, R.P.; Stush, A.M. Geometric and material parameters of a nickel-titanium and a beta titanium orthodontic arch wire alloy. *Dent. Mater.* **1987**, *3*, 207–217. [CrossRef]
222. Kusy, R.P. A review of contemporary archwires: Their properties and characteristics. *Angle Orthod.* **1997**, *67*, 197–207. [CrossRef]
223. Lee, J.H.; Park, J.B.; Andreasen, G.F.; Lakes, R.S. Thermomechanical study of Ni-Ti alloys. *J. Biomed. Mater. Res.* **1988**, *22*, 573–588. [CrossRef] [PubMed]
224. Marsicovetere, E.S.; Clement, D.J.; del Rio, C.E. Morphometric video analysis of the engine-driven nickel-titanium Lightspeed instrument system. *J. Endod.* **1996**, *22*, 231–235. [CrossRef]
225. Mayhew, M.J.; Kusy, R.P. Effects of sterilization on the mechanical properties and the surface topography of nickel-titanium arch wires. *Am. J. Orthod. Dentofacial Orthop.* **1988**, *93*, 232–236. [CrossRef]
226. Mercier, O.; Torok, E. Mechanical properties of the coldworked martensitic NiTi type alloys. *J. Phys.* **1982**, *43*, C4-267–C4-272. [CrossRef]
227. Miura, F.; Mogi, M.; Ohura, Y.; Hamanaka, H. The super-elastic property of the Japanese NiTi alloy wire for use in orthodontics. *Am. J. Orthod. Dentofacial Orthop.* **1986**, *90*, 1–10. [CrossRef]
228. Miura, F.; Mogi, M.; Okamoto, Y. New application of superelastic NiTi rectangular wire. *J. Clin. Orthod.* **1990**, *24*, 544–548.
229. Saburi, T.; Tatsumi, T.; Nenno, S. Effects of heat treatment on mechanical behaviour of Ti-Ni alloys. *J. Phys.* **1982**, *43*, C4-261–C4-266. [CrossRef]
230. Sachdeva, R.; Fukuyo, S.; Suzuki, K.; Oshida, Y.; Miyazaki, S. Shape memory NiTi alloys—Applications in dentistry. *Mater. Sci. Forum* **1990**, *56–58*, 693–698. [CrossRef]
231. Sarkar, N.K.; Redmond, W.; Schwaninger, B.; Goldberg, A.J. The chloride corrosion behaviour of four orthodontic wires. *J. Oral Rehabil.* **1983**, *10*, 121–128. [CrossRef]
232. Sarkar, N.K.; Schwaninger, B. The in vivo corrosion of Nitinol wire. *J. Dent. Res.* **1980**, *59A*, 528–Abstract 1035.
233. Schäfer, E. Root canal instruments for manual use: A review. *Dent. Traumatol.* **1997**, *13*, 51–64. [CrossRef]
234. Schäfer, E.; Tepel, J.; Hoppe, W. Properties of endodontic hand instruments used in rotary motion. Part 2. Instrumentation of curved canals. *J. Endod.* **1995**, *21*, 493–497. [CrossRef]
235. Schettler, D.; Baumgart, F.; Bensmann, G.; Haasters, J. Method of alveolar bracing in mandibular fractures using a new form of fixation made from memory alloy (preliminary report). *J. Maxillofac. Surg.* **1979**, *7*, 51–54. [CrossRef]
236. Serene, T.P.; Adams, J.D.; Saxena, A. *Nickel–Titanium Instruments: Applications in Endodontics*; Ishiyaku Euro America, Inc.: St. Louis, MO, USA, 1995.
237. Smith, G.A.; von Fraunhofer, J.A.; Casey, G.R. The effect of clinical use and sterilization on selected orthodontic arch wires. *Am. J. Orthod. Dentofacial Orthop.* **1992**, *102*, 153–159. [CrossRef]
238. Stoeckel, D.; Yu, W. Superelastic Ni-Ti wire. *Wire J. Int.* **1991**, 45–50. Available online: https://www.nitinol.com/wp-content/uploads/2012/01/056.pdf (accessed on 25 November 2021).
239. Thompson, S.A.; Dummer, P.M. Shaping ability of Lightspeed rotary nickel-titanium instruments in simulated root canals. Part 1. *J. Endod.* **1997**, *23*, 698–702. [CrossRef]
240. Thompson, S.A.; Dummer, P.M. Shaping ability of Lightspeed rotary nickel-titanium instruments in simulated root canals. Part 2. *J. Endod.* **1997**, *23*, 742–747. [CrossRef]
241. Thompson, S.A.; Dummer, P.M. Shaping ability of ProFile.04 Taper Series 29 rotary nickel-titanium instruments in simulated root canals. Part 1. *Int. Endod. J.* **1997**, *30*, 1–7. [CrossRef] [PubMed]
242. Thompson, S.A.; Dummer, P.M. Shaping ability of ProFile.04 Taper Series 29 rotary nickel-titanium instruments in simulated root canals. Part 2. *Int. Endod. J.* **1997**, *30*, 8–15. [CrossRef]
243. Thompson, S.A.; Dummer, P.M. Shaping ability of NT Engine and McXim rotary nickel-titanium instruments in simulated root canals. Part 1. *Int. Endod. J.* **1997**, *30*, 262–269. [CrossRef] [PubMed]
244. Thompson, S.A.; Dummer, P.M. Shaping ability of NT Engine and McXim rotary nickel-titanium instruments in simulated root canals. Part 2. *Int. Endod. J.* **1997**, *30*, 270–278. [CrossRef] [PubMed]
245. Thompson, S.A.; Dummer, P.M. Shaping ability of Mity Roto 360 degrees and Naviflex rotary nickel-titanium instruments in simulated root canals. Part 1. *J. Endod.* **1998**, *24*, 128–134. [CrossRef]
246. Thompson, S.A.; Dummer, P.M. Shaping ability of Mity Roto 360 degrees and Naviflex rotary nickel-titanium instruments in simulated root canals. Part 2. *J. Endod.* **1998**, *24*, 135–142. [CrossRef]
247. Thompson, S.A.; Dummer, P.M. Shaping ability of Quantec Series 2000 rotary nickel-titanium instruments in simulated root canals: Part 1. *Int. Endod. J.* **1998**, *31*, 259–267. [CrossRef]
248. Thompson, S.A.; Dummer, P.M. Shaping ability of Quantec Series 2000 rotary nickel-titanium instruments in simulated root canals: Part 2. *Int. Endod. J.* **1998**, *31*, 268–274. [CrossRef]

249. Walia, H.; Costas, J.; Brantley, W.; Gerstein, H. Torsional ductility and cutting efficiency of the Nitinol file. *J. Endod.* **1989**, *15*, 174–Abstract 22.
250. Wang, F.E.; Pickart, S.J.; Alperin, H.A. Mechanism of the TiNi martensitic transformation and the crystal structures of TiNi-II and TiNi-III phases. *J. Appl. Phys.* **1972**, *43*, 97–112. [CrossRef]
251. Yoneyama, T.; Doi, H.; Hamanaka, H.; Okamoto, Y.; Mogi, M.; Miura, F. Super-elasticity and thermal behavior of Ni-Ti alloy orthodontic arch wires. *Dent. Mater. J.* **1992**, *11*, 1–10. [CrossRef]
252. Robertson, S.W.; Launey, M.; Shelley, O.; Ong, I.; Vien, L.; Senthilnathan, K.; Saffari, P.; Schlegel, S.; Pelton, A.R. A statistical approach to understand the role of inclusions on the fatigue resistance of superelastic Nitinol wire and tubing. *J. Mech. Behav. Biomed. Mater.* **2015**, *51*, 119–131. [CrossRef]
253. Manoj Samson, R.; Prakash, M.; Nirmal, R.; Vajpayee, G. Vibration Analysis of Nitinol Shape Memory Alloy in Carbon Fibre Reinforced Polymer Composites. *IOP Conf. Ser. Mater. Sci. Eng.* **2020**, *912*, 052029. [CrossRef]
254. Cheung, G.S.; Shen, Y.; Darvell, B.W. Does electropolishing improve the low-cycle fatigue behavior of a nickel-titanium rotary instrument in hypochlorite? *J. Endod.* **2007**, *33*, 1217–1221. [CrossRef] [PubMed]
255. Kuhn, G.; Tavernier, B.; Jordan, L. Influence of structure on nickel-titanium endodontic instruments failure. *J. Endod.* **2001**, *27*, 516–520. [CrossRef]
256. Lopes, H.P.; Elias, C.N.; Vieira, V.T.; Moreira, E.J.; Marques, R.V.; de Oliveira, J.C.; Debelian, G.; Siqueira, J.F., Jr. Effects of electropolishing surface treatment on the cyclic fatigue resistance of BioRace nickel-titanium rotary instruments. *J. Endod.* **2010**, *36*, 1653–1657. [CrossRef] [PubMed]
257. Chekotu, J.C.; Groarke, R.; O'Toole, K.; Brabazon, D. Advances in Selective Laser Melting of Nitinol Shape Memory Alloy Part Production. *Materials* **2019**, *12*, 809. [CrossRef] [PubMed]
258. Zadafiya, K.; Bandhu, D.; Kumari, S.; Chatterjee, S.; Abhishek, K. Recent trends in non-traditional machining of shape memory alloys (SMAs): A review. *CIRP J. Manuf. Sci. Technol.* **2021**, *32*, 217–227. [CrossRef]
259. Bonaccorso, A.; Tripi, T.R.; Rondelli, G.; Condorelli, G.G.; Cantatore, G.; Schäfer, E. Pitting corrosion resistance of nickel-titanium rotary instruments with different surface treatments in seventeen percent ethylenediaminetetraacetic Acid and sodium chloride solutions. *J. Endod.* **2008**, *34*, 208–211. [CrossRef]
260. Tripi, T.R.; Bonaccorso, A.; Condorelli, G.G. Cyclic fatigue of different nickel-titanium endodontic rotary instruments. *Oral Surg. Oral Med. Oral Pathol. Oral Radiol. Endod.* **2006**, *102*, e106–e114. [CrossRef]
261. Lopes, H.P.; Elias, C.N.; Vieira, M.V.; Vieira, V.T.; de Souza, L.C.; Dos Santos, A.L. Influence of Surface Roughness on the Fatigue Life of Nickel-Titanium Rotary Endodontic Instruments. *J. Endod.* **2016**, *42*, 965–968. [CrossRef]
262. Bui, T.B.; Mitchell, J.C.; Baumgartner, J.C. Effect of electropolishing ProFile nickel-titanium rotary instruments on cyclic fatigue resistance, torsional resistance, and cutting efficiency. *J. Endod.* **2008**, *34*, 190–193. [CrossRef]
263. Condorelli, G.G.; Bonaccorso, A.; Smecca, E.; Schäfer, E.; Cantatore, G.; Tripi, T.R. Improvement of the fatigue resistance of NiTi endodontic files by surface and bulk modifications. *Int. Endod. J.* **2010**, *43*, 866–873. [CrossRef]
264. Praisarnti, C.; Chang, J.W.; Cheung, G.S. Electropolishing enhances the resistance of nickel-titanium rotary files to corrosion-fatigue failure in hypochlorite. *J. Endod.* **2010**, *36*, 1354–1357. [CrossRef]
265. Herold, K.S.; Johnson, B.R.; Wenckus, C.S. A scanning electron microscopy evaluation of microfractures, deformation and separation in EndoSequence and Profile nickel-titanium rotary files using an extracted molar tooth model. *J. Endod.* **2007**, *33*, 712–714. [CrossRef]
266. Mwangi, J.W.; Bui, V.D.; Thüsing, K.; Hahn, S.; Wagner, M.F.-X.; Schubert, A. Characterization of the arcing phenomenon in micro-EDM and its effect on key mechanical properties of medical-grade Nitinol. *J. Mater. Proc. Tech.* **2020**, *275*, 116334. [CrossRef]
267. COLTENE. HyFlex®Rotary Files. Available online: https://nam.coltene.com/pim/DOC/BRO/docbro03464-h-en-hyflex-cm-8-5-x-11-0senaindv1.pdf (accessed on 16 November 2021).
268. Pirani, C.; Iacono, F.; Generali, L.; Sassatelli, P.; Nucci, C.; Lusvarghi, L.; Gandolfi, M.G.; Prati, C. HyFlex EDM: Superficial features, metallurgical analysis and fatigue resistance of innovative electro discharge machined NiTi rotary instruments. *Int. Endod. J.* **2016**, *49*, 483–493. [CrossRef]
269. Singh, S.; Maheshwari, S.; Pandey, P.C. Some investigations into the electric discharge machining of hardened tool steel using different electrode materials. *J. Mater. Proc. Tech.* **2004**, *149*, 272–277. [CrossRef]
270. Bojorquez, B.; Marloth, R.T.; Es-Said, O.S. Formation of a crater in the workpiece on an electrical discharge machine. *Eng. Fail. Anal.* **2002**, *9*, 93–97. [CrossRef]
271. Daneshmand, S.; Kahrizi, E.F.; Abedi, E.; Abdolhosseini, M.M. Influence of machining parameters on electro discharge machining of NiTi shape memory alloys. *Int. J. Electrochem. Sci.* **2013**, *8*, 3095–3104.
272. Uslu, G.; Özyürek, T.; Yılmaz, K. Comparison of Alterations in the Surface Topographies of HyFlex CM and HyFlex EDM Nickel-titanium Files after Root Canal Preparation: A Three-dimensional Optical Profilometry Study. *J. Endod.* **2018**, *44*, 115–119. [CrossRef] [PubMed]
273. Iacono, F.; Pirani, C.; Generali, L.; Bolelli, G.; Sassatelli, P.; Lusvarghi, L.; Gandolfi, M.G.; Giorgini, L.; Prati, C. Structural analysis of HyFlex EDM instruments. *Int. Endod. J.* **2017**, *50*, 303–313. [CrossRef]
274. Kaval, M.E.; Capar, I.D.; Ertas, H. Evaluation of the Cyclic Fatigue and Torsional Resistance of Novel Nickel-Titanium Rotary Files with Various Alloy Properties. *J. Endod.* **2016**, *42*, 1840–1843. [CrossRef]

275. Pedullà, E.; Lo Savio, F.; Boninelli, S.; Plotino, G.; Grande, N.M.; La Rosa, G.; Rapisarda, E. Torsional and Cyclic Fatigue Resistance of a New Nickel-Titanium Instrument Manufactured by Electrical Discharge Machining. *J. Endod.* **2016**, *42*, 156–159. [CrossRef]
276. Pelton, A.R.; Russell, S.M.; DiCello, J. The physical metallurgy of nitinol for medical applications. *JOM* **2003**, *55*, 33–37. [CrossRef]
277. Brantley, W.A.; Svec, T.A.; Iijima, M.; Powers, J.M.; Grentzer, T.H. Differential scanning calorimetric studies of nickel titanium rotary endodontic instruments. *J. Endod.* **2002**, *28*, 567–572. [CrossRef] [PubMed]
278. Pereira, E.S.; Peixoto, I.F.; Viana, A.C.; Oliveira, I.I.; Gonzalez, B.M.; Buono, V.T.; Bahia, M.G. Physical and mechanical properties of a thermomechanically treated NiTi wire used in the manufacture of rotary endodontic instruments. *Int. Endod. J.* **2012**, *45*, 469–474. [CrossRef]
279. Gurley, A.; Lambert, T.R.; Beale, D.; Broughton, R. Dual measurement self-sensing technique of NiTi actuators for use in robust control. *Smart Mater. Struct.* **2017**, *26*, 105050. [CrossRef]
280. Dilibal, S.; Sahin, H.; Dursun, E.; Engeberg, E.D. Nickel–titanium shape memory alloy-actuated thermal overload relay system design. *Electr. Eng.* **2017**, *99*, 923–930. [CrossRef]
281. Mehrpouya, M.; Gisario, A.; Broggiato, G.B.; Puopolo, M.; Vesco, S.; Barletta, M. Effect of welding parameters on functionality of dissimilar laser-welded NiTi superelastic (SE) to shape memory effect (SME) wires. *Int. J. Adv. Manuf. Technol.* **2019**, *103*, 1593–1601. [CrossRef]
282. Casati, R.; Saghafi, F.; Biffi, C.A.; Vedani, M.; Tuissi, A. Improved functional properties and efficiencies of nitinol wires under high-performance shape memory effect (HP-SME). *J. Mater. Eng. Perform.* **2017**, *26*, 4964–4969. [CrossRef]
283. *Metale i Ich Stopy*; Dobrzański, L.A. (Ed.) Open Access Library VII(2); International OCSCO World Press: Gliwice, Poland, 2017; pp. 1–982.
284. Tadayyon, G.; Mazinani, M.; Guo, Y.; Zebarjad, S.M.; Tofail, S.A.M.; Biggs, M.J. The effect of annealing on the mechanical properties and microstructural evolution of Ti-rich NiTi shape memory alloy. *Mater. Sci. Eng. A* **2016**, *662*, 564–577. [CrossRef]
285. ASTM E8/E8M-21. *Standard Test Methods for Tension Testing of Metallic Materials*; ASTM International: West Conshohocken, PA, USA, 2021.
286. Sadiq, H.; Wong, M.B.; Al-Mahaidi, R.; Zhao, X.L. The effects of heat treatment on the recovery stresses of shape memory alloys. *Smart Mater. Struct.* **2010**, *19*, 035021. [CrossRef]
287. Gall, K.; Sehitoglu, H.; Chumlyakov, Y.I.; Kireeva, I.V.; Maier, H.J. The influence of aging on critical transformation stress levels and martensite start temperatures in NiTi: Part I—Aged microstructure and micro- mechanical modeling. *J. Eng. Mater. Technol.* **1999**, *121*, 19–27. [CrossRef]
288. Gall, K.; Sehitoglu, H.; Chumlyakov, Y.I.; Kireeva, I.V.; Maier, H.J. The Influence of Aging on Critical Transformation Stress Levels and Martensite Start Temperatures in NiTi: Part II—Discussion of Experimental Results. *J. Eng. Mater. Technol.* **1999**, *121*, 28–37. [CrossRef]
289. Funakubo, H. *Shape Memory Alloys*; University of Tokyo: Tokyo, Japan, 1984; p. 7.
290. Ren, X.; Miura, N.; Taniwaki, K.; Otsuka, K.; Suzuki, T.; Tanaka, K.; Chumlyakov, Y.I.; Asai, M. Understanding the martensitic transformations in TiNi-based alloys by elastic constants measurement. *Mater. Sci. Eng. A* **1999**, *273–275*, 190–194. [CrossRef]
291. Chenxi, N.; Xia, L. Research progress on the effect of root canal sealers on root fracture resistance. *Int. J. Stomatol.* **2020**, *47*, 711–716. [CrossRef]
292. Faus-Llácer, V.; Pérez, R.L.; Faus-Matoses, I.; Ruiz-Sánchez, C.; Zubizarreta-Macho, Á.; Sauro, S.; Faus-Matoses, V. Efficacy of Removing Thermafil and GuttaCore from Straight Root Canal Systems Using a Novel Non-Surgical Root Canal Re-Treatment System: A Micro-Computed Tomography Analysis. *J. Clin. Med.* **2021**, *10*, 1266. [CrossRef]
293. Kim, S.; Kim, S.; Park, J.-W.; Jung, I.-Y.; Shin, S.-J. Comparison of the Percentage of Voids in the Canal Filling of a Calcium Silicate-Based Sealer and Gutta Percha Cones Using Two Obturation Techniques. *Materials* **2017**, *10*, 1170. [CrossRef] [PubMed]
294. Teoh, Y.-Y.; Walsh, L.J. Residual Endodontic Filling Material after Post Space Preparation: A Confocal Microscopic Study. *Materials* **2017**, *10*, 1333. [CrossRef]
295. Zhang, L.; Yu, Y.; Joubert, C.; Bruder, G.; Liu, Y.; Chang, C.-C.; Simon, M.; Walker, S.G.; Rafailovich, M. Differentiation of Dental Pulp Stem Cells on Gutta-Percha Scaffolds. *Polymers* **2016**, *8*, 193. [CrossRef]
296. Ribeiro, M.A.; Queiroz, A.C.F.S.; Silva, P.G.; Yoshinari, G.H.; Guerisoli, D.M.Z.; Pereira, K.F.S. Comparative study of the area filled with gutta-percha in the TC, Thermafil and Lateral Condensation techniques. *Rev. Odontol. UNESP* **2009**, *38*, 65–71.
297. Fan, G.; Chen, W.; Yang, S.; Zhu, J.; Ren, X.; Otsuka, K. Origin of abnormal multi-stage martensitic transformation behavior in aged Ni-rich Ti–Ni shape memory alloys. *Acta Mater.* **2004**, *52*, 4351–4362. [CrossRef]
298. Wang, Z.; Everaerts, J.; Salvati, E.; Korsunsky, A.M. Evolution of thermal and mechanical properties of Nitinol wire as a function of ageing treatment conditions. *J. Alloys Compd.* **2020**, *819*, 153024. [CrossRef]
299. Chad Hornbuckle, B.; Yu, X.X.; Noebe, R.D.; Martens, R.; Weaver, M.L.; Thompson, G.B. Hardening behavior and phase decomposition in very Ni-rich Nitinol alloys. *Mater. Sci. Eng. A* **2015**, *639*, 336–344. [CrossRef]
300. Wang, X.; Kustov, S.; Verlinden, B.; Van Humbeeck, J. Fundamental development on utilizing the R-phase transformation in NiTi shape memory alloys. *Shap. Mem. Superelasticity* **2015**, *1*, 231–239. [CrossRef]
301. Shamimi, A.; Amin-Ahmadi, B.; Stebner, A.; Duerig, T. The effect of low temperature aging and the evolution of R-phase in Ni-rich NiTi. *Shap. Mem. Superelasticity* **2018**, *4*, 417–427. [CrossRef]
302. Zhang, X.; Qian, M.; Zhu, X.; Shang, C.; Geng, L. Elastocaloric effects in ultra-fine grained NiTi microwires processed by cold-drawing. *APL Mater.* **2018**, *6*, 036102. [CrossRef]

303. Świec, P.; Zubko, M.; Lekston, Z.; Stróż, D. Structure and properties of NiTi shape memory alloy after cold rolling in martensitic state. *Acta Phys. Pol. A* **2016**, *130*, 1081–1084. [CrossRef]
304. Burow, J.; Frenzel, J.; Somsen, C.; Prokofiev, E.; Valiev, R.; Eggeler, G. Grain nucleation and growth in deformed NiTi shape memory alloys: An in situ TEM study. *Shap. Mem. Superelast.* **2017**, *3*, 347–360. [CrossRef]
305. Tong, Y.X.; Hu, K.P.; Chen, F.; Tian, B.; Li, L.; Zheng, Y.F. Multiple-stage transformation behavior of Ti49.2Ni50.8 alloy with different initial microstructure processed by equal channel angular pressing. *Intermetallics* **2017**, *85*, 163–169. [CrossRef]
306. Velmurugan, C.; Senthilkumar, V.; Dinesh, S.; Arulkirubakaran, D. Review on phase transformation behavior of NiTi shape memory alloys. *Mater. Today Proc.* **2018**, *5*, 14597–14606. [CrossRef]
307. Kim, J.I.; Miyazaki, S. Effect of nano-scaled precipitates on shape memory behavior of Ti-50.9at.%Ni alloy. *Acta Mater.* **2005**, *53*, 4545–4554. [CrossRef]
308. Liang, X.; Xiao, F.; Chen, H.; Li, Z.; Li, Z.; Jin, X.; Fukuda, T. Internal friction of the R-phase in single crystalline Ti-50.8Ni (at.%) alloy containing controlled precipitate of Ti_3Ni_4. *Scr. Mater.* **2019**, *166*, 44–47. [CrossRef]
309. Pourbabak, S.; Orekhov, A.; Samaee, V.; Verlinden, B.; Van Humbeeck, J.; Schryvers, D. In-Situ TEM stress induced martensitic transformation in $Ni_{50.8}Ti_{49.2}$ microwires. *Shap. Mem. Superelast.* **2019**, *5*, 154–162. [CrossRef]
310. Wang, X.; VerlinDen, B.; Kustov, S. Multi-stage martensitic transformation in Ni-rich NiTi shape memory alloys. *Funct. Mater. Lett.* **2017**, *10*, 1740004. [CrossRef]
311. Liu, S.; Zhu, J.; Lin, X.; Wang, X.; Wang, G. Coupling effect of stretch-bending deformation and electric pulse treatment on phase transformation behavior and superelasticity of a Ti-50.8 at.% Ni alloy. *Mater. Sci. Eng. A* **2021**, *799*, 140164. [CrossRef]
312. Liang, C.L.; Lin, K.L. The microstructure and property variations of metals induced by electric current treatment: A review. *Mater. Charact.* **2018**, *145*, 545–555. [CrossRef]
313. Zhu, R.; Jiang, Y.; Guan, L.; Li, H.; Tang, G. Difference in recrystallization between electropulsing-treated and furnace-treated NiTi alloy. *J. Alloys Compd.* **2016**, *658*, 548–554. [CrossRef]
314. Chen, Y.; Tyc, O.; Kadeřávek, L.; Molnárová, O.; Heller, L.; Šittner, P. Temperature and microstructure dependence of localized tensile deformation of superelastic NiTi wires. *Mater. Des.* **2019**, *174*, 107797. [CrossRef]
315. Sun, Y.; Zhao, G.; Yang, F. Effect of electric current on nanoindentation of superelastic NiTi alloy. *Exp. Mech.* **2015**, *55*, 1503–1509. [CrossRef]
316. Delville, R.; Malard, B.; Pilch, J.; Sittner, P.; Schryvers, D. Microstructure changes during non-conventional heat treatment of thin Ni-Ti wires by pulsed electric current studied by transmission electron microscopy. *Acta Mater.* **2010**, *58*, 4503–4515. [CrossRef]
317. Malard, B.; Pilch, J.; Sittner, P.; Delville, R.; Curfs, C. In situ investigation of the fast microstructure evolution during electropulse treatment of cold drawn NiTi wires. *Acta Mater.* **2011**, *59*, 1542–1556. [CrossRef]
318. Malard, B.; Pilch, J.; Sittner, P.; Gartnerova, V.; Delville, R.; Schryvers, D.; Curfs, C. Microstructure and Functional Superelasticity Property Changes in Thin NiTi Wires Heat Treated by Electric Current. *ESOMAT* **2009**, *2009*, 06004. [CrossRef]
319. Wang, X.; Pu, Z.; Yang, Q.; Huang, S.; Wang, Z.; Kustov, S.; Van Humbeeck, J. Improved functional stability of a coarse-grained Ti-50.8 at.% Ni shape memory alloy achieved by precipitation on dislocation networks. *Scr. Mater.* **2019**, *163*, 57–61. [CrossRef]
320. Nishida, M.; Wayman, C.M.; Honma, T. Precipitation processes in near-equiatomic TiNi shape memory alloys. *Metall. Mater. Trans. A* **1986**, *17*, 1505–1515. [CrossRef]
321. Adharapurapu, R.R.; Jiang, F.; Vecchio, K.S. Aging effects on hardness and dynamic compressive behavior of Ti-55Ni (at.%) alloy. *Mater. Sci. Eng. A* **2010**, *527*, 1665–1676. [CrossRef]
322. Kuang, C.-H.; Chien, C.; Wu, S.-K. Multistage martensitic transformation in high temperature aged $Ti_{48}Ni_{52}$ shape memory alloy. *Intermetallics* **2015**, *67*, 12–18. [CrossRef]
323. Huang, X.; Liu, Y. Effect of annealing on the transformation behavior and superelasticity of NiTi shape memory alloy. *Scr. Mater.* **2001**, *45*, 153–160. [CrossRef]
324. Xue, D.; Zhou, Y.; Ren, X. The effect of ageing on the B2-R transformation behaviors in Ti-51at%Ni alloy. *Intermetallics* **2011**, *19*, 1752–1758. [CrossRef]
325. Jordan, L.; Chandrasekaran, M.; Masse, M.M.; Bouquet, G. Study of the phase transformation in Ni-Ti based shape memory alloys. *J. Phys. IV France* **1995**, *5*, C2-489–C2-494. [CrossRef]
326. Allafi, J.K.; Eggeler, G.; Schmahl, W.W. Quantitative phase analysis in microstructures which display multiple step martensitic transformations in Ni-rich NiTi shape memory alloys. *Mater. Sci. Eng. A* **2006**, *438–440*, 593–596. [CrossRef]
327. Miyazaki, S.; Otsuka, K. Deformation and transition behavior associated with the R-phase in Ti-Ni alloys. *Metall. Mater. Trans. A* **1986**, *17*, 53–63. [CrossRef]
328. Miyazaki, S.; Kimura, S.; Otsuka, K. Shape-memory effect and pseudoelasticity associated with the R-phase transition in Ti-50·5 at.% Ni single crystals. *Philos. Mag. A* **1988**, *57*, 467–478. [CrossRef]
329. Dautovich, D.P.; Purdy, G.R. Phase Transformations in TiNi. *Canad. Metall. Quart.* **1965**, *4*, 129–143. [CrossRef]
330. Vatanayon, S.; Hehemann, R.F. Martensitic Transformations in β Phase Alloys. In *Shape Memory Effects in Alloys*; Perkins, J., Ed.; Plenum: New York, NY, USA, 1975; pp. 115–145.
331. Goo, E.; Sinclair, R. The B2 To R Transformation in $Ti_{50}Ni_{47}Fe_3$ and $Ti_{49.5}Ni_{50.5}$ alloys. *Acta Metall.* **1985**, *33*, 1717–1723. [CrossRef]
332. Hara, T.; Ohba, T.; Okunishi, E.; Otsuka, K. Structural Study of R-Phase in Ti-50.23 at.%Ni and Ti-47.75 at.%Ni-1.50 at.%Fe Alloys. *Mater. Trans. JIM* **1997**, *38*, 11–17. [CrossRef]

333. Duerig, T.W.; Bhattacharya, K. The Influence of the R-Phase on the Superelastic Behavior of NiTi. *Shap. Mem. Superelast.* **2015**, *1*, 153–161. [CrossRef]
334. Šittner, P.; Landa, M.; Lukáš, P.; Novák, V. R-phase transformation phenomena in thermomechanically loaded NiTi polycrystals. *Mech. Mater.* **2006**, *38*, 475–492. [CrossRef]
335. Tobushi, H.; Kimura, K.; Sawada, T.; Hattori, T.; Lin, P.H. Recovery Stress Associated with R-Phase Transformation in TiNi Shape Memory Alloy: Properties under Constant Residual Strain. *JSME Int. J. A* **1994**, *37*, 138–142. [CrossRef]
336. Tobushi, H.; Yamada, S.; Hachisuka, T.; Ikai, A.; Tanaka, K. Thermomechanical properties due to martensitic and R-phase transformations of TiNi shape memory alloy subjected to cyclic loadings. *Smart Mater. Struct.* **1996**, *5*, 788. [CrossRef]
337. Pelton, A.R.; Huang, G.H.; Moine, P.; Sinclair, R. Effects of thermal cycling on microstructure and properties in Nitinol. *Mater. Sci. Eng. A* **2012**, *532*, 130–138. [CrossRef]
338. Uchil, J.; Kumara, K.G.; Mahesh, K.K. Effect of thermal cycling on R-phase stability in a NiTi shape memory alloy. *Mater. Sci. Eng. A* **2002**, *332*, 25–28. [CrossRef]
339. Miyazaki, S.; Igo, Y.; Otsuka, K. Effect of thermal cycling on the transformation temperatures of Ti-Ni alloys. *Acta Metall.* **1986**, *34*, 2045–2051. [CrossRef]
340. Miyazaki, S.; Otsuka, K. Mechanical behaviour associated with the premartensitic rhombohedral-phase transition in a $Ti_{50}Ni_{47}Fe_3$ alloy. *Philos. Mag. A* **1985**, *50*, 393–408. [CrossRef]
341. Ha, J.H.; Kim, S.K.; Cohenca, N.; Kim, H.C. Effect of R-phase heat treatment on torsional resistance and cyclic fatigue fracture. *J. Endod.* **2013**, *39*, 389–393. [CrossRef] [PubMed]
342. Wang, X.; Li, K.; Schryvers, D.; Verlinden, B.; Van Humbeeck, J. R-phase transition and related mechanical properties controlled by low-temperature aging treatment in a Ti–50.8at.% Ni thin wire. *Scr. Mater.* **2014**, *72–73*, 21–24. [CrossRef]
343. Lygin, K.; Langbein, S.; Labenda, P.; Sadek, T. A Methodology for the Development, Production, and Validation of R-Phase Actuators. *J. Mater. Eng. Perform.* **2012**, *21*, 2657–2662. [CrossRef]
344. Zheng, Y.; Jiang, F.; Li, L.; Yang, H.; Liu, Y. Effect of ageing treatment on the transformation behaviour of Ti–50.9 at.% Ni alloy. *Acta Mater.* **2008**, *56*, 736–745. [CrossRef]
345. Kim, J.I.; Liu, Y.; Miyazaki, S. Ageing-induced two-stage R-phase transformation in Ti-50.9at.%Ni. *Acta Mater.* **2004**, *52*, 487–499. [CrossRef]
346. Gall, K.; Tyber, J.; Wilkesanders, G.; Robertson, S.W.; Ritchie, R.O.; Maier, H.J. Effect of microstructure on the fatigue of hot-rolled and cold-drawn NiTi shape memory alloys. *Mater. Sci. Eng. A* **2008**, *486*, 389–403. [CrossRef]
347. Nishida, M.; Wayman, C.M. Electron microscopy studies of the "Premartensitic" transformations in an aged Ti-51 at%Ni shape memory alloy. *Metallography* **1988**, *21*, 255–273. [CrossRef]
348. Favier, D.; Liu, Y.; McCormick, P.G. Three stage transformation behaviour in aged NiTi. *Scr. Metall. Mater.* **1993**, *28*, 669–672. [CrossRef]
349. Liu, X.; Wang, Y.; Yang, D.; Qi, M. The effect of ageing treatment on shape-setting and superelasticity of a nitinol stent. *Mater. Charact.* **2008**, *59*, 402–406. [CrossRef]
350. Khalil-Allafi, J.; Eggeler, G.; Dlouhy, A.; Schmahl, W.W.; Somsen, C.H. On the influence of heterogeneous precipitation on martensitic transformations in a Ni-rich NiTi shape memory alloy. *Mater. Sci. Eng. A* **2004**, *378*, 148–151. [CrossRef]
351. Matsumoto, H. Appearance of an intermediate phase with thermal cycling on the transformation of NiTi. *J. Mater. Sci. Lett.* **1991**, *10*, 408–410. [CrossRef]
352. Matsumoto, H. Transformation behaviour with thermal cycling in NiTi alloys. *J. Alloys Compd.* **2003**, *350*, 213–217. [CrossRef]
353. Dilibal, S.; Hamilton, R.F.; Lanba, A. The effect of employed loading mode on the mechanical cyclic stabilization of NiTi shape memory alloys. *Intermetallics* **2017**, *89*, 1–9. [CrossRef]
354. Piekielny, M.; Jarmołowicz, M.; Dobrzyński, M. Odporność na cykliczne zmęczenie wybranych endodontycznych narzędzi maszynowych w świetle piśmiennictwa. *Inż. Fiz. Med.* **2020**, *9*, 143–144.
355. Fan, G.; Zhou, Y.; Chen, W.; Yang, S.; Ren, X.; Otsuka, K. Precipitation kinetics of Ti_3Ni_4 in polycrystalline Ni-rich TiNi alloys and its relation to abnormal multi-stage transformation behavior. *Mater. Sci. Eng. A* **2006**, *438–440*, 622–626. [CrossRef]
356. Zeng, C.Y.; Cao, S.; Li, Y.Y.; Zhao, Z.X.; Yao, X.Y.; Ma, X.; Zhang, X.P. A hidden single-stage martensitic transformation from B2 parent phase to B19′ martensite phase in an aged $Ni_{51}Ti_{49}$ alloy. *Mater. Lett.* **2019**, *253*, 99–101. [CrossRef]
357. Kaya, I.; Tobe, H.; Karaca, H.E.; Nagasako, M.; Kainuma, R.; Chumlyakov, Y. Positive and negative two-way shape memory effect in [111]-oriented $Ni_{51}Ti_{49}$ single crystals. *Mater. Sci. Eng. A* **2015**, *639*, 42–53. [CrossRef]
358. Chen, H.; Xiao, F.; Liang, X.; Li, Z.; Li, Z.; Jin, X.; Min, N.; Fukuda, T. Improvement of the stability of superelasticity and elastocaloric effect of a Ni-rich Ti-Ni alloy by precipitation and grain refinement. *Scr. Mater.* **2019**, *162*, 230–234. [CrossRef]
359. Poletika, T.M.; Girsova, S.L.; Lotkov, A.I. Ti_3Ni_4 precipitation features in heat-treated grain/subgrain nanostructure in Ni-rich TiNi alloy. *Intermetallics* **2020**, *127*, 106966. [CrossRef]
360. Liu, S.; Zhu, J.; Lin, Y.; Wang, G.; Wang, X. Effect of stretching-bending deformation and aging treatment on phase transformation behavior and superelasticity of Ti-50.8 at.% Ni alloy. *Intermetallics* **2021**, *129*, 107051. [CrossRef]
361. Xiao, F.; Fukuda, T.; Kakeshita, T. Inverse elastocaloric effect in a Ti-Ni alloy containing aligned coherent particles of Ti_3Ni_4. *Scr. Mater.* **2016**, *124*, 133–137. [CrossRef]

362. Cao, S.; Zeng, C.Y.; Li, Y.Y.; Yao, X.; Ma, X.; Samaee, V.; Schryvers, D.; Zhang, X.P. Quantitative FIB/SEM three-dimensional characterization of a unique Ni_4Ti_3 network in a porous $Ni_{50.8}Ti_{49.2}$ alloy undergoing a two-step martensitic transformation. *Mater. Charact.* **2020**, *169*, 110595. [CrossRef]
363. Kaya, I.; Acar, E.; Karaca, H.E. Effects of deformation temperature and amount on the two-way shape memory effect of solutionized $Ni_{50.8}Ti_{49.2}$ alloys. *Intermetallics* **2019**, *114*, 106607. [CrossRef]
364. Hirsch, P.; Howie, A.; Nicholson, R.B.; Pashley, D.W.; Whelan, M.J. *Electron Microscopy of Thin Crystals*, 2nd ed.; R. E. Krieger Publishing Company: Malabar, FL, USA, 1977; pp. 169, 317.
365. Honma, T. The effect of aging, on the spontaneous shape change and the all-round shape memory effect in Ni-rich TiNi alloy. In Proceedings of the International Conference on Martensitic Transformations ICOMAT-86, Nara, Japan, 26–30 August 1986; pp. 709–716.
366. Kainuma, R.; Matsumoto, M.; Honma, T. The mechanism of the all-round shape memory effect in a Ni-rich TiNi alloy. In Proceedings of the International Conference on Martensitic Transformations ICOMAT-86, Nara, Japan, 26–30 August 1986; pp. 717–722.
367. Koskimaki, D.; Marcinkowski, M.J.; Sastri, A.S. Solid State Diffusional Transformations in the Near Equiatomic Ni-Ti Alloys. *Trans. Metall. Soc. AIME* **1969**, *245*, 1883–1890.
368. Chen, Q.; Wu, X.F.; Ko, T. The effects of Ti_3Ni_4 precipitates on the R-phase transformation. *Scr. Metall. Mater.* **1993**, *29*, 49–53. [CrossRef]
369. Xie, C.Y.; Zhao, L.C.; Lei, T.C. Effect of precipitates on the electrical resistivity-temperature curves in an aged Ti-51.8 at % Ni shape memory alloy. *Scr. Metall.* **1989**, *23*, 2131–2136. [CrossRef]
370. Xie, C.Y.; Zhao, L.C.; Lei, T.C. Effect of Ti_3Ni_4 precipitates on the phase transitions in an aged Ti-51.8at% Ni shape memory alloy. *Scr. Metall. Mater.* **1990**, *24*, 1753–1758. [CrossRef]
371. Nishida, M.; Wayman, C.M.; Kainuma, R.; Honma, T. Further electron microscopy studies of the $Ti_{11}Ni_{14}$ phase in an aged Ti-52at%Ni shape memory alloy. *Scr. Metall.* **1986**, *20*, 899–904. [CrossRef]
372. Zou, W.H.; Han, X.D.; Wang, R.; Zhang, Z.; Zhang, W.-Z.; Lai, J.K.L. TEM and HREM study of the interphase interface structure of Ti_3Ni_4 precipitates and parent phase in an aged TiNi shape memory alloy. *Mater. Sci. Eng. A* **1996**, *219*, 142–147. [CrossRef]
373. Khalil-Allafi, J.; Ren, X.; Eggeler, G. The mechanism of multistage martensitic transformations in aged Ni-rich NiTi shape memory alloys. *Acta Mater.* **2002**, *50*, 793–803. [CrossRef]
374. Wang, X.; Li, C.; Verlinden, B.; Van Humbeeck, J. Effect of grain size on aging microstructure as reflected in the transformation behavior of a low-temperature aged Ti–50.8 at.% Ni alloy. *Scr. Mater.* **2013**, *69*, 545–548. [CrossRef]
375. Van Humbeeck, J. Non-medical applications of shape memory alloys. *Mater. Sci. Eng. A* **1999**, *273–275*, 134–148. [CrossRef]
376. Cao, S.; Nishida, M.; Schryvers, D. Quantitative three-dimensional analysis of Ni_4Ti_3 precipitate morphology and distribution in polycrystalline Ni-Ti. *Acta Mater.* **2011**, *59*, 1780–1789. [CrossRef]
377. Pushin, V.G.; Stolyarov, V.V.; Valiev, R.Z.; Lowe, T.C.; Zhu, Y.T. Nanostructured TiNi based shape memory alloys processed by severe plastic deformation. *Mater. Sci. Eng.* **2005**, *410–411*, 386–389. [CrossRef]
378. Moon, H.-j.; Chun, S.-j.; Liu, Y.; Yang, H.; Kim, Y.-w.; Nam, T.-h. Effect of alloy composition on the B2–R transformation in rapidly solidified Ti–Ni alloys. *J. Alloys Compd.* **2013**, *577*, S259–S264. [CrossRef]
379. Stróż, D.; Kwarciak, J.; Morawiec, H. Effect of ageing on martensitic transformation in NiTi shape memory alloy. *J. Mater. Sci.* **1988**, *23*, 4127–4131. [CrossRef]
380. Stróż, D.; Bojarski, Z.; Ilczuk, J.; Lekston, Z.; Morawiec, H. Effect of thermal cycling on as-quenched and aged nickel-rich Ni-Ti alloy. *J. Mater. Sci.* **1991**, *26*, 1741–1748. [CrossRef]
381. Meisel, L.V.; Cote, P.J. *Transient Phenomena Following Precipitation and Resolution Anneals in a NiTi Alloy*; Minerals, Metals and Materials Society: 173; US Army Armament Research, Development and Engineering Center: Warrendale, PA, USA, 1992; Volume 1.
382. Morawiec, H.; Stróż, D.; Chrobak, D. Effect of Deformation and Thermal Treatment of NiTi Alloy on Transition Sequence. *J. Phys. IV France* **1995**, *5*, C2-205–C2-210. [CrossRef]
383. Bataillard, L.; Gotthardt, R. Influence of Thermal Treatment on the Appearance of a Three Step Martensitic Transformation in NiTi. *J. Phys. IV Fr.* **1995**, *5*, C8-647–C8-652. [CrossRef]
384. Morawiec, H.; Stróż, D.; Goryczka, T.; Chrobak, D. Two-stage martensitic transformation in a deformed and annealed NiTi alloy. *Scr. Mater.* **1996**, *35*, 485–490. [CrossRef]
385. Morawiec, H.; Ilczuk, J.; Stróż, D.; Goryczka, T.; Chrobak, D. Two-Stage Martensitic Transformation in NiTi Alloys Caused by Stress Fields. *J. Phys. IV Fr.* **1997**, *7*, C5-155–C5-159. [CrossRef]
386. Bataillard, L.; Bidaux, J.-E.; Gotthardt, R. Interaction between microstructure and multiple-step transformation in binary NiTi alloys using in-situ transmission electron microscopy observations. *Philos. Mag. A* **1998**, *78*, 327–344. [CrossRef]
387. Khalil-Allafi, J.; Dlouhy, A.; Eggeler, G. Ni_4Ti_3-precipitation during aging of NiTi shape memory alloys and its influence on martensitic phase transformations. *Acta Mater.* **2002**, *50*, 4255–4274. [CrossRef]
388. Dlouhy, A.; Khalil-Allafi, J.; Eggeler, G. Multiple-step martensitic transformations in Ni-rich NiTi alloys—An in-situ transmission electron microscopy investigation. *Philos. Mag. A* **2003**, *83*, 339–363. [CrossRef]
389. Sitepu, H.; Schmahl, W.W.; Allafi, J.K.; Eggeler, G.; Dlouhy, A.; Toebbens, D.M.; Tovar, M. Neutron diffraction phase analysis during thermal cycling of a Ni-rich NiTi shape memory alloy using the Rietveld method. *Scr. Mater.* **2002**, *46*, 543–548. [CrossRef]

390. Nishida, M.; Hara, T.; Ohba, T.; Yamaguchi, K.; Tanaka, K.; Yamauchi, K. Experimental Consideration of Multistage Martensitic Transformation and Precipitation Behavior in Aged Ni-Rich Ti-Ni Shape Memory Alloys. *Mater. Trans.* **2003**, *44*, 2631–2636. [CrossRef]
391. Frick, C.P.; Ortega, A.M.; Tyber, J.; Gall, K.; Maier, H.J. Multiscale structure and properties of cast and deformation processed polycrystalline NiTi shape-memory alloys. *Metall. Mater. Trans. A* **2004**, *35*, 2013–2025. [CrossRef]
392. Tirry, W.; Schryvers, D. Quantitative determination of strain fields around Ni_4Ti_3 precipitates in NiTi. *Acta Mater.* **2005**, *53*, 1041–1049. [CrossRef]
393. Karaca, H.E.; Kaya, I.; Tobe, H.; Basaran, B.; Nagasako, M.; Kainuma, R.; Chumlyakov, Y. Shape memory behavior of high strength $Ni_{54}Ti_{46}$ alloys. *Mater. Sci. Eng. A* **2013**, *580*, 66–70. [CrossRef]
394. ASTM E8M–91. *Standard Test Methods for Tension Testing of Metallic Materials*; ASTM International: West Conshohocken, PA, USA, 1991.
395. Liu, Y.; Van Humbeeck, J.; Stalmans, R.; Delaey, L. Some aspects of the properties of NiTi shape memory alloy. *J. Alloys Compd.* **1997**, *247*, 115–121. [CrossRef]
396. Liu, Y. Detwinning process and its anisotropy in shape memory alloys. *Smart Mater.* **2001**, *4234*, 82–93. [CrossRef]
397. Liu, Y.; Xie, Z.; Van Humbeeck, J.; Delaey, L.; Liu, Y. On the deformation of the Twinned domain in NiTi shape memory alloys. *Philos. Mag. A* **2000**, *80*, 1935–1953. [CrossRef]
398. Chen, Y.; Jiang, H.-c.; Rong, L.-j.; Xiao, L.; Zhao, X.-q. Mechanical behavior in NiTiNb shape memory alloys with low Nb content. *Intermetallics* **2011**, *19*, 217–220. [CrossRef]
399. Tong, Y.X.; Jiang, P.C.; Chen, F.; Tian, B.; Li, L.; Zheng, Y.F.; Gunderov, D.V.; Valiev, R.Z. Microstructure and martensitic transformation of an ultrafine-grained TiNiNb shape memory alloy processed by equal channel angular pressing. *Intermetallics* **2014**, *49*, 81–86. [CrossRef]
400. Salje, E.K.H.; Koppensteiner, J.; Reinecker, M.; Schranz, W.; Planes, A. Jerky elasticity: Avalanches and the martensitic transition in $Cu_{74.08}Al_{23.13}Be_{2.79}$ shape-memory alloy. *Appl. Phys. Lett.* **2009**, *95*, 231908. [CrossRef]
401. Gallardo, M.C.; Manchado, J.; Romero, F.J.; del Cerro, J.; Salje, E.K.H.; Planes, A.; Vives, E.; Romero, R.; Stipcich, M. Avalanche criticality in the martensitic transition of $Cu_{67.64}Zn_{16.71}Al_{15.65}$ shape-memory alloy: A calorimetric and acoustic emission study. *Phys. Rev. B* **2010**, *81*, 174102. [CrossRef]
402. McCormick, P.G.; Liu, Y. Thermodynamic analysis of the martensitic transformation in NiTi—II. Effect of transformation cycling. *Acta Metall. Mater.* **1994**, *42*, 2407–2413. [CrossRef]
403. Liu, Y.; McCormick, P.G. Thermodynamic analysis of the martensitic transformation in NiTi—I. Effect of heat treatment on transformation behaviour. *Acta Metall. Mater.* **1994**, *42*, 2401–2406. [CrossRef]
404. Olson, G.B.; Cohen, M. Reply to "On the equilibrium temperature in thermoelastic martensitic transformations". *Scr. Metall.* **1977**, *11*, 345–347. [CrossRef]
405. Salzbrenner, R.J.; Cohen, M. On the thermodynamics of thermoelastic martensitic transformations. *Acta Metall.* **1979**, *27*, 739–748. [CrossRef]
406. Olson, G.B.; Owen, W.S. *Martenite*; ASM International: Materials Park, OH, USA, 1992.
407. Ortin, J.; Planes, A. Thermodynamic analysis of thermal measurements in thermoelastic martensitic transformations. *Acta Metall.* **1988**, *36*, 1873–1889. [CrossRef]
408. Zhou, H.; Peng, B.; Zheng, Y.F. An overview of the mechanical properties of nickel-titanium endodontic instruments. *Endod. Top.* **2013**, *29*, 42–54. [CrossRef]
409. McKelvey, A.L.; Ritchie, R.O. Fatigue-crack growth behavior in the superelastic and shape-memory alloy nitinol. *Metall. Mater. Trans. A* **2001**, *32*, 731–743. [CrossRef]
410. Shen, Y.; Zhou, H.M.; Zheng, Y.F.; Peng, B.; Haapasalo, M. Current challenges and concepts of the thermomechanical treatment of nickel-titanium instruments. *J. Endod.* **2013**, *39*, 163–172. [CrossRef]
411. Dentsply Sirona. Available online: https://www.dentsplysirona.com/pl-pl/explore/endodontics.html (accessed on 17 November 2021).
412. Kim, H.; Jeon, S.J.; Seo, M.S. Comparison of the canal transportation of ProTaper GOLD, WaveOne GOLD, and TruNatomy in simulated double-curved canals. *BMC Oral Health* **2021**, *21*, 533. [CrossRef]
413. Pereira, É.S.; Viana, A.C.; Buono, V.T.; Peters, O.A.; Bahia, M.G. Behavior of nickel-titanium instruments manufactured with different thermal treatments. *J. Endod.* **2015**, *41*, 67–71. [CrossRef] [PubMed]
414. Hu, W.; Whitten, B.; Sedgley, C.; Svec, T. Effect of three NiTi files on transportation of the apical foramen. *Int. Endod. J.* **2014**, *47*, 1064–1071. [CrossRef] [PubMed]
415. Hieawy, A.; Haapasalo, M.; Zhou, H.; Wang, Z.J.; Shen, Y. Phase Transformation Behavior and Resistance to Bending and Cyclic Fatigue of ProTaper Gold and ProTaper Universal Instruments. *J. Endod.* **2015**, *41*, 1134–1138. [CrossRef] [PubMed]
416. Shen, Y.; Zhou, H.M.; Zheng, Y.F.; Campbell, L.; Peng, B.; Haapasalo, M. Metallurgical characterization of controlled memory wire nickel-titanium rotary instruments. *J. Endod.* **2011**, *37*, 1566–1571. [CrossRef]
417. Özyürek, T. Cyclic Fatigue Resistance of Reciproc, WaveOne, and WaveOne Gold Nickel-Titanium Instruments. *J. Endod.* **2016**, *42*, 1536–1539. [CrossRef]
418. Plotino, G.; Grande, N.M.; Cotti, E.; Testarelli, L.; Gambarini, G. Blue treatment enhances cyclic fatigue resistance of vortex nickel-titanium rotary files. *J. Endod.* **2014**, *40*, 1451–1453. [CrossRef]

419. Shen, Y.; Zhou, H.; Coil, J.M.; Aljazaeri, B.; Buttar, R.; Wang, Z.; Zheng, Y.F.; Haapasalo, M. ProFile Vortex and Vortex Blue Nickel-Titanium Rotary Instruments after Clinical Use. *J. Endod.* **2015**, *41*, 937–942. [CrossRef]
420. De-Deus, G.; Silva, E.J.; Vieira, V.T.; Belladonna, F.G.; Elias, C.N.; Plotino, G.; Grande, N.M. Blue Thermomechanical Treatment Optimizes Fatigue Resistance and Flexibility of the Reciproc Files. *J. Endod.* **2017**, *43*, 462–466. [CrossRef]
421. Gao, Y.; Gutmann, J.L.; Wilkinson, K.; Maxwell, R.; Ammon, D. Evaluation of the impact of raw materials on the fatigue and mechanical properties of ProFile Vortex rotary instruments. *J. Endod.* **2012**, *38*, 398–401. [CrossRef] [PubMed]
422. Gagliardi, J.; Versiani, M.A.; de Sousa-Neto, M.D.; Plazas-Garzon, A.; Basrani, B. Evaluation of the shaping characteristics of ProTaper Gold, ProTaper NEXT, and ProTaper Universal in curved canals. *J. Endod.* **2015**, *41*, 1718–1724. [CrossRef]
423. Adıgüzel, M.; Capar, I.D. Comparison of cyclic fatigue resistance of WaveOne and WaveOne Gold small, primary, and large instruments. *J. Endod.* **2017**, *43*, 623–627. [CrossRef] [PubMed]
424. Duke, F.; Shen, Y.; Zhou, H.; Ruse, N.D.; Wang, Z.J.; Hieawy, A.; Haapasalo, M. Cyclic Fatigue of ProFile Vortex and Vortex Blue Nickel-Titanium Files in Single and Double Curvatures. *J. Endod.* **2015**, *41*, 1686–1690. [CrossRef] [PubMed]
425. Elnaghy, A.M.; Elsaka, S.E. Effect of sodium hypochlorite and saline on cyclic fatigue resistance of WaveOne Gold and Reciproc reciprocating instruments. *Int. Endod. J.* **2017**, *50*, 991–998. [CrossRef]
426. Serafin, M.; De Biasi, M.; Franco, V.; Generali, L.; Angerame, D. Influence of different motions on the cyclic fatigue resistance of Reciproc and Reciproc Blue endodontic instruments. *J. Conserv. Dent.* **2019**, *22*, 449–453. [CrossRef]
427. Keskin, C.; Inan, U.; Demiral, M.; Keleş, A. Cyclic Fatigue Resistance of Reciproc Blue, Reciproc, and WaveOne Gold Reciprocating Instruments. *J. Endod.* **2017**, *43*, 1360–1363. [CrossRef] [PubMed]
428. Nguyen, H.H.; Fong, H.; Paranjpe, A.; Flake, N.M.; Johnson, J.D.; Peters, O.A. Evaluation of the resistance to cyclic fatigue among ProTaper Next, ProTaper Universal, and Vortex Blue rotary instruments. *J. Endod.* **2014**, *40*, 1190–1193. [CrossRef]
429. Topçuoğlu, H.S.; Düzgün, S.; Aktı, A.; Topçuoğlu, G. Laboratory comparison of cyclic fatigue resistance of WaveOne Gold, Reciproc and WaveOne files in canals with a double curvature. *Int. Endod. J.* **2017**, *50*, 713–717. [CrossRef]
430. Topçuoğlu, H.S.; Topçuoğlu, G. Cyclic Fatigue Resistance of Reciproc Blue and Reciproc Files in an S-shaped Canal. *J. Endod.* **2017**, *43*, 1679–1682. [CrossRef] [PubMed]
431. Uygun, A.D.; Kol, E.; Topcu, M.K.; Seckin, F.; Ersoy, I.; Tanriver, M. Variations in cyclic fatigue resistance among ProTaper Gold, ProTaper Next and ProTaper Universal instruments at different levels. *Int. Endod. J.* **2016**, *49*, 494–499. [CrossRef] [PubMed]
432. Serafin, M.; De Biasi, M.; Franco, V.; Angerame, D. In vitro comparison of cyclic fatigue resistance of two rotary single-file endodontic systems: OneCurve vs. OneShape. *Odontology* **2019**, *107*, 196–201. [CrossRef]
433. Duque, J.A.; Vivan, R.R.; Cavenago, B.C.; Amoroso-Silva, P.A.; Bernardes, R.A.; Vasconcelos, B.C.; Duarte, M.A. Influence of NiTi alloy on the root canal shaping capabilities of the ProTaper Universal and ProTaper Gold rotary instrument systems. *J. Appl. Oral Sci.* **2017**, *25*, 27–33. [CrossRef] [PubMed]
434. Elnaghy, A.M.; Elsaka, S.E. Shaping ability of ProTaper Gold and ProTaper Universal files by using cone-beam computed tomography. *Indian J. Dent. Res.* **2016**, *27*, 37–41. [CrossRef] [PubMed]
435. Özyürek, T.; Yılmaz, K.; Uslu, G. Shaping Ability of Reciproc, WaveOne GOLD, and HyFlex EDM Single-file Systems in Simulated S-shaped Canals. *J. Endod.* **2017**, *43*, 805–809. [CrossRef]
436. Pinheiro, S.R.; Alcalde, M.P.; Vivacqua-Gomes, N.; Bramante, C.M.; Vivan, R.R.; Duarte, M.A.H.; Vasconcelos, B.C. Evaluation of apical transportation and centring ability of five thermally treated NiTi rotary systems. *Int. Endod. J.* **2018**, *51*, 705–713. [CrossRef]
437. Silva, E.J.; Muniz, B.L.; Pires, F.; Belladonna, F.G.; Neves, A.A.; Souza, E.M.; De-Deus, G. Comparison of canal transportation in simulated curved canals prepared with ProTaper Universal and ProTaper Gold systems. *Restor. Dent. Endod.* **2016**, *41*, 1–5. [CrossRef] [PubMed]
438. Vasconcelos, R.A.; Arias, A.; Peters, O.A. Lateral and axial cutting efficiency of instruments manufactured with conventional nickel-titanium and novel gold metallurgy. *Int. Endod. J.* **2018**, *51*, 577–583. [CrossRef] [PubMed]
439. Dentsply Sirona. TruNatomy Brochure. Available online: https://www.dentsplysirona.com/en/explore/endodontics/trunatomy.html (accessed on 18 November 2021).
440. Elnaghy, A.M.; Elsaka, S.E.; Mandorah, A.O. In vitro comparison of cyclic fatigue resistance of TruNatomy in single and double curvature canals compared with different nickel-titanium rotary instruments. *BMC Oral Health* **2020**, *20*, 38. [CrossRef]
441. FKG Swiss Endo. Catalogue. Available online: https://www.fkg.ch/sites/default/files/FKG_Catalogue%202019_EN_WEB.pdf (accessed on 17 November 2021).
442. Gambarini, G.; Grande, N.M.; Plotino, G.; Somma, F.; Garala, M.; De Luca, M.; Testarelli, L. Fatigue resistance of engine-driven rotary nickel-titanium instruments produced by new manufacturing methods. *J. Endod.* **2008**, *34*, 1003–1005. [CrossRef]
443. Berendt, C. US Patent 20070072147A1: Method of Preparing Nitinol for Use in Manufacturing Instruments with Improved Fatigue Resistance. 2007. Available online: https://patentimages.storage.googleapis.com/24/b9/52/82a5ccc8031262/US20070072147A1.pdf (accessed on 19 November 2021).
444. Alapati, S.B.; Brantley, W.A.; Iijima, M.; Clark, W.A.; Kovarik, L.; Buie, C.; Liu, J.; Johnson, W.B. Metallurgical characterization of a new nickel-titanium wire for rotary endodontic instruments. *J. Endod.* **2009**, *35*, 1589–1593. [CrossRef]
445. Braga, L.C.; Faria Silva, A.C.; Buono, V.T.; de Azevedo Bahia, M.G. Impact of heat treatments on the fatigue resistance of different rotary nickel-titanium instruments. *J. Endod.* **2014**, *40*, 1494–1497. [CrossRef]
446. Ye, J.; Gao, Y. Metallurgical characterization of M-Wire nickel-titanium shape memory alloy used for endodontic rotary instruments during low-cycle fatigue. *J. Endod.* **2012**, *38*, 105–107. [CrossRef]

447. Johnson, E.; Lloyd, A.; Kuttler, S.; Namerow, K. Comparison between a novel nickel-titanium alloy and 508 nitinol on the cyclic fatigue life of ProFile 25/.04 rotary instruments. *J. Endod.* **2008**, *34*, 1406–1409. [CrossRef] [PubMed]
448. Pereira, E.S.; Gomes, R.O.; Leroy, A.M.; Singh, R.; Peters, O.A.; Bahia, M.G.; Buono, V.T. Mechanical behavior of M-Wire and conventional NiTi wire used to manufacture rotary endodontic instruments. *Dent. Mater.* **2013**, *29*, e318–e324. [CrossRef]
449. Montalvão, D.; Alçada, F.S. Numeric comparison of the static mechanical behavior between ProFile GT and ProFile GT series X rotary nickel-titanium files. *J. Endod.* **2011**, *37*, 1158–1161. [CrossRef]
450. Al-Hadlaq, S.M.; Aljarbou, F.A.; AlThumairy, R.I. Evaluation of cyclic flexural fatigue of M-wire nickel-titanium rotary instruments. *J. Endod.* **2010**, *36*, 305–307. [CrossRef]
451. Larsen, C.M.; Watanabe, I.; Glickman, G.N.; He, J. Cyclic fatigue analysis of a new generation of nickel titanium rotary instruments. *J. Endod.* **2009**, *35*, 401–403. [CrossRef]
452. Kramkowski, T.R.; Bahcall, J. An in vitro comparison of torsional stress and cyclic fatigue resistance of ProFile GT and ProFile GT Series X rotary nickel-titanium files. *J. Endod.* **2009**, *35*, 404–407. [CrossRef]
453. Shen, Y.; Coil, J.M.; Zhou, H.; Zheng, Y.; Haapasalo, M. HyFlex nickel-titanium rotary instruments after clinical use: Metallurgical properties. *Int. Endod. J.* **2013**, *46*, 720–729. [CrossRef]
454. Zhou, H.M.; Shen, Y.; Zheng, W.; Li, L.; Zheng, Y.F.; Haapasalo, M. Mechanical properties of controlled memory and superelastic nickel-titanium wires used in the manufacture of rotary endodontic instruments. *J. Endod.* **2012**, *38*, 1535–1540. [CrossRef]
455. Saber, S.E.; Nagy, M.M.; Schäfer, E. Comparative evaluation of the shaping ability of ProTaper Next, iRaCe and Hyflex CM rotary NiTi files in severely curved root canals. *Int. Endod. J.* **2015**, *48*, 131–136. [CrossRef]
456. Marceliano-Alves, M.F.; Sousa-Neto, M.D.; Fidel, S.R.; Steier, L.; Robinson, J.P.; Pécora, J.D.; Versiani, M.A. Shaping ability of single-file reciprocating and heat-treated multifile rotary systems: A micro-CT study. *Int. Endod. J.* **2015**, *48*, 1129–1136. [CrossRef] [PubMed]
457. Bürklein, S.; Börjes, L.; Schäfer, E. Comparison of preparation of curved root canals with Hyflex CM and Revo-S rotary nickel-titanium instruments. *Int. Endod. J.* **2014**, *47*, 470–476. [CrossRef] [PubMed]
458. Kumar, B.S.; Pattanshetty, S.; Prasad, M.; Soni, S.; Pattanshetty, K.S.; Prasad, S. An in-vitro Evaluation of canal transportation and centering ability of two rotary Nickel Titanium systems (Twisted Files and Hyflex files) with conventional stainless Steel hand K-flexofiles by using Spiral Computed Tomography. *J. Int. Oral Health* **2013**, *5*, 108–115. [PubMed]
459. Rubio, J.; Zarzosa, J.I.; Pallarés, A. A Comparative Study of Shaping Ability of four Rotary Systems. *Acta Stomatol. Croat.* **2015**, *49*, 285–293. [CrossRef]
460. COLTENE. Nowa Generacja Pilników NiTi, HyFlex™ CM & EDM. Available online: https://global.coltene.com/pim/DOC/BRO/docbro60013831-03-18-pl-hyflex-cm-edm-a4splaindv1.pdf (accessed on 19 November 2021).
461. Morgental, R.D.; Vier-Pelisser, F.V.; Kopper, P.M.; de Figueiredo, J.A.; Peters, O.A. Cutting efficiency of conventional and martensitic nickel-titanium instruments for coronal flaring. *J. Endod.* **2013**, *39*, 1634–1638. [CrossRef] [PubMed]
462. Peters, O.A.; Morgental, R.D.; Schulze, K.A.; Paqué, F.; Kopper, P.M.; Vier-Pelisser, F.V. Determining cutting efficiency of nickel-titanium coronal flaring instruments used in lateral action. *Int. Endod. J.* **2014**, *47*, 505–513. [CrossRef]
463. Soares, R.G.; Lopes, H.P.; Elias, C.N.; Viera, M.V.B.; Vieira, V.T.L.; de Paula, C.B.; Alves, F.R.F. Comparative study of the mechanical properties of instruments made of conventional, M-wire, R-phase, and controlled memory nickel-titanium alloys. *ENDO—Endod. Pract. Today* **2017**, *11*, 271–277.
464. Testarelli, L.; Plotino, G.; Al-Sudani, D.; Vincenzi, V.; Giansiracusa, A.; Grande, N.M.; Gambarini, G. Bending properties of a new nickel-titanium alloy with a lower percent by weight of nickel. *J. Endod.* **2011**, *37*, 1293–1295. [CrossRef] [PubMed]
465. Goo, H.J.; Kwak, S.W.; Ha, J.H.; Pedullà, E.; Kim, H.C. Mechanical Properties of Various Heat-treated Nickel-titanium Rotary Instruments. *J. Endod.* **2017**, *43*, 1872–1877. [CrossRef]
466. Pongione, G.; Pompa, G.; Milana, V.; Di Carlo, S.; Giansiracusa, A.; Nicolini, E.; De Angelis, F. Flexibility and resistance to cyclic fatigue of endodontic instruments made with different nickel-titanium alloys: A comparative test. *Ann. Stomatol.* **2012**, *3*, 119–122.
467. Santos, L.A.; de Azevedo Bahia, M.G.; Las Casas, E.B.; Buono, V.T. Comparison of the mechanical behavior between controlled memory and superelastic nickel-titanium files via finite element analysis. *J. Endod.* **2013**, *39*, 1444–1447. [CrossRef]
468. AlShwaimi, E. Cyclic fatigue resistance of a novel rotary file manufactured using controlled memory Ni-Ti technology compared to a file made from M-wire file. *Int. Endod. J.* **2018**, *51*, 112–117. [CrossRef]
469. Capar, I.D.; Ertas, H.; Arslan, H. Comparison of cyclic fatigue resistance of novel nickel-titanium rotary instruments. *Aust. Endod. J.* **2015**, *41*, 24–28. [CrossRef]
470. Shen, Y.; Qian, W.; Abtin, H.; Gao, Y.; Haapasalo, M. Fatigue testing of controlled memory wire nickel-titanium rotary instruments. *J. Endod.* **2011**, *37*, 997–1001. [CrossRef] [PubMed]
471. Casper, R.B.; Roberts, H.W.; Roberts, M.D.; Himel, V.T.; Bergeron, B.E. Comparison of autoclaving effects on torsional deformation and fracture resistance of three innovative endodontic file systems. *J. Endod.* **2011**, *37*, 1572–1575. [CrossRef]
472. Chang, S.W.; Shim, K.S.; Kim, Y.C.; Jee, K.K.; Zhu, Q.; Perinpanayagam, H.; Kum, K.Y. Cyclic fatigue resistance, torsional resistance, and metallurgical characteristics of V taper 2 and V taper 2H rotary NiTi files. *Scanning* **2016**, *38*, 564–570. [CrossRef] [PubMed]
473. Peters, O.A.; Gluskin, A.K.; Weiss, R.A.; Han, J.T. An in vitro assessment of the physical properties of novel Hyflex nickel-titanium rotary instruments. *Int. Endod. J.* **2012**, *45*, 1027–1034. [CrossRef] [PubMed]

474. Bouska, J.; Justman, B.; Williamson, A.; DeLong, C.; Qian, F. Resistance to cyclic fatigue failure of a new endodontic rotary file. *J. Endod.* **2012**, *38*, 667–669. [CrossRef]
475. Bulem, Ü.K.; Kececi, A.D.; Guldas, H.E. Experimental evaluation of cyclic fatigue resistance of four different nickel-titanium instruments after immersion in sodium hypochlorite and/or sterilization. *J. Appl. Oral Sci.* **2013**, *21*, 505–510. [CrossRef]
476. Aminsobhani, M.; Meraji, N.; Sadri, E. Comparison of Cyclic Fatigue Resistance of Five Nickel Titanium Rotary File Systems with Different Manufacturing Techniques. *J. Dent.* **2015**, *12*, 636–646.
477. Bhagabati, N.; Yadav, S.; Talwar, S. An in vitro cyclic fatigue analysis of different endodontic nickel-titanium rotary instruments. *J. Endod.* **2012**, *38*, 515–518. [CrossRef]
478. Ersoy, I.; Kol, E.; Uygun, A.D.; Tanriver, M.; Seckin, F. Comparison of cyclic fatigue resistance between different NiTi instruments with 4% taper. *Microsc. Res. Tech.* **2016**, *79*, 345–348. [CrossRef]
479. Kim, H.C.; Yum, J.; Hur, B.; Cheung, G.S. Cyclic fatigue and fracture characteristics of ground and twisted nickel-titanium rotary files. *J. Endod.* **2010**, *36*, 147–152. [CrossRef]
480. Pedullà, E.; Plotino, G.; Grande, N.M.; Pappalardo, A.; Rapisarda, E. Cyclic fatigue resistance of four nickel-titanium rotary instruments: A comparative study. *Ann. Stomatol.* **2012**, *3*, 59–63.
481. Pedullà, E.; Grande, N.M.; Plotino, G.; Pappalardo, A.; Rapisarda, E. Cyclic fatigue resistance of three different nickel-titanium instruments after immersion in sodium hypochlorite. *J. Endod.* **2011**, *37*, 1139–1142. [CrossRef]
482. Rodrigues, R.C.; Lopes, H.P.; Elias, C.N.; Amaral, G.; Vieira, V.T.; De Martin, A.S. Influence of different manufacturing methods on the cyclic fatigue of rotary nickel-titanium endodontic instruments. *J. Endod.* **2011**, *37*, 1553–1557. [CrossRef]
483. Choi, J.; Oh, S.; Kim, Y.C.; Jee, K.K.; Kum, K.; Chang, S. Fracture Resistance of K3 Nickel-Titanium Files Made from Different Thermal Treatments. *Bioinorg. Chem. Appl.* **2016**, *2016*, 6374721. [CrossRef] [PubMed]
484. Hou, X.; Yahata, Y.; Hayashi, Y.; Ebihara, A.; Hanawa, T.; Suda, H. Phase transformation behaviour and bending property of twisted nickel-titanium endodontic instruments. *Int. Endod. J.* **2011**, *44*, 253–258. [CrossRef]
485. Shen, Y.; Zhou, H.M.; Wang, Z.; Campbell, L.; Zheng, Y.F.; Haapasalo, M. Phase transformation behavior and mechanical properties of thermomechanically treated K3XF nickel-titanium instruments. *J. Endod.* **2013**, *39*, 919–923. [CrossRef] [PubMed]
486. Gambarini, G.; Pongione, G.; Rizzo, F.; Testarelli, L.; Cavalleri, G.; Gerosa, R. Bending properties of nickel-titanium instruments: A comparative study. *Minerva Stomatol.* **2008**, *57*, 393–398.
487. Gambarini, G.; Gerosa, R.; De Luca, M.; Garala, M.; Testarelli, L. Mechanical properties of a new and improved nickel-titanium alloy for endodontic use: An evaluation of file flexibility. *Oral Surg. Oral Med. Oral Pathol. Oral Radiol. Endod.* **2008**, *105*, 798–800. [CrossRef]
488. Otsuka, K.; Wayman, C.M. *Shape Memory Alloys*, 1st ed.; Cambridge University Press: Cambridge, UK, 1998; pp. 1–284.
489. Wu, S.K.; Lin, H.C.; Chou, T.S. A study of electrical resistivity, internal friction and shear modulus on an aged $Ti_{49}Ni_{51}$ alloy. *Acta Metall. Mater.* **1990**, *38*, 95–102. [CrossRef]
490. Liaw, Y.C.; Su, Y.Y.; Lai, Y.L.; Lee, S.Y. Stiffness and frictional resistance of a superelastic nickel-titanium orthodontic wire with low-stress hysteresis. *Am. J. Orthod. Dentofacial Orthop.* **2007**, *131*, 578.E12–578.E18. [CrossRef]
491. El Batouty, K.M.; Elmallah, W.E. Comparison of canal transportation and changes in canal curvature of two nickel-titanium rotary instruments. *J. Endod.* **2011**, *37*, 1290–1292. [CrossRef]
492. Hashem, A.A.; Ghoneim, A.G.; Lutfy, R.A.; Foda, M.Y.; Omar, G.A. Geometric analysis of root canals prepared by four rotary NiTi shaping systems. *J. Endod.* **2012**, *38*, 996–1000. [CrossRef] [PubMed]
493. Rejula, F.; Christalin, R.; Ahmed, W.; Dinakaran, S.; Gopinathan, A.S.; Babu, A. Measure and compare the Degree of Root Canal Transportation and Canal-centering ability of Twisted, ProTaper, and Conventional Stainless Steel K Files using Spiral Computed Tomography: An in vitro Study. *J. Contemp. Dent. Pract.* **2017**, *18*, 463–469. [CrossRef] [PubMed]
494. Reddy, P.J.; Kumar, V.S.; Aravind, K.; Kumar, H.T.; Vishal, M.B.; Vizaikumar, V.N.; Das, R.; Vamsilatha, K. Canal shaping with one shape file and twisted files: A comparative study. *J. Clin. Diagn. Res.* **2014**, *8*, ZF01–ZF03. [CrossRef]
495. Braga, L.C.; Magalhães, R.R.; Nakagawa, R.K.; Puente, C.G.; Buono, V.T.; Bahia, M.G. Physical and mechanical properties of twisted or ground nickel-titanium instruments. *Int. Endod. J.* **2013**, *46*, 458–465. [CrossRef] [PubMed]
496. Higuera, O.; Plotino, G.; Tocci, L.; Carrillo, G.; Gambarini, G.; Jaramillo, D.E. Cyclic fatigue resistance of 3 different nickel-titanium reciprocating instruments in artificial canals. *J. Endod.* **2015**, *41*, 913–915. [CrossRef]
497. Elsaka, S.E.; Elnaghy, A.M.; Badr, A.E. Torsional and bending resistance of WaveOne Gold, Reciproc and Twisted File Adaptive instruments. *Int. Endod. J.* **2017**, *50*, 1077–1083. [CrossRef]
498. Wycoff, R.C.; Berzins, D.W. An in vitro comparison of torsional stress properties of three different rotary nickel-titanium files with a similar cross-sectional design. *J. Endod.* **2012**, *38*, 1118–1120. [CrossRef]
499. Rapisarda, E.; Bonaccorso, A.; Tripi, T.R.; Condorelli, G.G. Effect of sterilization on the cutting efficiency of rotary nickel-titanium endodontic files. *Oral Surg. Oral Med. Oral Pathol. Oral Radiol. Endod.* **1999**, *88*, 343–347. [CrossRef]
500. Plotino, G.; Costanzo, A.; Grande, N.M.; Petrovic, R.; Testarelli, L.; Gambarini, G. Experimental Evaluation on the Influence of Autoclave Sterilization on the Cyclic Fatigue of New Nickel-Titanium Rotary Instruments. *J. Endod.* **2012**, *38*, 222–225. [CrossRef] [PubMed]
501. La Chapelle, C.F.; Veersema, S.; Brölmann, H.A.M.; Jansen, F.W. Effectiveness and feasibility of hysteroscopic sterilization techniques: A systematic review and meta-analysis. *Fertil. Steril.* **2015**, *103*, 1516–1525.e3. [CrossRef]

502. Haïkel, Y.; Serfaty, R.; Bleicher, P.; Lwin, T.-T.C.; Allemann, C. Effects of cleaning, disinfection, and sterilization procedures on the cutting efficiency of endodontic files. *J. Endod.* **1996**, *22*, 657–661. [CrossRef]
503. Laneve, E.; Raddato, B.; Dioguardi, M.; Di Gioia, G.; Troiano, G.; Lo Muzio, L. Sterilisation in Dentistry: A Review of the Literature. *Int. J. Dent.* **2019**, *2019*, 6507286. [CrossRef] [PubMed]
504. Raju, T.B.; Garapati, S.; Agrawal, R.; Reddy, S.; Razdan, A.; Kumar, S.K. Sterilizing Endodontic Files by four different sterilization methods to prevent cross-infection—An In-vitro Study. *J. Int. Oral. Health* **2013**, *5*, 108–112. [PubMed]
505. Venkatasubramanian, R.; Jayanthi; Das, U.M.; Bhatnagar, S. Comparison of the effectiveness of sterilizing endodontic files by 4 different methods: An in vitro study. *J. Indian Soc. Pedod. Prev. Dent.* **2010**, *28*, 2–5. [CrossRef]
506. Sheth, N.C.; Rathod, Y.V.; Shenoi, P.R.; Shori, D.D.; Khode, R.T.; Khadse, A.P. Evaluation of new technique of sterilization using biological indicator. *J. Conserv. Dent.* **2017**, *20*, 346–350. [CrossRef]
507. Bourgeois, D.; Dussart, C.; Saliasi, I.; Laforest, L.; Tramini, P.; Carrouel, F. Observance of Sterilization Protocol Guideline Procedures of Critical Instruments for Preventing Iatrogenic Transmission of Creutzfeldt-Jakob Disease in Dental Practice in France, 2017. *Int. J. Environ. Res. Public Health* **2018**, *15*, 853. [CrossRef]
508. Schafer, E. Effect of sterilization on the cutting efficiency of PVD-coated nickel-titanium endodontic instruments. *Int. Endod. J.* **2002**, *35*, 867–872. [CrossRef] [PubMed]
509. Seago, S.T.; Bergeron, B.E.; Kirkpatrick, T.C.; Roberts, M.D.; Roberts, H.W.; Himel, V.T.; Sabey, K.A. Effect of Repeated Simulated Clinical Use and Sterilization on the Cutting Efficiency and Flexibility of Hyflex CM Nickel-Titanium Rotary Files. *J. Endod.* **2015**, *41*, 725–728. [CrossRef]
510. Haïkel, Y.; Serfaty, R.; Wilson, P.; Speisser, J.M.; Allemann, C. Cutting efficiency of nickel-titanium endodontic instruments and the effect of sodium hypochlorite treatment. *J. Endod.* **1998**, *24*, 736–739. [CrossRef]
511. Neal, R.G.; Craig, R.G.; Powers, J.M. Effect of sterilization and irrigants on the cutting ability of stainless steel files. *J. Endod.* **1983**, *9*, 93–96. [CrossRef]
512. Morrison, S.W.; Newton, C.W.; Brown, C.E. The effects of steam sterilization and usage on cutting efficiency of endodontic instruments. *J. Endod.* **1989**, *15*, 427–431. [CrossRef]
513. Haïkel, Y.; Serfaty, R.; Lwin, T.T.; Allemann, C. Measurement of the cutting efficiency of endodontic instruments: A new concept. *J. Endod.* **1996**, *22*, 651–656. [CrossRef]
514. Webber, J.; Moser, J.B.; Heuer, M.A. A method to determine the cutting efficiency of root canal instruments in linear motion. *J. Endod.* **1980**, *6*, 829–834. [CrossRef]
515. Villalobos, R.L.; Moser, J.B.; Heuer, M.A. A method to determine the cutting efficiency of root canal instruments in rotary motion. *J. Endod.* **1980**, *6*, 667–671. [CrossRef]
516. Molven, O. A comparison of the dentin-removing ability of five root canal instruments. *Scand. J. Dent. Res.* **1970**, *78*, 500–511. [CrossRef] [PubMed]
517. Oliet, S.; Sorin, S.M. Cutting efficiency of endodontic reamers. *Oral Surg. Oral Med. Oral Pathol.* **1973**, *36*, 243–252. [CrossRef]
518. Fromme, H.G.; Riedel, H. Treatment of Dental Root Canals and the Marginal Contact between Filling Material and Tooth, studied by Scanning Electronic Microscopy. *Int. Endod. J.* **1972**, *6*, 17–20. [CrossRef]
519. Stefanescu, T.; Popovici, R.A.; Antoniac, I.V.; Galuscan, A.; Tirca, T. Ni-Ti Rotary Instrument Fracture Analysis after Clinical Use. Structure Changes in Used Instruments. *Environ. Eng. Manag. J.* **2016**, *15*, 981–988. [CrossRef]
520. Matei, A.; Pencea, I.; Stanciu, S.; Hristu, R.; Antoniac, I.; Coman, E.C.; Sfat, C.; Stanciu, G. Structural characterization and adhesion appraisal of TiN and TiCN coatings deposited by CAE-PVD technique on a new carbide composite cutting tool. *J. Adhes. Sci. Technol.* **2015**, *29*, 2576–2589. [CrossRef]
521. Inan, U.; Keskin, C. Torsional Resistance of ProGlider, Hyflex EDM, and One G Glide Path Instruments. *J. Endod.* **2019**, *45*, 1253–1257. [CrossRef]
522. Spagnuolo, G.; Ametrano, G.; d'Antò, V.; Rengo, C.; Simeone, M.; Riccitiello, F.; Amato, M. Effect of autoclaving on the surfaces of TiN-coated and conventional nickel-titanium rotary instruments. *Int. Endod. J.* **2012**, *45*, 1148–1155. [CrossRef]
523. Razavian, H.; Iranmanesh, P.; Mojtahedi, H.; Nazeri, R. Effect of Autoclave Cycles on Surface Characteristics of S-File Evaluated by Scanning Electron Microscopy. *Iran. Endod. J.* **2015**, *11*, 29–32. [CrossRef]
524. Nair, A.S.; Tilakchand, M.; Naik, B.D. The effect of multiple autoclave cycles on the surface of rotary nickel-titanium endodontic files: An in vitro atomic force microscopy investigation. *J. Conserv. Dent.* **2015**, *18*, 218–222.
525. Fayyad, D.M.; Elgendy, A.A.E. Cutting Efficiency of Twisted versus Machined Nickel-Titanium Endodontic Files. *J. Endod.* **2011**, *37*, 1143–1146. [CrossRef] [PubMed]
526. Hilt, B.R.; Cunningham, C.J.; Shen, C.; Richards, N. Torsional Properties of Stainless-Steel and Nickel-Titanium Files After Multiple Autoclave Sterilizations. *J. Endod.* **2000**, *26*, 76–80. [CrossRef]
527. Silvaggio, J.; Hicks, M.L. Effect of heat sterilization on the torsional properties of rotary nickel-titanium endodontic files. *J. Endod.* **1997**, *23*, 731–734. [CrossRef]
528. Khabiri, M.; Ebrahimi, M.; Saei, M.R. The Effect of Autoclave Sterilization on Resistance to Cyclic Fatigue of Hero Endodontic File #642 (6%) at Two Artificial Curvature. *J. Dent.* **2017**, *18*, 277–281.
529. Hilfer, P.B.; Bergeron, B.E.; Mayerchak, M.J.; Roberts, H.W.; Jeansonne, B.G. Multiple Autoclave Cycle Effects on Cyclic Fatigue of Nickel-Titanium Rotary Files Produced by New Manufacturing Methods. *J. Endod.* **2011**, *37*, 72–74. [CrossRef] [PubMed]

530. Alshwaimi, E.O. Effect of Sterilization on Cyclic Fatigue Resistance of Proflexendo Endodontic Rotary Files. *Saudi J. Med. Med. Sci.* **2019**, *7*, 151–155. [CrossRef]
531. Testarelli, L.; Gallottini, L.; Gambarini, G. Mechanical properties of nickel-titanium files following multiple heat sterilizations. *Minerva Stomatol.* **2003**, *52*, 169–173. [PubMed]
532. King, J.B.; Roberts, H.W.; Bergeron, B.E.; Mayerchak, M.J. The effect of autoclaving on torsional moment of two nickel-titanium endodontic files. *Int. Endod. J.* **2012**, *45*, 156–161. [CrossRef] [PubMed]
533. Viana, A.C.; Gonzalez, B.M.; Buono, V.T.; Bahia, M.G. Influence of sterilization on mechanical properties and fatigue resistance of nickel-titanium rotary endodontic instruments. *Int. Endod. J.* **2006**, *39*, 709–715. [CrossRef] [PubMed]
534. Alfoqom Alazemi, M.; Bryant, S.T.; Dummer, P.M. Deformation of HyFlex CM instruments and their shape recovery following heat sterilization. *Int. Endod. J.* **2015**, *48*, 593–601. [CrossRef]
535. Yilmaz, K.; Uslu, G.; Ozyurek, T. Effect of multiple autoclave cycles on the surface roughness of HyFlex CM and HyFlex EDM files: An atomic force microscopy study. *Clin. Oral. Investig.* **2018**, *22*, 2975–2980. [CrossRef]
536. Zhao, D.; Shen, Y.; Peng, B.; Haapasalo, M. Effect of autoclave sterilization on the cyclic fatigue resistance of thermally treated Nickel-Titanium instruments. *Int. Endod. J.* **2016**, *49*, 990–995. [CrossRef]
537. Valois, C.R.; Silva, L.P.; Azevedo, R.B. Multiple autoclave cycles affect the surface of rotary nickel-titanium files: An atomic force microscopy study. *J. Endod.* **2008**, *34*, 859–862. [CrossRef]
538. Canalda-Sahli, C.; Brau-Aguadé, E.; Sentís-Vilalta, J. The effect of sterilization on bending and torsional properties of K-files manufactured with different metallic alloys. *Int. Endod. J.* **1998**, *31*, 48–52. [CrossRef]
539. Li, X.F.; Zheng, P.; Xu, L.; Su, Q. The influence of autoclave sterilization on surface characteristics and cyclic fatigue resistance of 3 nickel-titanium rotary instruments. *Shanghai Kou Qiang Yi Xue* **2015**, *24*, 690–695.
540. Mize, S.B.; Clement, D.J.; Pruett, J.P.; Carnes, D.L., Jr. Effect of sterilization on cyclic fatigue of rotary nickel-titanium endodontic instruments. *J. Endod.* **1998**, *24*, 843–847. [CrossRef]
541. Özyürek, T.; Yılmaz, K.; Uslu, G. The effects of autoclave sterilization on the cyclic fatigue resistance of ProTaper Universal, ProTaper Next, and ProTaper Gold nickel-titanium instruments. *Restor. Dent. Endod.* **2017**, *42*, 301–308. [CrossRef] [PubMed]
542. Alexandrou, G.; Chrissafis, K.; Vasiliadis, L.; Pavlidou, E.; Polychroniadis, E.K. Effect of heat sterilization on surface characteristics and microstructure of Mani NRT rotary nickel-titanium instruments. *Int. Endod. J.* **2006**, *39*, 770–778. [CrossRef] [PubMed]